Spatiotemporal Drivers of CO_2 Dynamics and Evasion Fluxes from Mountain Streams

Thèse N° 7583

Présentée le 8 novembre 2019

à la Faculté de l'environnement naturel, architectural et construit
Laboratoire de recherche en biofilms et écosystèmes fluviaux
Programme doctoral en génie civil et environnement

pour l'obtention du grade de Docteur ès Sciences

par

Åsa Lovisa Viktoria HORGBY

Acceptée sur proposition du jury

Prof. A. Meibom, président du jury
Prof. T. I. Battin, directeur de thèse
Dr S. Sobek, rapporteur
Prof. P. Regnier, rapporteur
Prof. B. Wehrli, rapporteur

2019

ÉCOLE POLYTECHNIQUE
FÉDÉRALE DE LAUSANNE

Acknowledgements

There are many people that have supported me during the four years that it has taken me to accomplish the work leading to this thesis. First of all, I would like to thank my PhD advisor Tom Battin that have helped me a lot during last years. I am grateful to you for your inspiration, innovative ideas, for pushing me and helping me to improve my work and develop professionally.

Secondly, I would like to thank all my great colleagues at the Stream Biofilm and Ecosystem Research Laboratory. A special thanks to Amber Ulseth for your involvement and support in the beginning of my PhD, and to Lluís Gómez-Gener for your involvement and support at the end of my PhD. I would also like to thank Hannes Peter, Marta Boix Canadell, Sabine Flury, Alexandre Bagnoud, Janine Rüegg and Torsten Vennemann for all the fruitful discussions we had throughout the years. I am also very thankful to Nicolas Escoffier for bouncing ideas of each other, in the laboratory and while driving home from field work. Moreover, I would like to direct a special thanks to Pier Luigi Segatto. Your help with statistics and coding has been crucial for the last chapter of my thesis, when my PhD thesis took a more modelling turn. Furthermore, I would like to Aline Adler, Hannes Peter, Robert Niederdorfer and Nicola Deluigi for helping me translating the abstract of this thesis into French, German and Italian.

I am very happy about having been a part of the C-CASCADES project during my PhD. Through the C-CASCADES project, I did not only find great friends but also got the opportunity to network and meet a lot of interesting people, such as Ronny Lauerwald that have been of great help for the fourth chapter of this thesis. I would also like to thank Gesa Weyhenmeyer and Anna Nydahl for welcoming me during my research stay at Uppsala University, and Pier Fietzek, Nadia Kinski and Anna Canning for welcoming me during my research stay at Kongsberg-CONTROS.

A lot of things has been processed over coffee with my great coffee mates Pier Luigi, David, Amin, Katka and Oscar, as well as at satellite with Anh Chi, Niels, Conny, Tomás, Lucia, Emma and Solenne, or over dinner at home with Aline and Matt. I would like to thank all of you for being there. Those years have been truly life changing, however not always easy. I would not have been able to complete this thesis without the amazing support I got from colleagues and friends. With the skiing accident half a year into my PhD, I sometimes doubted if I would be able to continue or not, and without all great support, I do not know how this would have finished. I want to direct a special thanks to Hannes, Marta and Amber for accompanying me to doctor's appointments and visiting me in hospital. I also want to thank Tania for all the support and laughter that we have shared, Paraskevi for driving me to physiotherapy, Anh Chi for watching all seasons of Friends with me, and Kathi for all your visits. I would like to thank all my Swedish friends that came down to keep me company during my sick leaves (especially Ingela for taking the train for 30 hours!). The rough beginning of my time in Switzerland really showed me how much easier everything is when you have amazing and supportive friends and colleagues around you.

I am forever grateful for the support from my family – mum, dad, Anna, Simon Pierre and Gustav – for always believing in me and approaching life with humor.

Most of all, I would like to thank Robert for all the strength that you have given me during those years. I am excited to see what the future will bring next and I am so happy to have you by my side.

Denna doktorsavhandling tillägnar jag två av mina stora inspirationskällor: till mormor för att du alltid har inspirerat mig till att följa mina drömmar och ta till vara på chanserna i ett allt mer jämställt samhälle, och till farmor för ditt fulla stöd i alla lägen.

Lausanne, 13 August 2019

Abstract

Inland waters are key components of the global carbon cycle, emitting a substantial amount of carbon dioxide (CO_2) to the atmosphere. Climate change and global warming affect mountain catchments significantly, leading to glacier retreat and changing precipitation patterns. What this means for the streams in the mountains, and for CO_2 sources, dynamics and fluxes from those streams, is poorly understood. Generally, mountain streams have low CO_2 concentrations, largely due to low organic carbon content in catchments above the tree line and poorly developed soil horizons. However, it is yet unclear from where the streamwater CO_2 is coming, what drives the CO_2 dynamics, and the magnitudes of the CO_2 evasion fluxes from the stream surfaces to the atmosphere.

This PhD thesis aims to fill this knowledge gap. By using a combination of field sampling, sensor monitoring stations, and analyses of stable isotopes, I identify potential drivers of CO_2 concentrations and fluxes from mountain streams across different spatial and temporal scales. Moreover, in combination with recent insights of gas exchange from mountain streams, this thesis comprises new quantifications of CO_2 evasion fluxes from Swiss mountain streams, as well as mountain streams worldwide.

Within the frame of this thesis, two major field studies were carried out. The first field study consisted of repeated seasonal sampling campaigns every 50 meter across an Alpine stream network. We found large seasonal and spatial variations in streamwater CO_2 concentrations, and identified soil respiration as the major source of streamwater CO_2. With spring snowmelt, and increased catchment connectivity, more respiratory CO_2 could be transported to the stream, however due to high gas transfer velocities, the CO_2 was rapidly evaded downstream.

The second major field study consisted of high-frequency (10 minutes) monitoring of streamwater CO_2 in 12 streams located in 4 Alpine catchments. This enabled us to further explore the role of snowmelt for CO_2 dynamics in mountain streams. We identified different responses in CO_2 concentration and CO_2 evasion fluxes to increasing runoff across different temporal scales. On annual time scales, increasing runoff led to lower streamwater CO_2 concentration. However, during the onset of snowmelt we found increasing CO_2 concentrations with higher runoff, leading to higher CO_2 evasion fluxes.

To better contextualize our results and estimate CO_2 evasion fluxes from mountain streams, we combined insights gained from the two field studies with recent insights of gas exchange in turbulent streams. We developed a simple CO_2 prediction model, and modelled the CO_2 evasion fluxes from all small mountain streams in Switzerland, as well as all mountain streams worldwide. We estimate that mountain streams worldwide emit 167 ± 1.5 Tg C yr^{-1}. This estimate is unexpectedly high given the small total surface area of small mountain streams.

This thesis brings new light on the CO_2 dynamics in mountain streams, not only by highlighting the role of spatiotemporal catchment dynamics and in particular the important role of snowmelt for facilitating transport of catchment-derived CO_2 to the streams, but also by providing one of the first global estimates of the quantity of CO_2 that is evaded from mountain streams every year.

Keywords

Mountain streams, headwater streams, CO_2 sources, CO_2 drivers, CO_2 evasion fluxes, spatiotemporal scales

Resumé

Les eaux continentales sont des composants clés du cycle global du carbone, car elles émettent une quantité importante de CO_2 dans l'atmosphère. Les changements climatiques et le réchauffement de la planète affectent considérablement les bassins versants des montagnes, entraînant le retrait des glaciers et la modification des régimes de précipitations. Les conséquences pour les ruisseaux de montagnes, ainsi que pour les sources, la dynamique et les flux de CO_2 de ces ruisseaux, est mal compris. On sait que les ruisseaux de montagne contiennent généralement de faibles concentrations de CO_2, principalement en raison de la faible teneur en carbone organique dans les bassins versants situés au-dessus de la limite des arbres et des horizons pédologiques peu développés. Cependant, on ne sait pas encore d'où provient le CO_2 contenus dans les cours d'eau, ce qui détermine la dynamique du CO_2 ou l'ampleur des flux d'évasion de CO_2 de la surface des cours d'eau vers l'atmosphère.

Dans cette thèse de doctorat, mon objectif est de mieux comprendre ces phénomènes. En combinant échantillonnages sur le terrain, stations de surveillance de capteurs et analyses d'isotopes stables, j'identifie les facteurs potentiels qui influencent les concentrations et flux de CO_2 des cours d'eau de montagne à différentes échelles spatiales et temporelles. De plus, la combinaison des connaissances récentes sur les échanges de gaz dans les ruisseaux de montagne et des résultats acquis durant cette thèse ont permis de nouvelles quantifications des flux d'évasion de CO_2 des ruisseaux de montagne en Suisses et dans le monde entier.

Dans le cadre de cette thèse, deux études de terrain majeures ont été réalisées. La première consistait en campagnes d'échantillonnage saisonnières avec une résolution de 50 mètres sur un réseau de cours d'eau alpin. Nous avons trouvé de grandes variations spatiales et saisonnières dans les concentrations de CO_2 des ruisseaux et identifié la respiration du sol comme la principale source de CO_2 dans les cours d'eau. Avec la fonte des neiges au printemps et la connectivité accrue des bassins versants davantage de CO_2 issus de la respiration était transporté dans le ruisseau. Cependant, en raison des vitesses élevées de transfert, le CO_2 était rapidement dissipé en aval.

La seconde étude de terrain a consisté en une surveillance du CO_2 dans les eaux de ruissellement, ainsi que des potentiels facteurs influençant les concentrations et flux de CO_2, avec une haute fréquence (10 minutes) dans 12 cours d'eau situés dans 4 bassins versants des Alpes. Cela nous a permis d'explorer plus avant le rôle de la fonte des neiges dans la dynamique du CO_2 dans les cours d'eau de montagne. Nous avons identifié des réponses différentes aux ruissellement accrus en termes de concentration et de flux d'évasion de CO_2 à différentes échelles temporelles. Sur une échelle de temps annuelle, des débits accrus ont mené à de plus faibles concentrations de CO_2 dans les ruisseaux. Cependant, durant le début de la fonte des neiges, nous avons trouvé des concentrations croissantes de CO_2 malgré de plus grands débits, résultant en des flux d'évasion plus élevés.

Afin de mieux contextualiser nos résultats et estimer les flux de CO_2 provenant des cours d'eaux des montagnes, nous avons combiné les connaissances acquises grâce aux deux campagnes de terrain avec les connaissances récentes en matière d'échanges gazeux dans les cours d'eaux turbulent. Nous avons développé un modèle simple de prévision du CO_2, et modélisé les flux d'évasion de CO_2 de tous les petits cours d'eau de montagne en Suisse et dans le monde entier. Nous avons estimé ces derniers à 167 ± 1,5 Tg C an^{-1}. Cette estimation est étonnamment élevée étant donné petite superficie que représente les petits ruisseaux de montagne.

Cette thèse apporte un éclairage nouveau sur la dynamique du CO_2 dans les cours d'eau de montagne, non seulement en soulignant l'importance de la dynamique spatio-temporelle des flux en provenance du bassin versant et en particulier le rôle majeur de la fonte des neiges dans la facilitation du transport du CO_2 depuis le bassin versant vers les cours d'eau, mais également en fournissant l'une des premières estimations mondiales de la quantité de CO_2 s'échappant chaque année des ruisseaux de montagne.

Mots-clés

Ruisseaux de montagne, cours d'eaux supérieurs, sources de CO_2, flux d'évasion de CO_2, échelle spatiotemporelle.

Zusammenfassung

Binnengewässer sind Schlüsselkomponenten des globalen Kohlenstoffkreislaufs und geben eine erhebliche Menge an CO_2 an die Atmosphäre ab. Der Klimawandel und die globale Erwärmung wirken sich erheblich auf alpine Einzugsgebiete aus und führen zu einem Rückgang der Gletscher und sich veränderndem Niederschlag. Was dies für die CO_2-Quellen, Dynamiken und Emissionen aus Gebirgsbäche bedeutet ist kaum bekannt. Es ist bekannt, dass Gebirgsbäche im Allgemeinen niedrige CO_2-Konzentrationen aufweisen, was hauptsächlich auf den geringen Gehalt an organischem Kohlenstoff in Einzugsgebieten oberhalb der Baumgrenze und schlecht entwickelte Bodenhorizonte zurückzuführen ist. Es ist jedoch noch unklar, woher das gelöste CO_2 in den Gebirgsbächen kommt, welche Mechanismen die CO_2-Dynamiken antreibt und wie groß die CO_2-Emissionen von den Bächen zur Atmosphäre sind.

In dieser Doktorarbeit möchte ich diese Wissenslücke schließen. Mithilfe einer Kombination aus Feldproben, Sensorenmessungen und der Analyse stabiler Isotope identifiziere ich die potenziellen Treiber von CO_2-Konzentrationen und -Emissionen aus Gebirgsbächen auf verschiedenen räumlichen und zeitlichen Skalen. In Kombination mit den jüngsten Erkenntnissen zum Gasaustausch aus Gebirgsbächen umfasst diese Arbeit außerdem neueste Quantifizierungen von CO_2-Emissionen aus Schweizer Gebirgsbächen sowie aus Gebirgsbächen weltweit.

Im Rahmen dieser Arbeit wurden zwei große Feldstudien durchgeführt. Die erste Feldstudie bestand aus einer regelmäßigen, saisonalen Probenahme eines alpinen Bach Netzwerkes. Wir fanden große saisonale und räumliche Schwankungen in den CO_2-Konzentrationen des Stromwassers und identifizierten Bodenatmung als Hauptquelle für CO_2 im Bachwasser. Durch die Schneeschmelze und erhöhter Konnektivität der Einzugsgebiete, wurde mehr CO_2 aus dem Einzugsgebiet in den Bach transportiert, welches jedoch aufgrund der hohen Geschwindigkeit des Gastransfers stromabwärts schnell an die Atmosphäre abgegeben wurde.

Die zweite große Feldstudie im Rahmen dieser Dissertation bestand aus hochauflösenden (10-Minuten-Intervalle), kontinuierlichen Messungen der CO_2-Emissionen in 12 Bächen in 4 alpinen Einzugsgebieten. Diese Messungen erlaubten uns den Einfluss der Schneeschmelze auf die CO_2-Dynamiken in Gebirgsbächen genauer zu untersuchen. Die Hochfrequenzdaten ergaben unterschiedliche Reaktionen der CO_2-Konzentration und Emission auf verschiedenen Zeitskalen. Während der frühen Schneeschmelze wurde signifikante mehr CO2 von den Bächen transportiert und an die Atmosphäre abgegeben, über das ganze Jahr betrachtet hatte dieses Phänomen jedoch nur einen geringen Einfluss.

Um unsere Ergebnisse besser zu kontextualisieren haben wir die Erkenntnisse über CO_2-Quellen und -Dynamiken mit den jüngsten Erkenntnissen über den Gastransfer aus Gebirgsbächen kombiniert. Dazu haben wir ein einfaches CO_2-Vorhersagemodell entwickelt, welches mit Hilfe von Geodaten auf die Gebirgsbäche der Schweiz sowie auf alle Gebirgsbäche weltweit angewandt wurde. Wir schätzen, dass Gebirgsbäche 167 ± 1,5 Tg C yr^{-1} emittieren. Diese Schätzung ist unerwartet hoch, da die Fläche kleiner Gebirgsbäche nur 4 bis 6% der weltweiten Ausdehnung von Bächen und Flüssen ausmacht.

Diese Arbeit untersucht die CO_2-Dynamik in Gebirgsbächen neu, indem sie nicht nur die Rolle der räumlichen und zeitlichen Einzugsdynamik und insbesondere die wichtige Rolle der Schneeschmelze für den Transport von CO_2 aus Einzugsgebieten hervorhebt, sondern auch eine der ersten globalen Schätzungen der Menge an CO_2, die jedes Jahr aus Gebirgsbächen austritt ermöglicht.

Schlüsselwörter

Gebirgsbäche, Quellgebiet, CO_2-Quellen, CO_2-Treiber, CO_2-Ausweichflüsse, Raum-zeit Skalierung

Riassunto

Le acque superficiali sono componenti chiave del ciclo globale del carbonio, emettendo una notevole quantità di anidride carbonica (CO_2) nell'atmosfera. Il cambiamento climatico e il riscaldamento globale influenzano in modo significativo i bacini di montagna, portando al ritiro dei ghiacciai e a modifiche nella frequenza e nell'intensità delle precipitazioni. Ciò significa che per i corsi d'acqua di montagna, e per le fonti di CO_2, le dinamiche e i flussi di tali corsi d'acqua sono tuttora poco compresi. In generale, i torrenti montani hanno basse concentrazioni di CO_2, in gran parte a causa del basso contenuto di carbonio organico dei bacini imbriferi posti al di sopra della linea degli alberi e con orizzonti pedologici poco sviluppati. Tuttavia, non è ancora totalmente chiaro da dove provenga il CO_2 disciolto nell'acqua e che cosa ne controlli le dinamiche e le dimensioni dei flussi di evasione di CO_2 dalle superfici dei corsi d'acqua all'atmosfera.

In questa tesi di dottorato investigo questa tematica in dettaglio. Utilizzando una combinazione tecniche che spaziano dal campionamento sul campo, all'installazione di stazioni di monitoraggio provviste di sensori e all'analisi di isotopi stabili, ho identificato i potenziali fattori che controllano le concentrazioni e i flussi di CO_2 espulsi dai corsi d'acqua di montagna a diverse scale temporali e spaziali. Inoltre, in combinazione con le recenti scoperte nel campo degli scambi di gas dai corsi d'acqua di montagna, questa tesi propone nuove quantificazioni dei flussi di evasione di CO_2 provenienti dai torrenti montani svizzeri, così come dai corsi d'acqua di montagna in tutto il mondo.

Nell'ambito di questa tesi, sono stati condotti due importanti studi sul campo. Il primo consiste in ripetute campagne di campionamento stagionale ogni 50 metri in una rete di ruscelli alpini. In questo ambito sono state osservate grandi variazioni stagionali e spaziali nelle concentrazioni di CO_2 dell'acqua per le quali la respirazione del suolo è stata identificata come la principale fonte di CO_2 disciolto. Con lo scioglimento delle nevi primaverili e una maggiore connettività del bacino imbrifero, è stato possibile osservare un maggior trasporto di CO_2 proveniente dalla respirazione del suolo che, tuttavia, viene rapidamente espulso poco più a valle a causa delle elevate velocità di trasferimento del gas.

Il secondo importante studio sul campo consiste nel monitoraggio ad alta frequenza (10 minuti) di CO_2 disciolto in dodici corsi d'acqua situati in quattro bacini alpini. Questa rete di misure ha permesso di esplorare ulteriormente il ruolo dello scioglimento della neve nelle dinamiche di CO_2 nei ruscelli di montagna ed osservare diverse risposte nella concentrazione e nei flussi di evasione di questo gas all'aumentare del deflusso del corso d'acqua. Su scale temporali annuali, l'aumento del deflusso porta generalmente a una minore concentrazione di CO_2 nell'acqua. Tuttavia, durante l'insorgere dello scioglimento delle nevi è stato riscontrato un aumento delle concentrazioni di CO_2 con un deflusso più elevato, che porta a flussi di evasione di CO_2 maggiori.

Per contestualizzare meglio i nostri risultati e stimare i flussi di evasione di CO_2 dai corsi d'acqua montani, abbiamo combinato le intuizioni acquisite dai due studi sul campo con le più recenti scoperte sullo scambio di gas in flussi turbolenti. Abbiamo sviluppato un modello di previsione del CO_2 e ne abbiamo modellato i flussi di evasione per tutti i piccoli corsi d'acqua di montagna della Svizzera, così come per tutti quelli di tutto il mondo. Stimiamo che i corsi d'acqua di montagna del globo emettano 167 x 1,5 Tg C yr-1. Questa stima è inaspettatamente elevata data la piccola superficie totale di piccoli corsi d'acqua di montagna.

Questa tesi porta nuove contribuzioni sulle dinamiche di CO_2 nei torrenti montani, non solo evidenziando il ruolo delle dinamiche spazio-temporali che occorrono nei bacini imbriferi, e in particolare riguardo l'importante ruolo dello scioglimento della neve quale facilitazione al trasporto di CO_2 proveniente dalla respirazione dei suoli dei bacini stessi, ma anche fornendo una delle prime stime globali della quantità di CO_2 che viene espulsa dai torrenti di montagna ogni anno.

Parole chiave

Ruscelli di montagna, acque superficiali, fonti di CO_2, driver di CO_2, flussi di evasione di CO_2, scale spazio-temporali

Sammanfattning

Inlandsvatten är en viktig komponent i den globala koldioxidcykeln och avger en betydande mängd koldioxid (CO_2) till atmosfären. Klimatförändringar och den globala uppvärmningen påverkar bergsområden avsevärt, och leder till smältande glaciärer och förändrade nederbördsmönster. Det är oklart vad detta kommer att innebära för bäckar och forsar i bergsområden, samt för CO_2-källor, CO_2-dynamik och avgivning av gas från dessa vattendrag. Bergsbäckar har ofta låga halter av CO_2, vilket till stor del beror på litet organiskt kolinnehåll i avrinningsområden ovanför trädgränsen samt outvecklade jordmånshorisonter. Det är emellertid oklart varifrån koldioxiden i bergsbäckarna kommer ifrån, vad som påverkar förändringar av vattnets koldioxidhalter samt hur mycket koldioxid som avges från bergsbäckar ut i atmosfären.

Denna doktorsavhandling strävar efter att fylla detta kunskapsgap. Genom att använda en kombination av fältprovtagning, sensorstationer och analyser av isotoper, identifieras potentiella drivkrafter för förändringar i CO_2-halter samt avgivning av gas från bäckar i bergsområden över tid och rum. Genom att kombinera detta med nya forskningsrön om gasers transport mellan vattendrag och atmsofären, så uppskattas hur mycket koldioxid som avges från bäckar i de Schweiziska alperna samt hur mycket CO_2 som avges av alla bergsbäckar över hela världen.

Inom ramen för doktorsavhandlingen har två stora fältstudier genomförts. Den första fältstudien bestod av fyra upprepade provtagningsomgångar i ett alpint avrinningsområde där huvudbäcken och sidobäckar provtogs varje 50:e meter. CO_2 producerad av bakterier i omgivande mark identifierades som den viktigaste CO_2-källan. Ett specifikt område med hög grundvattentillrinning fungerade som en "kontrollpunkt" och styrde bäckens biogeokemiska sammansättning. Med vårens snösmältning ökade transportvägarna mellan bäcken och den omigvande marken, och mer koldioxid kunde transporteras till bäcken. Denna CO_2 avgas dock snabbt nedströms på grund av de höga gasöverföringshastigheterna.

Den andra stora fältstudien bestod av högfrekvensmätningar (var 10:e minut) av CO_2 i 12 vattendrag i fyra alpina avrinningsområden. Tidsserierna möjliggjorde ytterligare analyser av snösmältningens roll för CO_2-dynamik i bergsbäckar. Trots övergripande utspädningsrespons på årlig basis så identifierade vi betydande händelser under tidig snösmältning, då bäckarna innehöll högre halter av CO_2 och därmed mer CO_2 som kunde avges till atmosfären.

För att kunna pröva och sätta in resultaten i en vetenskaplig kontext kombinerades resultat från de båda ovanstående studierna med nya forskningsrön om gasöverföring från branta och turbulenta bäckar. I denna studie utvecklade vi en förutsägelsemodell för CO_2 i bergsbäckar och modellerade avgasning av CO_2 från alla bergsbäckar i Schweiz, liksom från alla bergsbäckar över hela världen. Vi uppskattar att bäckar som rinner i bergsområden avger 167 ± 1,5 Tg C per år. Denna uppskattning är oväntat hög med tanke på de små bergsbäckarnas blygsamma yta.

Denna doktorsavhandling ger ny information om hur CO_2-dynamiken fungerar i bergsströmmar. Den gör det inte bara genom att lyfta fram vikten av spatiotemporära mätningar och persepektiv, och då särskilt betydelsen av snösmältning för transport av CO_2 till bäckarna, utan också genom att presentera en första global uppskattning av mängden koldioxid som avges varje år från bäckar i bergsområden.

Nyckelord

Bergsbäckar, CO_2-källor, CO_2-dynamik, avgasning av CO_2, spatiotemporära skalor

Contents

List of Figures

List of Tables

List of Equations

Chapter 1 Introduction

1.1 Facing a climate emergency

On May 12 this year, 2019, a new record was reached when atmospheric carbon dioxide (CO_2) exceeded 415 ppm at the Mauna Loa monitoring station in Hawaii. Never before in human history had atmospheric CO_2 concentrations been this high[1].

The exponential increase of greenhouse gases in the atmosphere, including CO_2, methane (CH_4) and nitrous oxide (N_2O), started with the industrial revolution in the 1850th and is projected to continue to increase in the future. Anomalies in air temperatures and precipitation patterns, predicted by the Intergovernmental Panel of Climate Change (IPCC), are currently causing, and will continue to cause, extreme weather events, glacier melt, permafrost thawing and sea level rise[2]. Climate change is difficult to assess and mitigate, nonetheless, it is highly likely that climate change will indirectly or directly impact most of our lives and the life of the coming generations. Consequently, many jurisdictions and nations[3] have now declared that we are not only facing climate change – we are facing a climate emergency.

Glaciers have historically shown to be one of the more responsive physical systems to climate change[4] and the rate of glacier shrinkage is accelerating[5]. The periods of glacier volume loss increases in intensity due to higher greenhouse gas concentrations in the atmosphere[6], changes in albedo and moraine cover[7], as well as changes in atmospheric oscillation patterns[8] and changes in local precipitation and wind patterns[7]. As an example, the total glacial coverage area in the European Alps decreased with 35 % during 80 years (1850-1970)[9] and most Alpine glaciers will be gone within the coming 20 to 80 years; glaciers situated below 2000 m (a.s.l.) are predicted to be gone by 2050 and glaciers below 2500 predicted to be gone by 2100[5]. A projected 3℃ temperature increase in the Alpine regions, together with a 10-30 % precipitation decrease, would lead to a shift in the seasonal distribution of precipitation[10]. In Switzerland, effects of climate change can already be seen. Average summer temperatures during the last 30 years exceeds all previous periods since 1685 and the near-surface temperature has increased by 2℃ during the last 150 years (1864-2017). This can be compared by a 0.9℃ increase globally. As a result, the days of snowfall below 800 m (a.s.l.) have now decreased with half of the days compared to the 1970s, as the winter precipitation has shifted to more rain. In the coming 80 years, climate projections (RCP8.5) indicate a precipitation decrease in Switzerland during summer (-43 to +2 %) along with a precipitation increase in winter (2 to 24 %). Depending on the climate scenario, the temperature rise in Switzerland is predicted to be between 0.6 and 1.9 ℃ (RCP2.6) and 3.3 and 5.4 ℃ (RCP8.5) by the end of the century, resulting in a snow cover decrease by up to 80 % at lower elevations[11]. Hence, drastic alterations of hydrological regimes are to be expected for the streams and rivers in the Alps. Glacial and nival hydrological regimes, common regimes in the Swiss Alps (Federal Office for the Environment, FOEN, Switzerland, 2013), will transit into pluvial regimes. Thus, high-altitude streams are highly susceptible to global warming, where shifting hydrological regimes impact stream and river biogeochemistry and carbon cycling[12].

1.2 Inland waters and the global carbon cycle

During the last decade, the role of inland waters (i.e. streams, rivers, lakes, wetlands, estuaries and reservoirs) in the global carbon cycle has caught more attention from the scientific community. In 2007, Cole and colleagues emphasized that inland waters indeed are key components of the global carbon cycle: transporting, storing and transforming organic and inorganic carbon, and emitting CO_2 and CH_4 to the atmosphere[13]. This differed substantially from previous views of inland waters as passive pipes, transporting carbon along the land to ocean aquatic continuum (LOAC) (Figure 1:1).

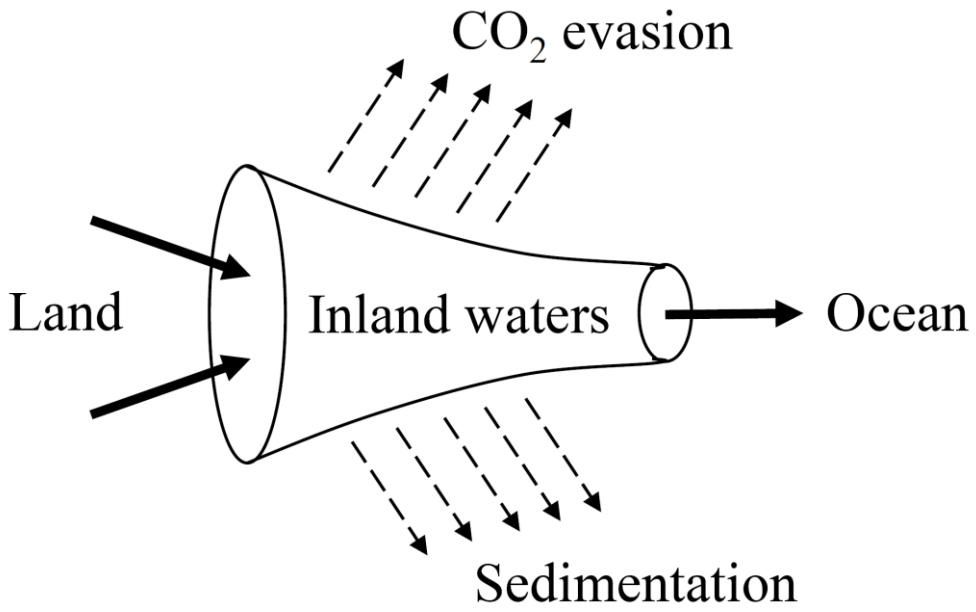

Figure 1:1: Conceptual view of inland waters as funnels, not only transporting carbon along the land to ocean aquatic continuum; carbon also gets transformed, sedimented and evaded along the way. Figure modified from Cole and colleagues in 2007[13].

Inland waters were for the first time included in the report from the International Panel of Climate Change (IPCC) in 2013, when freshwaters were estimated to emit 1.0 Pg C per year[14]. Since those first acknowledgements of the contributions of inland waters to the global carbon cycle, a number of studies have focused on better quantifying CO_2 (e.g., refs. [15–18]), CH_4 (e.g., ref. [19]) and N_2O (e.g., ref. [20]) evasion fluxes from inland waters. The estimate of the total CO_2 evasion flux from inland waters has increased since estimates from contributing components. This includes revised estimates of CO_2 fluxes from deltas (e.g., ref. [21]), reservoirs (e.g., ref. [22]), and lakes (e.g., refs. [23,24]). Moreover, more studies from poorly studied parts of the world, such as African streams and rivers (e.g., ref. [25]), Chinese rivers (e.g., ref. [26]) and Indian estuaries (e.g., ref. [27]) have been included. Nevertheless, current estimates of CO_2 evasion fluxes from inland waters vary considerably between publications, from 0.75 to 3.88 Pg C per year[28] (Figure 1:2). Thus, the research community is far from a consensus of the quantity of CO_2 emitted from inland waters and there are still major components left to be better quantified. One example of this are the streams in the very beginning of the land to ocean aquatic continuum: the headwater streams[29,30]).

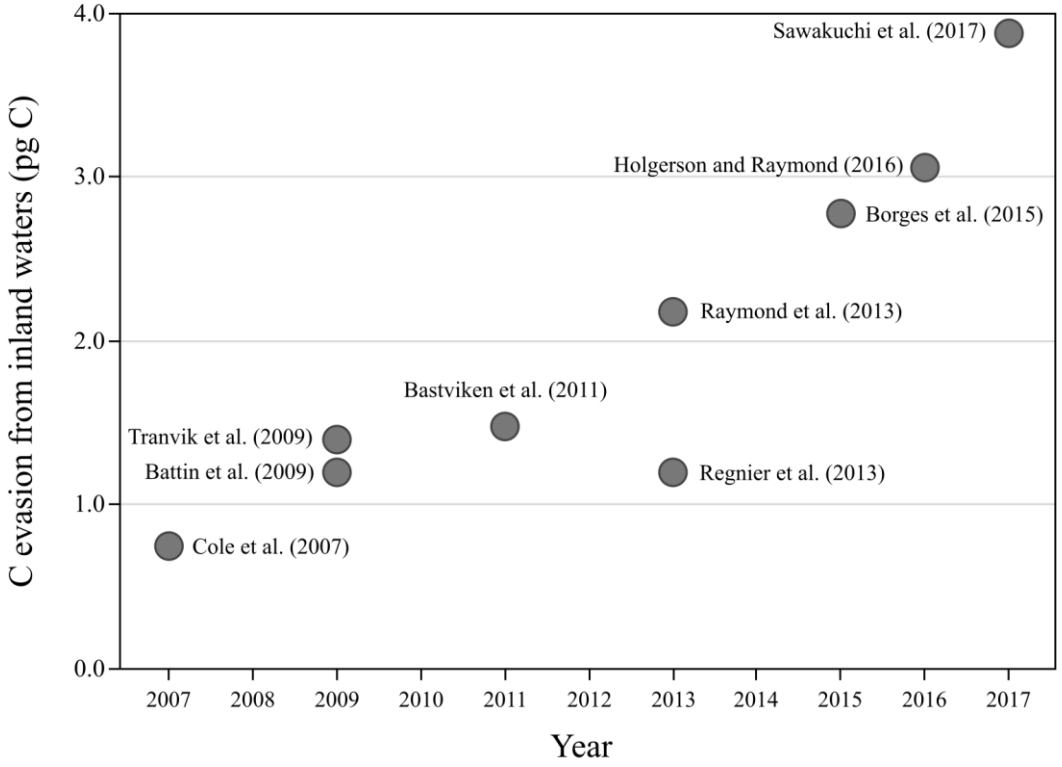

Figure 1:2 The estimate of the total carbon evasion flux has been revised upwards during the last decade. Figure created with data synthetized from Drake and colleagues in 2018 (ref. [28]) based on several studies[13,15,17–19,25,31–33].

1.3 Mountain headwater streams and the global carbon cycle

Headwater streams are estimated to comprise approximately 89% of the total stream and river length[34,35], although streams and rivers contribute with only 0.6 % of the Earth's non-glaciated land surface[36]. Nevertheless, headwater streams are estimated to emit an very high amount of CO_2 with respect to their surface area[30,37,38]. Most of those estimates are based on studies from high-latitude headwater streams[16,39–41], where partial pressure of the streamwater CO_2 (pCO_2) generally is high due to high quantities of organic carbon present[42,43] (Figure 1:3a, Figure 1:3b). Fewer studies have been conducted on more carbon-poor systems, such as mountain stream networks, despite the fact that mountains cover one fourth of the land surface[44,45] and mountain streams and rivers contribute with 32 % of the global runoff[45]. In fact, median altitude of the CO_2 data included in the global river chemistry database (GLORICH)[46] is 409 m above sea level (Figure 1:3c). Overall, high-altitude streams have comparably low pCO_2 and sporadically also undersaturated CO_2 concentrations with respect to the atmosphere[47–50], the magnitude of their CO_2 emissions to the atmosphere is still debated[47,49].

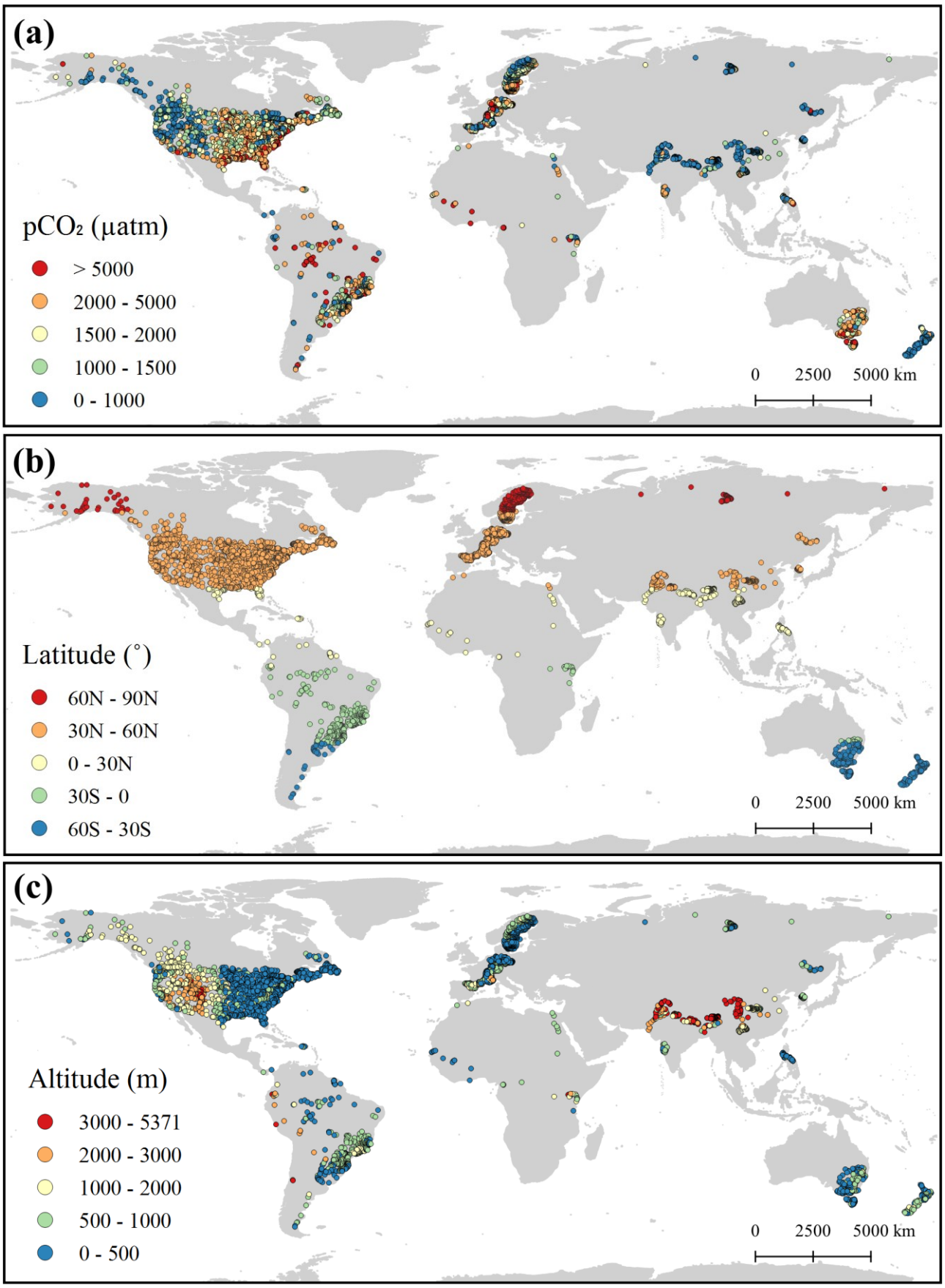

Figure 1:3 Streamwater pCO_2 data included in the GLORICH database (a) is highly biased towards high latitude streams (b) as well as streams located at lower altitudes (c). Figure based on data from the GLORICH database[46].

1.4 CO_2 evasion fluxes from mountain streams: high gas exchange and low streamwater CO_2

CO_2 fluxes (F_{CO2}) depend both on the CO_2 concentration gradient between water and atmosphere (CO_{2water} – CO_{2air}) and on the CO_2 gas exchange between the streamwater surface and the atmosphere (Equation 1:1). The gas exchange can be described as a function of the gas transfer velocity (k), as shown in Equation 1:1. Gas transfer velocity varies between different gases and can be translated into CO_2 gas transfer velocity (k_{CO2}) using the Schmidt number for CO_2. The Schmidt number is an empirically calculated parameter of the water's kinematic viscosity divided the gas molecular diffusion coefficient. It is gas specific and temperature specific, meaning that every gas has a different Schmidt number (the Schmidt number is also influenced by salinity which has to be considered in non-freshwater environments)[51].

$$F_{CO2} = (CO_{2water} - CO_{2air}) \times k_{CO2}$$

Equation 1:1 – CO_2 evasion fluxes

The CO_2 concentration gradient between the streamwater and the atmosphere generally increases in downstream stream and river networks due to higher inputs of organic carbon and higher rates of *in-situ* CO_2 production from aquatic metabolism, in comparison to dominating catchment-derived CO_2 sources in headwater streams (Figure 1:4a)[38]. Oppositely, the gas exchange might be high in headwater[41,52] (Figure 1:4b) since the gas transfer velocity increases with stream channel slopes[41,53,54]. In fact, gas transfer velocity rates in mountain high-energy streams are disproportionally high due to high turbulence and bubble formation within the water column[54]. For mountain streams, this implies that even a slight CO_2 oversaturation might lead to high CO_2 evasion fluxes.

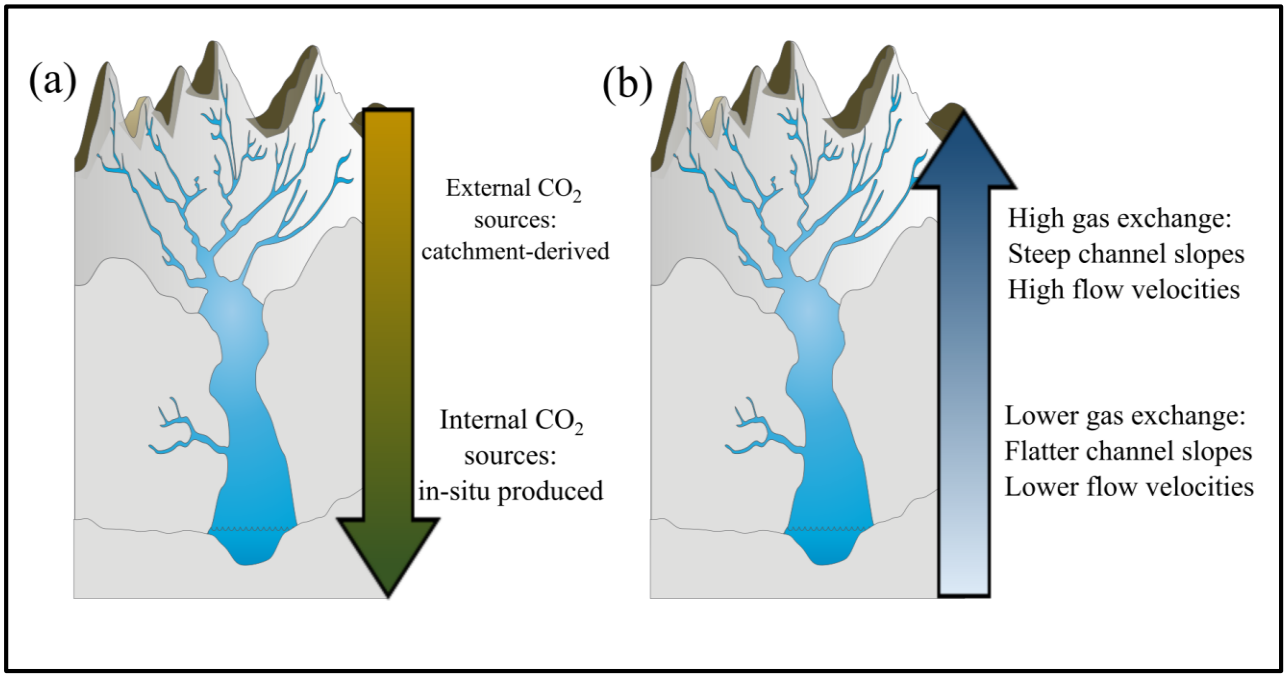

Figure 1:4 Streamwater CO_2 sources are known to vary along the land to ocean aquatic continuum, where headwaters have a higher contribution of catchment-derived CO_2 (external CO_2 sources) compared to downstream rivers that have higher proportions of in-situ produced CO_2 (internal sources) (a). The gas exchange between the stream and the atmosphere is higher in steeper, high-energy, streams due to the higher turbulence, compared to in flatter, low-energy, streams (b). Figure modified from: Tracey Saxby, Integration and Application Network, University of Maryland Center for Environmental Science (ian.umces.edu/imagelibrary/).

1.5 Spatiotemporal CO_2 dynamics in mountain streams

Due to the high gas exchange in mountain streams, combined with pCO_2 close to atmospheric equilibrium, those streams in particular require accurate estimations of streamwater pCO_2. There are different methods for estimating streamwater CO_2. Traditionally, streamwater CO_2 has been estimated indirectly through calculations based on the carbonate equilibria where the speciation of dissolved inorganic carbon (DIC) (i.e., dissolved CO_2, carbonic acid, bicarbonate and carbonate) depend on pH and temperature[55,56]. This method is relatively simple and cost-effective, although associated with high errors, especially at low pH[57]. A more accurate method is to estimate streamwater CO_2 from grab samples using a headspace equilibrium method, where a headspace is created *in-situ* or in a laboratory. The headspace it then let to equilibrate with the remaining water in the vial, either through shaking[39] or heating[49]. Thereafter, the gas in the headspace can be extracted and measured an infrared gas analyzer[58], gas chromatography[59] or cavity ring-down mass spectrometry[60]. CO_2 can also be measured via drifting chamber measurements[61]. During the last couple of decades, there has been an increasing availability pCO_2 sensors that directly measure the stream water mole fraction of CO_2. A major advantage using the pCO_2 sensors is that they can continuously measure CO_2, enabling more long-term monitoring[62,63]. With an increasing possibility of more accurate estimations and monitoring of CO_2, higher resolution of sampling is possible. This is a major breakthrough, since streamwater pCO_2 is known be highly variable both spatially and temporally[64–66], causing spatiotemporally dynamic CO_2 'hotspots' and 'hot moments'[67–69].

In mountain streams, hydrological regimes drives temporal variations in stream biogeochemistry, where the sources of water (precipitation, groundwater, snowmelt and glacier ice melt) changes throughout the year[12,70]. The hydrological connectivity of the catchment, enhancing the transport of soil CO_2 and weathered products, has been identified as a major driver of streamwater CO_2 dynamics in headwater streams[37,66,71,72] where groundwater upwelling may cause CO_2 hotspots[37,62] that significantly alter the stream biogeochemistry[73]. Streamwater hydrology is also important for the gas exchange, where gas transfer velocities increases with increasing turbulence[54,74]. The relationship between streamwater hydrology and streamwater CO_2 dynamics in mountain streams, and how this varies over different spatial and temporal scales, is yet today poorly constrained. This includes both streamwater CO_2 sources and CO_2 evasion fluxes – from Swiss mountain streams as well as from mountain streams worldwide. Mountain streams are exposed to present and future alterations due to the ongoing climate emergency, with biogeochemical and hydrological shifts[12,75], such as a tree line advancing to higher altitudes[76] and increased catchment connectivity due to glacier retreat[77]. This makes it even more important to better understand the drivers and mechanisms behind CO_2 dynamics and evasion fluxes from mountain streams.

1.6 Thesis objectives and chapters

We are facing a threat of a changing climate that human kind has never experienced before. Despite this, many components of the global carbon cycles remain to be refined. This includes the role of mountain streams for global carbon fluxes. This is remarkable given the probability of mountain streams contributing significantly to global CO_2 emissions[49], as well as the susceptibility of mountain streams to climate change[12,78]. **The objective of my PhD thesis is therefore to better constrain CO_2 sources, CO_2 dynamics, and CO_2 evasion fluxes from mountain streams.** My thesis is divided into five chapters, where the first chapter is this thesis introduction. The following two chapters aim to assess mountain stream CO_2 dynamics and fluxes at different spatial and temporal scales; high-resolution spatial scale and high-resolution temporal scale. The forth chapter of my thesis focuses on a global scale and aims to assess the overall role of mountain streams in the global carbon cycle. Finally, the fifth chapter contains a conclusion of all results of this thesis, and an outlook with future perspectives.

1.6.1 Chapter 2: High-resolution spatial sampling identifies groundwater as driver of CO_2 dynamics in an Alpine stream network

This chapter focuses on spatial and seasonal variations in CO_2 sources and drivers in a high-altitude Alpine stream network. I present a case study from a small headwater catchment in the Swiss Alps were we have conducted highly resolved spatial sampling campaigns repetitively during four periods of the year; winter, spring, summer and autumn (2016). In total, streamwater samples from 300 sites were collected, and approximately 3000 samples analyzed. By interpreting the data, we reconstructed seasonal hydrological changes and the important role of catchment connectivity for streamwater CO_2 dynamics, sources and evasion fluxes from the stream network.

1.6.2 Chapter 3: Dynamics and potential drivers of CO_2 concentration and evasion across temporal scales in high-alpine streams

In this chapter, unique results from a study in the Swiss Alps are presented. We monitored streamwater pCO_2 and water levels continuously (every 10 minutes) during two years (August 2016 to September 2018). By relating the responses in streamwater CO_2 concentration, and CO_2 evasion fluxes, with discharge dynamics, we identified the importance of temporal scale for assessment of CO_2 evasion fluxes from streams that are low in CO_2. Despite overall diluting responses in CO_2 concentration to increasing flow, we identified pulses of CO_2 during early snowmelt, when soil-derived CO_2 was flushed from the catchments to the streams.

1.6.3 Chapter 4: Unexpected large evasion fluxes of carbon dioxide from turbulent streams draining the world's mountains

The fourth chapter of my thesis contains an estimation of the total contribution from mountain streams to the global carbon cycle. I used, together with my colleagues, insights from the two previous chapters and upscaled the results to cover larger areas: first to cover all small mountain streams in Switzerland, and then to all small mountain streams in the world. We constructed a prediction model of streamwater CO_2 in mountain streams that we coupled with estimates of gas exchange and derived a new estimate of the total CO_2 annually emitted from the world's mountain streams.

1.6.4 Chapter 5: Conclusions and future perspectives

The fifth chapter starts with a summary of achieved results and then continuing with an outlook of future development. Altogether, the chapters in this thesis brings together a new perspective of CO_2 dynamics, sources and fluxes from mountain streams, and stresses that a better implementation of mountain streams in the global carbon budgets is needed – not only to enable better prediction models of the global carbon cycle but also to better monitor and predict future alterations for the world's mountain streams due to climate change.

Chapter 2 High-resolution spatial sampling identifies groundwater as driver of CO_2 dynamics in an Alpine stream network

Research article published in *Journal of Geophysical Research: Biogeosciences*

Publishing date: 07 June 2019

doi: 10.1029/2019JG005047

Contributing authors:

Åsa Horgby[1], Marta Boix Canadell[1], Amber J. Ulseth[1,2], Torsten W. Vennemann[3] and Tom J. Battin[1]

[1]Stream Biofilm and Ecosystem Research Laboratory, École Polytechnique Fédérale de Lausanne (EPFL), Station 2, CH-1015, Lausanne, Switzerland
[2]Now at Department of Biological Sciences, Sam Houston State University, Huntsville, TX 77341, USA
[3]Institute of Earth Surface Dynamics, University of Lausanne, CH-1015, Lausanne, Switzerland

T.J.B., Å.H. and A.J.U planned and designed the research. A.J.U. and M.B.C. led the field work, and Å.H led the laboratory work. Å.H. performed all data analyses. Å.H. wrote with the help of T.J.B and A.J.U the first draft of the manuscript; all other authors contributed to the final version of the manuscript.

2.1 Abstract

Inland waters are major sources of CO_2 to the atmosphere. The origin of this CO_2 is often elusive, especially in high-altitude streams that remain poorly studied at present. Here we study the spatial and seasonal variations in streamwater CO_2, its potential sources and drivers in an Alpine stream network (Switzerland). High-resolution sampling combined with stable isotope analysis and mixing models enabled us to capture the fine-scale spatial heterogeneity in streamwater pCO_2 as the stream network expanded and contracted during seasons. We identified soil respiration as a major source of CO_2 to the stream. We also identified a major groundwater upwelling zone as an ecosystem 'control point' that disproportionately influenced stream biogeochemistry. This was particularly pronounced when the stream network expanded during snowmelt, when it covered a five times larger area compared to winter (35,300 m^2 compared to 7,100 m^2). Downstream from this control point, CO_2 evaded rapidly owing to high gas transfer velocity. The stream network was a net source of CO_2 to the atmosphere with an average areal evasion flux of 30.1 (18.0–43.1) µmol m^{-2} s^{-1} and a total flux at network scale ranging from 237 (141–339) kg C d^{-1} in winter to 1793 (1069–2565) kg C d^{-1} during spring snowmelt. Our study highlights the role of stream network dynamics and control points for the CO_2 dynamics in high-altitude streams.

2.2 Introduction

Inland waters are key components of the global carbon cycle. They transport and store organic and inorganic carbon, but also transform carbon with the ultimate emission of carbon dioxide (CO_2) and methane (CH_4) to the atmosphere[13,15,17,79]. While high-latitude streams are recognized as large emitters of CO_2 (e.g., refs. [39–41]), the emissions of CO_2 from high-altitude streams are less well studied at present[16,49,80]. This is remarkable given the susceptibility of high-altitude streams to climate change, where glacier retreat and shifts in precipitation patterns, with consequences for snowpack distribution, change the hydrological and thermal regimes[12,75] and carbon fluxes[81].

While a third of the CO_2 evasion from streams and rivers occurs in headwater catchments[30], it is only recently that attempts are being made to constrain the sources of the CO_2 in these streams[37,38]. Overall, these studies suggest that terrestrial deliveries of CO_2 prevail in headwaters and that autochthonous CO_2 sources (e.g., from aquatic ecosystem respiration) become more important downstream. This is, among other reasons, because of the typically high hydrological connectivity between groundwater with their adjacent soils in headwater streams[66,71,80]. Shallow groundwater transports CO_2 derived from soil respiration[82], while deeper groundwater can entrain dissolved inorganic carbon (DIC) from carbonaceous rock weathering[83] into the streams. The upwelling of groundwater may therefore locally enrich streamwater in CO_2 (and DIC) and subsequently increase CO_2 evasion fluxes along downstream reaches[37,62]. Such zones of local groundwater upwelling may function as 'control points' that spatially and temporally control ecosystem dynamics and related biogeochemical fluxes[73]. If not properly accounted for, the rapid local CO_2 evasion downstream from such control points may lead to an underestimation of CO_2 evasion rates at larger scales (i.e., reach scale and beyond)[37,67]. Thus, insights in catchment hydrology and streamwater sources are helpful for tracking the sources and fate of streamwater CO_2.

The sources of CO_2 in streamwater can be identified using stable carbon isotope analyses[82,84,85]. $\delta^{13}C$ values of streamwater CO_2 depend on the relative contribution of carbon from respiration, weathering and atmospheric exchange[86]. Isotopic discrimination occurs during CO_2 assimilation by plants, where the lighter isotope is preferentially used over the heavier isotope. CO_2 originating from in-stream or soil respiration (either from root respiration or heterotrophic oxidation of soil organic matter) has $\delta^{13}C$ values similar to those of the organic carbon being respired[87], commonly ranging between -34 to -24 ‰[88] in temperate environments where C3 is the most abundant photosynthetic pathway[89]. In the presence of carbonate bedrock, calcium carbonate dissolution (with $\delta^{13}C$ values close to zero) commonly occurs due to a reaction with carbonic acid (H_2CO_3) originating from soil respiration[90]. Therefore, in streams with carbonate mineral dissolution, streamwater CO_2 is typically enriched in ^{13}C with values ranging from -23 to -11 ‰[91]. Moreover, during exchange with atmospheric CO_2, the lighter ^{12}C isotopes evade more easily from the streamwater, which results in an enrichment of streamwater CO_2 and DIC in the heavier isotope ^{13}C[85,92].

The aim of this study was, using high-resolution spatial surveys, to study the dynamics of CO_2, its sources and evasion fluxes from an Alpine headwater stream network as it expands and contracts during seasons. Alpine catchments, with their hydrology being dominated by snow and glacier ice melt, are well suited to study the dynamics of hydrological connectivity and its impact on stream biogeochemistry. In fact, the hydrology of alpine streams is shaped by the relative contributions from groundwater, precipitation, snowmelt and glacier ice melt, all of them changing seasonally and becoming increasingly altered because of global warming[12]. We hypothesized that the spatial and temporal variability of groundwater upwelling is a major driver of the dynamics of streamwater pCO_2 and CO_2 evasion fluxes from the stream network. We also anticipated that local valley geomorphology can act as a control point[73] that, depending on the hydrology, modulates groundwater upwelling and hence CO_2 delivery into the stream. Furthermore, we expected the hydrological connectivity as modulated by seasonal expansion and contraction of the stream network, together with seasonal fluctuation of shallow groundwater dynamics, to influence pCO_2 dynamics and CO_2 evasion fluxes.

2.3 Materials and Methods

2.3.1 Study site description

We conducted field surveys in the stream network draining the Vallon de Nant catchment (13.4 km^2, 46° 15'12.3''N, 7° 06'34.7''E) in the Swiss Alps (Figure 2:1). Catchment boundaries were delineated in ArcGIS 10.5 (Environmental Systems Research Institute, USA) using a digital elevation model (DEM; 2 m^2 resolution) (Geodata © Swisstopo). The catchment elevation ranges from 1190 to 3051 m above sea level (a.s.l.). The upstream catchment is characterized by a wide valley bottom with braided and low-sloped channels. Downstream from this braided area, the valley geomorphology constrains the stream into a canyon-like channel that gradually opens up again further downstream (Figure 2:1). The average catchment slope is 0.32 m m^{-1} and the average stream channel slope is 0.093 ± 0.033 m m^{-1}. The stream network, with a maximum stream length of 4500 m, expands and contracts throughout the year depending on the variable contributions from snowmelt, glacier ice melt, groundwater and precipitation (Figure 2:2). The glacier, situated in the southeast part of the catchment, covers 5 % of the catchment area.Vegetation cover consists of natural grassland (18 %), coniferous forest (15 %), sparsely vegetated areas (13 %) and moors and peatland (4 %); roughly 45 % of the catchment consists of bare rock, including calcareous minerals, estimated in ArcGIS from CORINE land cover (European Environment Agency, Denmark). In 2016, the annual air temperature averaged 5.9 ± 6.1 °C and streamwater temperature averaged 4.8 ± 2.8 °C.

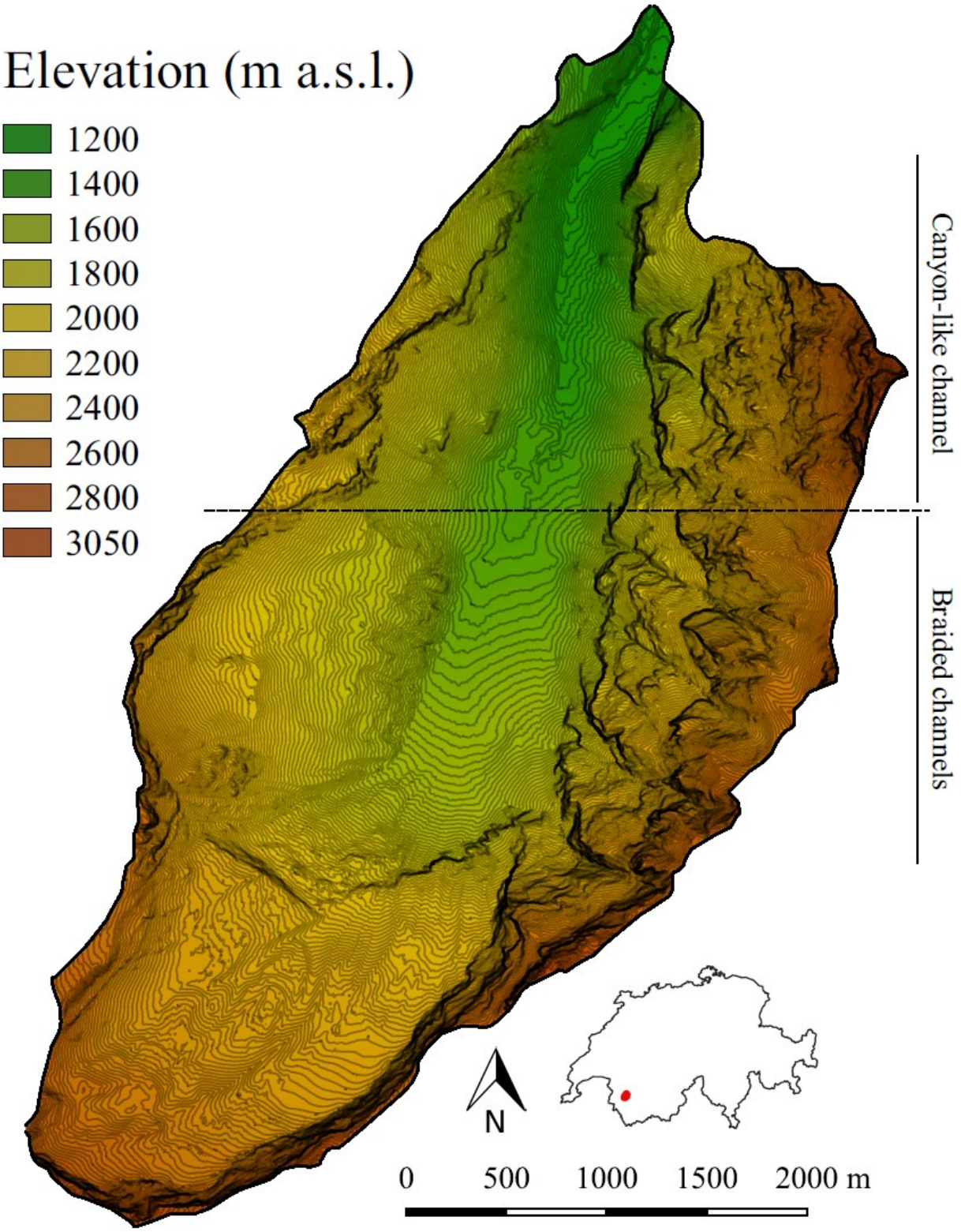

Figure 2:1 Topographic map of the study catchment, Vallon de Nant (Switzerland) with an elevation ranging from 1190 to 3051 m above sea level (a.s.l.). The geomorphological transition partitions the stream channels in an upstream braided system and a downstream canyon-like system. Shown are 10 m elevation contour lines derived from a digital elevation model, derived in QGIS 3.2.1 (QGIS Development Team, Switzerland) Data source: Geodata © Swisstopo.

2.3.2 Sampling design

We conducted sampling campaigns (2016) in winter (March), spring (May), summer (September) and autumn (November) and timed them to capture the seasonal hydrological variability typical for Alpine catchments. During each season, streamwater samples were collected during 3 to 4 days along the main channel and intermittent tributaries approximately every 50 to 80 m, starting from the catchment outlet, to a maximal length of 4500 m upstream depending on the network expansion. Hereafter, we refer to the various sampling sites as the linear distance upstream from the catchment outlet (i.e., from the most downstream site in our sampling sequence). We systematically restricted the sampling window and only sampled between 6 am and 12 am in order to avoid effects from diurnal fluctuations in streamwater chemistry owing to glacier ice melt and snowmelt later during the day. Moreover, we compared the daily fluctuations in streamwater temperature in the catchment outlet (measured every 10 minutes) to the instantaneous values measured during sampling to verify that we sampled well within that window of relative stability. During sampling in winter, large parts of the stream network were snow-covered, which precluded sampling in the reaches beyond a distance of 2700 m upstream from the outlet. During this time the stream network was at maximum contraction. During spring snowmelt, water flow in tributaries and locally emerging subsurface flow paths transiently expanded the network. In summer, glacier ice melt provided water flow to the stream reach directly downstream from the glacier, a channel which fell dry again in autumn. In autumn, various springs along the northwestern flank of the catchment contributed to stream flow in the main channel. The network behavior allowed us to collect streamwater samples from a total of 43 sites in late winter (March), 118 sites in spring (May), 75 sites in summer (September) and 64 sites in autumn (November); sampling sites along the main stem slightly differed between seasons.

2.3.3 Chemical composition of streamwater

Streamwater was collected from the thalweg to analyze a suite of parameters. Samples were stored in the dark (4˚C) pending analyses in the laboratory within 24 h. We also measured streamwater pH, temperature and specific conductivity (SC) in the field with daily calibrated WTW multi-parameter probes (Xylem Inc., USA).

We collected water samples for CO_2 concentration and isotopic composition ($\delta^{13}C\text{-}CO_2$). Duplicate samples were collected in glass vials (60 mL) that contained crystalized sodium azide (300 µL) for sample preservation[49]. In the field, vials were carefully submerged in the water to avoid bubble formation and turbulence-induced CO_2 loss, and while still submerged, the vials were sealed with rubber stoppers and metal caps. Back in the lab, a headspace with synthetic air (< 5 ppm CO_2) was created and the water phase and the headspace were equilibrated (2 hours)[49]. We measured the CO_2 concentrations and isotopic compositions using a cavity ring-down spectrometer (G2201-*i*, Picarro Instruments, USA). In the beginning and end of each laboratory day, we analyzed blanks with synthetic air to ensure that it contained less than 5 ppm of CO_2. At each sampling site in the field, we also sampled air into glass vials (60 mL) for the determination of atmospheric CO_2 using the same cavity ring-down spectrometer as above.

For dissolved inorganic carbon (DIC) concentrations and isotopic compositions ($\delta^{13}C\text{-}DIC$), streamwater was filtered directly in the field (0.47 µm nylon filter) into 40 mL glass vials (one vial per site). We assessed the possibility of degassing CO_2 because of filtration; the risk of underestimation of DIC was found to be small since DIC mostly consisted of HCO_3^- (97 ± 0.6 %) and the proportion of dissolved free CO_2 was 2.4 ± 0.7 % due to elevated streamwater pH (8.14 ± 0.12). For the measurements of DIC in the laboratory, we added 200 µL of 85 % orthophosphoric acid into empty glass vials, which we flushed with helium to avoid background CO_2. We then injected 1.5 mL of streamwater and equilibrated the samples for two hours in the helium headspace. Next, we measured DIC as the CO_2 released by the reaction with the orthophosphoric acid using isotope ratio mass spectrometry (Finnigan™ GasBench II, Thermo Finnigan DeltaPlus XL, USA)[93]. The measured values were normalized with an in-house standard, Carrara Marble II, which was analyzed in the beginning and the end of each sequence as well as dispersed throughout the sequence between every 8 to 10 samples.

Streamwater samples were also analyzed for DOC, alkalinity, major anions and cations and deuterium (δD) and oxygen ($\delta^{18}O$) stable isotopes. Samples for DOC analysis were filtered through double GF/F filters (Whatman) into 40 mL acid-washed and pre-combusted glass vials and analyzed within 1 to 3 days (Sievers M5310c TOC Analyzer, GE Analytical Instruments, USA). The accuracy of the instrument is ± 2 %, precision <1 % and detection limit 1.83 µmol C L^{-1} (N. Escoffier, personal communication). Non-filtered samples for the estimation of streamwater alkalinity were collected in 500 mL polyethylene bottles and analyzed by titration with 0.05 N HCl. For quality control, titrations were performed on freshly opened Evian© bottled water, which has a constant and known alkalinity. We performed the alkalinity measurements with both manual and automatic titration (916_Ti-touch automatic titrator, Metrohm, Switzerland). Concentrations of major anions and cations were measured on streamwater filtered through 0.22-µm filtered (Mixed Cellulose Ester) using ion chromatography (ICS-3000 Dionex, USA). Finally, values of streamwater δD and $\delta^{18}O$ were determined on filtered (0.47 µm) samples using a Picarro cavity ring-down spectrometer (L1102-i).

Discharge (Q) was estimated approximately every 300 m using slug additions of dissolved sodium chloride (NaCl) into the streamwater and measuring the changes of streamwater SC downstream. We established an empirical relationship between NaCl concentration and SC and calculated the discharge from the breakthrough curves[66]. We measured channel width at every sampling site to estimate the surface area of the stream network for each season. We also calculated streambed area between sites with Q measurements, from which we inferred areal specific stream discharge (Δq).

2.3.4 Data analysis

The relative contributions from groundwater, snowmelt and glacier ice melt (Table 2:1) were estimated using a Bayesian end-member mixing model with the *R* package *simmr*[94]. A dual tracer approach was used to achieve a two-dimensional plane of the potential water source contributions. Due to the similarity of the stable isotopic composition of groundwater and glacier ice melt, we performed mixing analyses using $\delta^{18}O$ as the first tracer and SC as the second tracer; these are common tracers for end-member mixing analyses[95]. The glacial stream end-member was sampled close to the glacier during summer (n = 12). Several nival tributaries were sampled during the spring campaign, across the stream network, and the $\delta^{18}O$ and SC of these sites served as the nival stream source (n = 27). The groundwater end-member values were obtained from a 5 m deep groundwater well installed in a large alluvial aquifer system below the braided reach 2800 m upstream. Groundwater is generally well mixed here and expected to be relatively stable in terms of its geochemistry (J. Thornton, personal communication). We received groundwater $\delta^{18}O$ data from this well in August 2017 and determined SC, pCO_2, DIC and isotopic compositions of CO_2 and DIC in October 2017.

Parameters	Glacial stream	Groundwater	Nival stream
$\delta^{18}O$ (‰ VSMOW)	-12.8 (0.03)	-12.7 (N/A)	-14.6 (0.16)
Specific Conductivity (µS cm^{-1})	165.6 (0.67)	272.0 (N/A)	138.1 (7.35)

Table 2:1 End-members for the mixing model; glacial stream (n = 12), groundwater (n = 1) and nival stream (n = 27). Values are means (standard deviations). Abbreviation: N/A, not available.

We used changepoint analysis[96,97] with the *R* package *changepoint*[96] to detect shifts in streamwater constituents along the main channel.

Sources of CO_2 and DIC were explored using Keeling[98] and Miller-Tans[99] linear mixing models. Both models are based on the assumption that the mixing of two different sources with different isotopic compositions create a two-dimensional space that can be described by a simple linear model (y = ax + b). The mass balances for CO_2 and $\delta^{13}C$-CO_2 (and correspondingly for DIC and $\delta^{13}C$-DIC) give the following relationship,

$$\delta^{13}C_M \times C_M = \delta^{13}C_S \times C_S + \delta^{13}C_B \times C_B$$

Equation 2:1 – Isotopic mass balance

where the measured isotopic composition ($\delta^{13}C_M$) and concentration (C_M) equal the sum of the isotopic composition and concentration of the source ($\delta^{13}C_S$ and C_S) and the background ($\delta^{13}C_B$ and C_B). $\delta^{13}C_S$ and C_S represent the sum of all carbon sources while $\delta^{13}C_B$ and C_B is the composition of atmospheric CO_2[98–100]. From Equation 2:1, the equations for the Keeling (Equation 2:2) and Miller-Tans (Equation 2:3) plots are derived as

$$\delta^{13}C_M = C_B(\delta^{13}C_B \times \delta^{13}C_S) \times (1/C_M) + \delta^{13}C_S$$

Equation 2:2 – Mixing model: Keeling

$$\delta^{13}C_M \times C_M = \delta^{13}C_S \times C_M - C_B(\delta^{13}C_B - \delta^{13}C_S)$$

Equation 2:3 – Mixing model: Miller-Tans

In the Keeling plot, the measured streamwater $\delta^{13}C$ is plotted against the inverse carbon concentration (1/C) where the y-intercept equals to the $\delta^{13}C$ of the source[98,101]. In the Miller-Tans plot, the observed isotopic ratio is multiplied by the concentration and expressed as a function of the measured concentration, where the slope represents the $\delta^{13}C_S$ value. Keeling and Miller-Tans models are based on linear mixing and we acknowledge that isotopic fractionation (e.g., during CO_2 evasion) can violate that assumption.

Therefore, additional to applying the Keeling and Miller-Tans models to the measured CO_2 and DIC concentrations and isotopic compositions, we also estimated CO_2 sources from theoretically calculated CO_2 concentrations (e.g., ref. [102]) and theoretically calculated isotopic compositions[56,103] (from DIC concentration, δ^{13}C-DIC and streamwater temperature) assuming an isotopic fractionation of δ^{13}C-CO_2 in equilibrium with DIC. Hence, we could better constrain the effect of CO_2 evasion for the estimation of CO_2 sources because rapid CO_2 evasion can drastically change its isotopic composition.

We estimated CO_2 evasion fluxes for winter, spring, summer and autumn, using seasonal median pCO_2 values combined with the empirical k_{600} equation from Ulseth and colleagues in 2019[54]. Briefly, we derived k_{600} from seasonal average energy dissipation (eD, $m^2\ s^{-3}$), where eD is a product of flow velocity (V, $m\ s^{-1}$), channel slope (S, $m\ m^{-1}$) and the gravitational acceleration ($m\ s^{-2}$) equation (2:4). To incorporate the large variation in stream channel slope along the stream network, and the potential impact slope might have on the resulting flux estimates, we used average stream channel slope (± standard deviation) for the calculations. Since eD was higher than 0.02 $m^2\ s^{-3}$ we used the equation established for turbulent and high-energy streams.

$$k_{600} = exp^{6.43+1.18 \times \ln(eD)}$$

Equation 2:4 – Normalized gas transfer velocity

k_{CO2} was then estimated from k_{600} using the Schmidt number scaling (Sc_{CO2})[104], which is temperature (T˚C) dependent, where the exponent of -0.5 is commonly used for turbulent water[105].

$$Sc_{CO2} = 1911.1 - 118.11 \times T + 3.4527 \times T^2 - 0.041320 \times T^3$$

Equation 2:5 – Schmidt scaling for CO_2

$$k_{CO2} = k600 \times \frac{Sc_{CO2}}{600}^{-0.5}$$

Equation 2:6 – Gas transfer velocity of CO_2

2.4 Results

2.4.1 Variation in discharge

Discharge in the main channel of the stream network varied seasonally and spatially (Figure 2:2). Average discharge was lowest during winter baseflow (70 L s^{-1}), increased tenfold and was highest in spring during snowmelt (970 L s^{-1}) to gradually decrease again during glacier ice melt in summer (230 L s^{-1}), and back to baseflow in autumn (140 L s^{-1}). Along the mainstem, discharge increased markedly around 2800 m upstream where the braided channels transited into constrained canyon-like channel (Figure 2:1). Here, the specific discharge was 1.30, 0.25 and 0.13 L m^{-2} s^{-1} in spring, summer and autumn, respectively; changes in specific discharge could not be estimated in winter because of snow cover. The spatial variation in discharge downstream of this gaining reach was generally low.

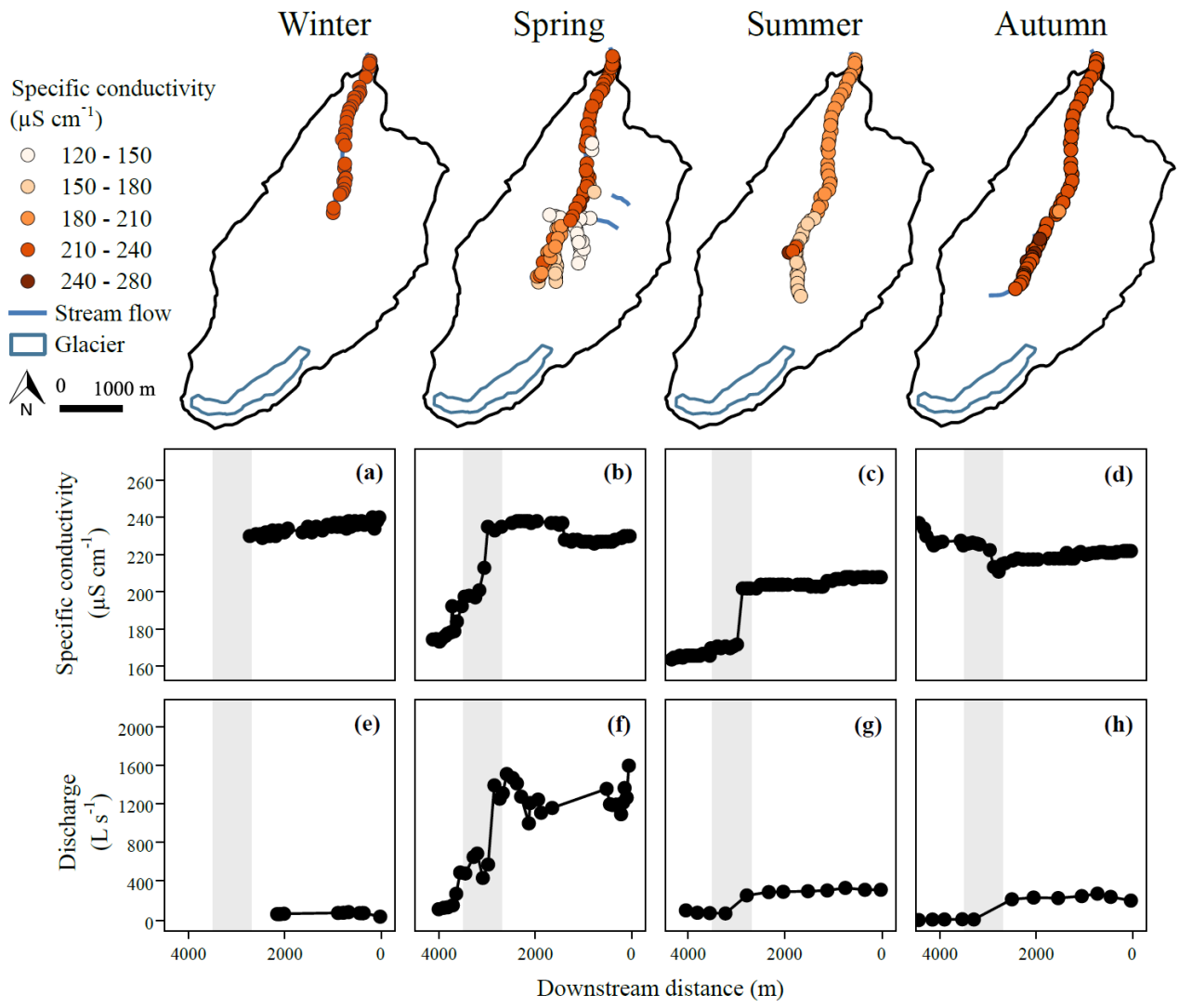

Figure 2:2 Samples were taken every 50 m along the nivo-glacial headwater stream network, during winter, spring, summer, and autumn. The circles specify each sampling location during the four campaigns. The steam network expanded and contracted throughout the year. A distinct increase in specific conductivity (maps and panel a-d) is noted approximately 2800 m (± 100 m) upstream, in a braided stream segment. This corresponds to an increase in discharge (e-h) in the same stream segment.

2.4.2 Spatial and seasonal variations in source contributions to stream flow

Contributions from groundwater, glacial ice melt and snowmelt to streamflow changed seasonally and were linked to the expansion and contraction dynamics of the stream network. The end-member mixing analysis showed that groundwater was the dominant source of water in winter, spring and autumn (Figure 2:3). Groundwater was relatively stable downstream (< 2800 m) from the braided reach, with contributions of 65.5 ± 2.8, 61.8 ± 2.9, 40.8 ± 1.5, and 54.1 ± 2.1 % in winter, spring, summer and autumn, respectively. No mixing model estimates were computed for the upstream reaches (> 2800 m) in winter because of the lack of data owing to the snow cover. In spring, however, groundwater contributions were lower in the upstream reaches (34.2 ± 12.2 %) compared to downstream reaches, while snow melt contributed 58.1 ± 10.8 % to the stream flow upstream. In summer, glacier ice melt was the primary source (92.2 ± 18.5 %) to streamwater flow in reaches above 2800 m. Owing to lateral groundwater upwelling, glacier ice melt contributed only 45.4 ± 6.2 % to the streamflow in the downstream reaches. During autumn, groundwater contributed on average 45.9 ± 23.9 % to the streamflow in the upstream reaches (2800 m) and were relatively constant along the mainstem.

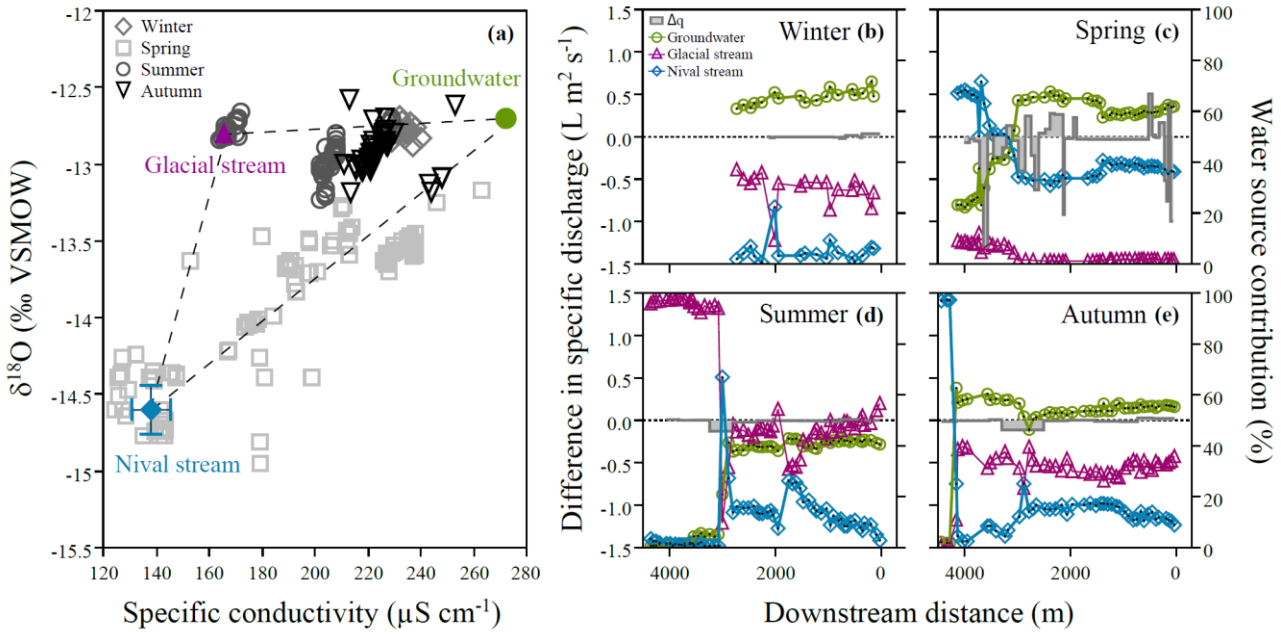

Figure 2:3 $\delta^{18}O$ values and specific conductivity of the streamwater sources and of the water collected along the stream network across the four seasonal sampling campaigns. The dashed line indicates the 2-dimensional space between the three identified water source contributions as obtained from the Bayesian mixing model; groundwater, glacial stream flow and nival stream flow (a). Water source contribution and difference in specific stream discharge (Δq) varied across winter (b), spring (c), summer (d), and autumn (e). The difference in specific discharge (Δq) was highest in the braided stream reach, where groundwater contributions increased in spring and summer.

2.4.3 Spatial and seasonal CO_2 dynamics

Streamwater pCO_2 averaged 634 ± 108 µatm during the study year and varied seasonally and spatially along the mainstem of the stream network (Figure 2:4; Table 2:2). Streamwater was supersaturated in CO_2 with respect to the atmosphere for 92 % of all sample sites across the stream network and over all four seasons (n=247). In the mainstem, streamwater CO_2 supersaturation was observed in 93 % of the sampling sites (n=159). The maximum streamwater pCO_2 (1305 µatm) was measured in a spring-fed stream draining into the braided reach (2800 m); the lowest pCO_2 was sampled in a snowmelt-fed tributary during spring (309 µatm). Of all streamwater samples, 8 % were undersaturated in CO_2 with respect to the atmosphere. The undersaturation was observed in nival tributaries in spring (13 % undersaturation) and in the reaches closest to the glacier in summer. The sites with CO_2 undersaturation had one commonality: low concentration of calcium ions, low DIC concentrations and an enriched $\delta^{13}C$-CO_2 and $\delta^{13}C$-DIC isotopic compositions. A possible explanation for this CO_2 undersaturation is carbonate buffering in the stream, where snow and ice meltwater, low in CO_2, mix with the streamwater. DIC represented the vast majority of the total dissolved carbon (DIC and DOC) in the streamwater (99.0 ± 0.8 % across the stream network). Of the DIC species (CO_2, HCO_3^- and CO_3^{2-}) CO_2 accounted for 2.9 ± 0.6 % of the DIC given the high pH (8.14 ± 0.12).

Streamwater DOC concentration averaged 0.011 ± 0.003 mmol C L^{-1} in the mainstem across all seasons; it was highest in spring (0.017 ± 0.004 mmol C L^{-1}) and lowest in summer (0.006 ± 0.001 mmol C L^{-1}). The largest spatial variation in DOC concentration was observed in spring, when DOC concentration in snow-fed tributaries (0.026 ± 0.010 mmol C L^{-1}) was up to 66 % higher than in the mainstem. Linear regression analysis detected a weak positive relationship between streamwater DOC concentration and pCO_2 for all sites along the mainstem and across all four seasons (R^2 = 0.17, p < 0.0001); however, when including the tributaries, there was no relation between DOC concentration and pCO_2 (R^2 = 0.0005, p > 0.05). Streamwater DIC concentration was positively related to pCO_2 across all mainstem sites and seasons (R^2 = 0.26, p < 0.0001), and across the entire network (R^2 = 0.33, p < 0.0001). Streamwater DIC concentration was related to pCO_2 in spring (R^2 = 0.59, p < 0.0001) and summer (R^2 = 0.42, p < 0.0001), but not in winter and autumn.

Furthermore, the isotopic composition of DIC and CO_2 varied spatially and across seasons (Figure 2:4). δ^{13}C-DIC was negatively related to streamwater pCO_2 for all mainstem sites (R^2 = 0.49, p < 0.0001), and also for the entire stream network (R^2 = 0.42, p < 0.0001). δ^{13}C-CO_2 was negatively related to streamwater pCO_2 for all mainstem sites (R^2 = 0.49, p < 0.0001) and for the entire stream network (R^2 = 0.45, p < 0.0001). The theoretically calculated δ^{13}C-CO_2 values (i.e., estimated from DIC concentration, δ^{13}C-DIC and temperature) were negatively related to streamwater pCO_2 for all mainstem sites (R^2 = 0.66, p < 0.0001) and the entire stream network (R^2 = 0.39, p < 0.0001). In spring, δ^{13}C-DIC (R^2 = 0.68, p < 0.0001), measured δ^{13}C-CO_2 (R^2 = 0.74, p < 0.0001) and calculated δ^{13}C-CO_2 (R^2 = 0.66, p < 0.0001) were all inversely related to pCO_2. Those three parameters were also significantly (p < 0.0001) related with pCO_2 in summer (R^2 = 0.41, R^2 = 0.38 and R^2 = 0.39, respectively). No corresponding relationships were observed in winter or autumn.

Season	Mainstem sampling sites	Mean pCO_2 (µatm)	Mean DOC (mmol L^{-1})	Mean DIC (mmol L^{-1})	Mean δ^{13}C-DIC (‰VPDB)	Mean δ^{13}C-CO_2 (‰VPDB)	Mean Atm. CO_2 (µatm)
Winter	35	671 (74)	0.011 (0.001)	1.645 (0.152)	-5.02 (0.39)	-10.69 (0.79)	404 (16)
Spring	49	744 (146)	0.017 (0.004)	1.733 (0.323)	-5.76 (1.34)	-11.15 (1.16)	402 (18)
Summer	61	544 (133)	0.006 (0.001)	1.331 (0.272)	-4.39 (0.81)	-8.91 (1.84)	405 (25)
Autumn	46	578 (78)	0.011 (0.004)	1.890 (0.203)	-5.08 (0.70)	-10.23 (1.02)	399 (13)
Yearly	190	634 (108)	0.011 (0.003)	1.649 (0.237)	-5.06 (0.81)	-10.25 (1.20)	402 (3)

Table 2:2 Dissolved organic and inorganic carbon concentrations, isotopic values of DIC, CO_2, and pCO_2. Values are seasonal means (standard deviations). Abbreviations: DOC, dissolved organic carbon; DIC, dissolved inorganic carbon; VPDB, Vienna Peedee belemnite.

Change point analyses detected spatial shifts in streamwater pCO_2 and related chemical constituents. In winter, spatial shifts were detected at 1600 m and 2600 m from the outlet where decreasing streamwater pCO_2 was associated with an increase in pH and enrichment in isotopic compositions of CO_2 and DIC. These changes indicate local upwelling of groundwater delivering CO_2 to the stream. Similarly, in summer, we identified a local increase in streamwater pCO_2 at 3000 m, which was associated with elevated SC, alkalinity and calcium concentrations, and with more depleted δ^{13}C-CO_2 values. In autumn, decreases in pCO_2 at 2600 m and 300 m were associated with an increase in pH and an enrichment in the isotopic compositions of CO_2 and DIC. Interestingly, this spatial pattern with local upwelling was not pronounced in spring. Rather, there was a gradual increase in pCO_2 along the braided channels (Figure 2:4), which was associated with increases in streamwater temperature, SC, pH, alkalinity and calcium concentrations, but also with more depleted isotopic compositions of CO_2 and DIC.

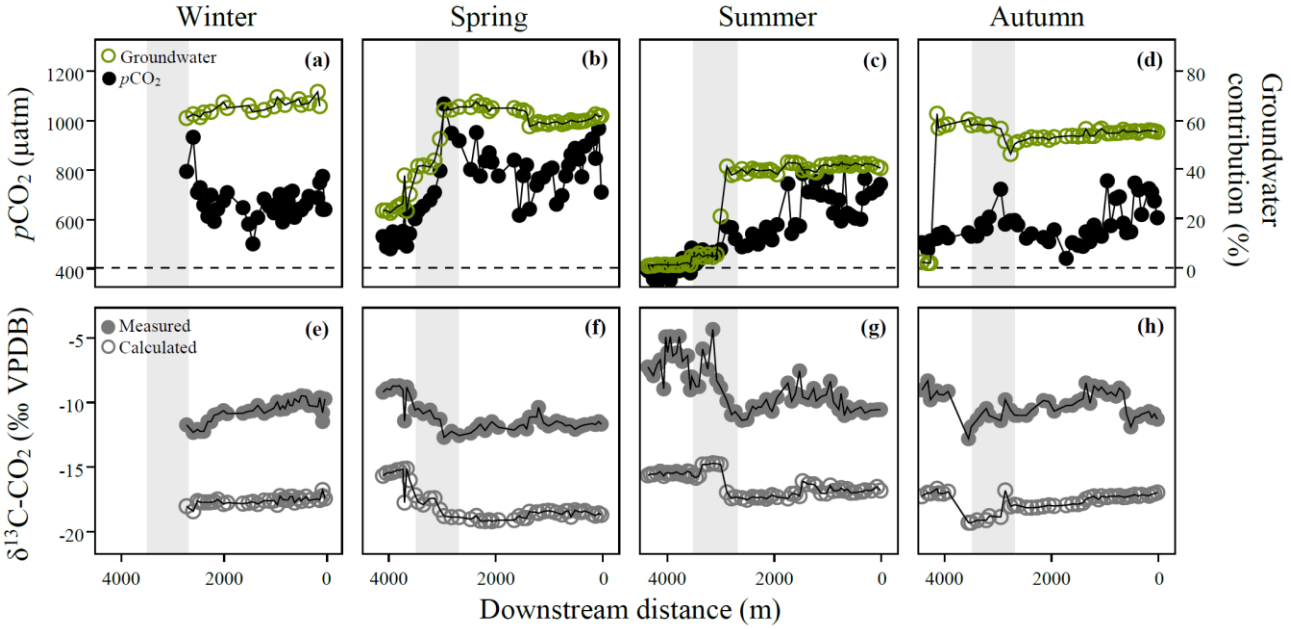

Figure 2:4 Spatial variations in pCO_2 and groundwater contributions (upper row, a-d), and measured and calculated $\delta^{13}C\text{-}CO_2$ (lower row, e-h). The mainstem streamwater pCO_2 varied across winter (a), spring (b), summer (c), and autumn (d). The groundwater contributions increased in the braided stream segment during spring and summer (marked with a grey band) simultaneously as the isotopic compositions of CO_2 became more depleted in ^{13}C. The calculated isotopic compositions of CO_2 followed the same spatial dynamic patterns as the measured isotopic compositions of CO_2.

2.4.4 Sources of streamwater CO_2

Relative groundwater contributions to the streamflow coincided with elevated streamwater pCO_2 for all data pooled across seasons ($R^2 = 0.47$, $p < 0.0001$) (Figure 2:5, a); it was not significantly related to streamwater pCO_2 in winter or autumn, but in spring (mainstem: $R^2 = 0.73$, $p < 0.0001$; braided reach: $R^2 = 0.93$, $p < 0.0001$) and in summer (mainstem: $R^2 = 0.66$, $p < 0.0001$; braided reach: $R^2 = 0.66$, $p < 0.01$). Streamwater pCO_2 was inversely related to the relative snowmelt contributions in spring ($R^2 = 0.74$, $p < 0.0001$). Streamwater pCO_2 was also inversely related to the relative glacier ice melt in spring ($R^2 = 0.56$, $p < 0.0001$) and summer ($R^2 = 0.51$, $p < 0.0001$). Across all seasons, relative groundwater contributions were negatively related to streamwater $\delta^{13}C$-DIC ($R^2 = 0.62$, $p < 0.0001$), suggesting groundwater as a major source of DIC. Relative groundwater contributions were also negatively related to streamwater $\delta^{13}C\text{-}CO_2$ ($R^2 = 0.59$, $p < 0.0001$) (Figure 2:5, b) and to the theoretically calculated $\delta^{13}C\text{-}CO_2$ ($R^2 = 0.68$, $p < 0.0001$) (Figure 2:5, c), suggesting that groundwater was also an important CO_2 source to the streamwater.

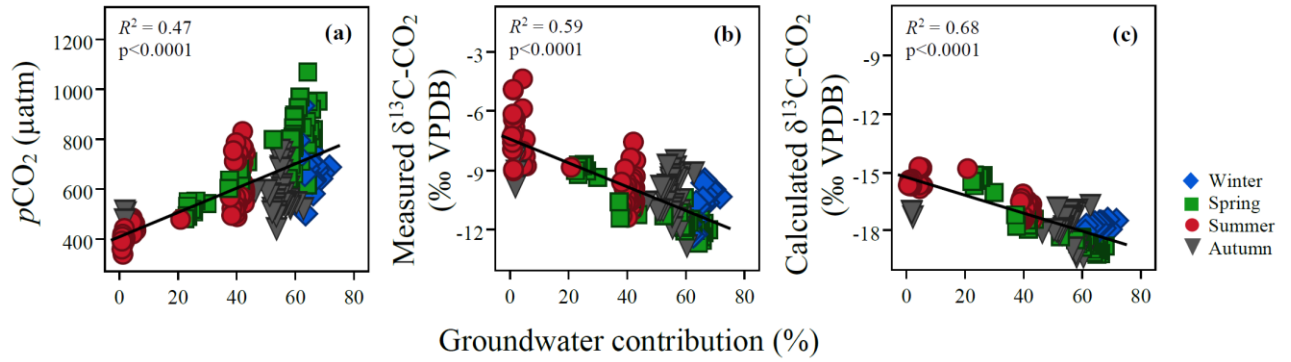

Figure 2:5 Groundwater contributions were significant positively related to pCO_2 (a), and significantly negatively related to measured $\delta^{13}C\text{-}CO_2$ (b) and calculated $\delta^{13}C\text{-}CO_2$ as (CO_2 in equilibrium with dissolved inorganic carbon) (c).

The results obtained from the Miller-Tans and Keeling linear mixing models suggest that the DIC sources to the stream-water were enriched in ^{13}C. An equal contribution from abiotic CO_2 originating from carbonate bedrock dissolution/precipitation (i.e., 0 ‰[90]) and heterotrophic and autotrophic soil respiration (approximated to -21.5 ‰, calculated from groundwater $\delta^{13}C$-DIC values,

DIC concentration and temperature) would imply a δ^{13}C-DIC value of -10.8 ‰. However, measured streamwater δ^{13}C-DIC source estimates (from Miller-Tans and Keeling plot averages) deviated from this prediction and changed seasonally from -4.9 to -11.2 ‰ (Figure 2:6, Table 2:3). Linear mixing suggests that carbonate bedrock weathering likely was the dominant DIC source throughout the year, comprising 72, 48, 66, and 76 % of the DIC source in winter, spring, summer and autumn, respectively. The DIC sources did not only vary temporally. They also varied spatially with DIC in the braided reach being isotopically more depleted in ^{13}C (annual mean of -9.45 ± 0.69 ‰, most ^{13}C depleted in spring with -10.20 ‰) than the downstream reaches (annual mean -5.57 ± 1.33 ‰, most enriched in autumn with -4.44 ‰) and upstream reaches (annual mean -4.59 ± 1.34 ‰, most enriched in summer with -3.09 ‰).

Season	Model	n	Equation	DIC source (‰VPDB)	R^2	Std. error	*p*-value
Winter	Miller-Tans	35	δ^{13}C-DIC x [DIC] = - 4.72 x [DIC] - 0.49	-4.72	0.54	0.76	<0.0001
	Keeling		δ^{13}C-DIC = 0.21 x 1/[DIC] - 5.15	-5.15	0.0009	0.76	<0.0001
Spring	Miller-Tans	49	δ^{13}C-DIC x [DIC] = -10.96 x [DIC] + 8.66	-10.96	0.94	0.40	<0.0001
	Keeling		δ^{13}C-DIC = 9.43 x 1/[DIC] - 11.42	-11.42	0.80	0.42	<0.0001
Summer	Miller-Tans	61	δ^{13}C-DIC x [DIC] = -7.40 x [DIC] + 3.83	-7.40	0.91	0.31	<0.0001
	Keeling		δ^{13}C-DIC = 3.85 x 1/[DIC] - 7.42	-7.42	0.67	0.28	<0.0001
Autumn	Miller-Tans	46	δ^{13}C-DIC x [DIC] = -5.39 x [DIC] + 0.59	-5.39	0.40	0.99	<0.0001
	Keeling		δ^{13}C-DIC = -0.14 x 1/[DIC] - 5.01	-5.01	0.0002	0.81	<0.0001

Table 2:3 Equations and DIC source estimates obtained from the Miller-Tans and Keeling plots. The standard errors and *p*-values represent the accuracy of the slopes (Miller-Tans) and intercepts (Keeling). Abbreviation: DIC, dissolved inorganic carbon.

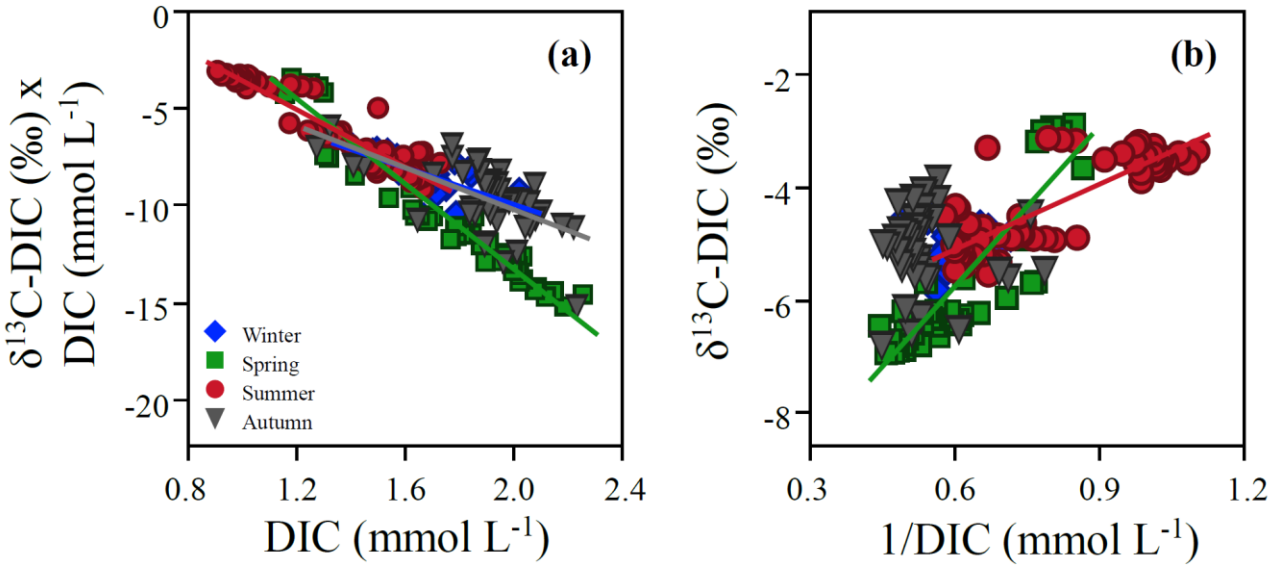

Figure 2:6 Estimation of the isotopic composition of the DIC sources by season (winter, spring, summer and autumn). The isotopic composition of the carbon source is the slope of the linear regression in the Miller-Tans plot (a) and the intercept with the y-axis in the Keeling plot (b). The Miller-Tans and Keeling plots indicate a DIC source enriched in ^{13}C in winter relative to a more depleted source in spring. In summer, the isotopic composition of the DIC source becomes more ^{13}C enriched and in autumn the ^{13}C source composition is similar to the composition in winter. All plots were significant ($p < 0.0001$).

The annual mean isotopic composition of the CO_2 source was -13.23 ± 2.28 ‰ (Miller-Tans) and -13.50 ± 2.56 ‰ (Keeling). The isotopic composition of the source was more enriched in winter (-12.41 ± 1.39 ‰) and autumn (-10.72 ± 2.13 ‰) than in spring (-15.96 ± 0.26 ‰) and summer (-14.37 ± 0.35 ‰) (Figure 2:7, Table 2:4). This suggests that a relevant contribution of CO_2 from soil respiration to the streamwater across all seasons (58, 74, 67, and 50 % in winter, spring, summer and autumn, respectively). Similar spatial isotopic variation as for the DIC sources could be seen for CO_2 sources, where CO_2 in the braided reach was isotopically more depleted in ^{13}C (annual mean of -15.59 ± 3.58 ‰) than in the downstream (annual mean of -10.47 ± 2.11 ‰) and upstream (annual mean of -10.95 ± 3.07 ‰) reaches. Using linear mixing, we estimated the mean annual contribution of respiratory soil CO_2 to streamwater to 73 ± 0.2 %. However, all above estimates were likely influenced by atmospheric exchange. In fact, the theoretically calculated δ^{13}C-CO_2 was more depleted in ^{13}C compared to the measured δ^{13}C-CO_2, which suggests that the CO_2 is not in equilibrium with the rest of the DIC species. It also implies that a proportion of the CO_2 measured in the stream may originate from the speciation within

the carbonate equilibria, such as weathering-derived carbon with a heavier isotopic composition. Applying the Miller-Tans and Keeling mixing models on the theoretically calculated CO_2 concentrations and isotopic compositions resulted in CO_2 source estimates substantially more depleted in ^{13}C compared to the models applied to the measured values (Miller-Tans: -19.08 ± 1.95 ‰; Keeling: -18.97 ± 2.25) (Figure 2:7, Table 2:4). CO_2 evasion can shift $\delta^{13}C$-DIC isotopic compositions by 1 to 4 ‰[82] and thereby bias those estimates. However, a more depleted DIC would reflect an even higher ^{13}C depletion of the CO_2. Thus, source estimates based on those 'pre-evaded' theoretically calculated $\delta^{13}C$-CO_2 revealed that respiratory soil CO_2 most likely contribute to the vast majority of the CO_2 in the streamwater. As estimated by linear mixing from the theoretically calculated $\delta^{13}C$-CO_2 values, the mean annual contribution of respiratory soil CO_2 to streamwater CO_2 was 88 ± 0.1 %, while the remaining CO_2 originated from weathered products by conversion of HCO_3^- to CO_2 due to the speciation within the carbonate equilibria.

		Miller-Tans		Keeling		Mean (± std.)
	Season	Slope $\delta^{13}C$-CO2 x $[CO_2]$ vs. $[CO_2]$	Slope $\delta^{13}C$-CO_2 x [DIC] vs. [DIC]	Intercept $\delta^{13}C$-CO_2 vs. 1/$[CO_2]$	Intercept $\delta^{13}C$-CO_2 vs. 1/[DIC]	CO_2 source
Measured	Winter	-11.97	-12.85	-10.77	-14.05	-12.41 (± 1.39)
	Spring	-15.79	-15.71	-16.29	-16.03	-15.96 (± 0.26)
	Summer	-14.09	-14.11	-14.83	-14.43	-14.37 (± 0.35)
	Autumn	-12.55	-8.75	-12.56	-9.00	-10.72 (± 2.13)
Calculated	Winter	-18.35	-17.01	-17.76	-17.21	-17.58 (± 0.60)
	Spring	-20.28	-23.12	-20.86	-23.54	-21.95 (± 1.62)
	Summer	-18.94	-19.45	-18.31	-19.42	-19.03 (± 0.53)
	Autumn	-17.49	-17.96	-16.86	-17.76	-17.52 (± 0.48)

Table 2:4 Estimate of the CO_2 source isotopic compositions obtained from the Miller-Tans and Keeling plots. Both the CO_2 concentrations and the total DIC concentrations were used, to reduce potential errors caused by decreasing concentrations due to loss of CO_2 to the atmosphere. All plots were significant ($p < 0.0001$).

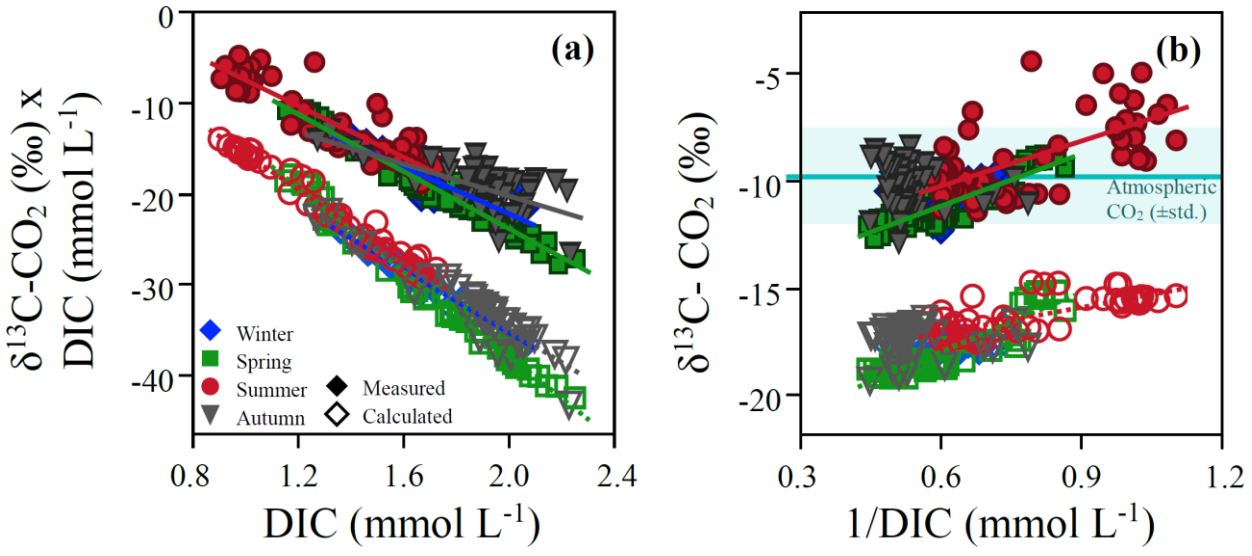

Figure 2:7 Estimation of the isotopic composition of the CO_2 sources by season (winter, spring, summer and autumn). Measured $\delta^{13}C$-CO_2 (full symbols) were higher than $\delta^{13}C$-CO_2 calculated from $\delta^{13}C$-DIC, DIC concentration and temperature (open symbols). The annual mean isotopic composition of the CO_2 source, predicted by Miller-Tans (a) and Keeling (b) plots, were -13.36 ± 2.35 ‰ and -19.02 ± 2.04 ‰ for the measured and calculated $\delta^{13}C$-CO_2 source respectively. All plots were significant ($p < 0.0001$).

2.4.5 Fate of streamwater CO_2

We observed a longitudinal pattern in streamwater $\delta^{13}C\text{-}CO_2$ with more depleted values in the braided reach compared to those downstream from the valley nexus (Figure 2:4). $\delta^{13}C\text{-}CO_2$ became rapidly enriched (on average 6.9 ± 1.3 %) within 500 m downstream from the braided reach. Across all seasons, the source of CO_2 in the mainstem was generally enriched by 1.62 ‰ (estimated from measured $\delta^{13}C\text{-}CO_2$) and 1.73 ‰ (estimated from calculated $\delta^{13}C\text{-}CO_2$) ($p < 0.0001$ for all seasons) compared to the braided reach; this translates into an enrichment by 10 and 8 %, for the measured and calculated samples respectively. Similarly, there was a ^{13}C enrichment of the DIC source downstream of the groundwater discharge zone (on average by 1.7 ‰ for the Miller-Tans and Keeling plots, $p < 0.0001$ for all seasons). The difference in isotopic compositions (both $\delta^{13}C\text{-}CO_2$ and $\delta^{13}C\text{-DIC}$) between the braided reach and downstream reaches can be attributed to the loss of ^{12}C due to CO_2 evasion. In fact, the ^{13}C enrichment downstream from the groundwater upwelling zone in the braided reach (where isotopic data suggest additions of biogenic carbon to the stream) coincided with a decrease in pCO_2 (12 to 27 % within 500 m downstream from the braided reach) and a simultanous increase in pH (with 2.1 to 2.9 %). This implies a loss of CO_2 and a subsequent shift in the carbonate equilibria.

Due to the high channel slope (0.093 ± 0.033 m m^{-1}) and high flow velocity (0.51–0.79 m s^{-1}), we found areal CO_2 evasion fluxes, which were on average eight times higher as those reported from other headwater streams (Table 2:5). In fact, areal CO_2 evasion fluxes averaged across the entire stream network 32.1 (19.1–45.9), 48.9 (29.1–69.9), 17.8 (10.6–25.5), and 21.7 (12.9–31.0) µmol m^{-2} s^{-1} in winter, spring, summer and autumn, respectively. Across all seasons, this gives a mean CO_2 evasion flux of 30.1 (18.0–43.1) µmol m^{-2} s^{-1} (Table 2:5). However, areal CO_2 evasion fluxes were even higher in the reaches with significant groundwater upwelling. For instance, in spring, we calculated CO_2 evasion fluxes from the braided stream reach to be more than 15-fold higher (477 µmol m^{-2} s^{-1}) compared to the seasonal mean. We estimated the mean areal CO_2 evasion fluxes from the entire stream network at 237 (141–339), 2793 (1069–2565), 299 (179–428) and 344 (205–493) kg C d^{-1} for winter, spring, summer and autumn, respectively. These fluxes translate into an annual CO_2 evasion flux of 244 (145–349) tons of C from the entire stream network. We estimate an average DIC export flux to be in the same order of magnitude as the CO_2 evasion flux (115, 1692, 302 and 327 kg C d^{-1} for winter, spring, summer and autumn, respectively); this translates into an annual DIC export flux of 222 tons of C from the entire stream network.

Location	pCO_2 (µatm)	CO_2 flux (µmol C m^{-2} s^{-1})	Reference
Switzerland, Alpine stream	634	30.1	This study
Austria, Alpine streams	794	3.12	*Schelker et al. (2016)*
Alaska, USA, boreal stream	1417	5.21	*Crawford et al. (2013)*
Wyoming, USA, alpine streams	391	-0.02	*Kuhn et al. (2017)*
Tibetan Plateau, China, high altitude rivers	982	5.16	*Qu et al. (2017)*
Loess Plateau, China, river	1068	1.86	*Ran et al. (2017)*
Sweden, 1st order streams	1445	8.00	*Humborg et al. (2010)*

Table 2:5 Comparison of pCO_2 and CO_2 evasion rates from headwater streams.

2.5 Discussion

High-resolution spatial sampling revealed the importance of catchment geomorphology and stream network expansion and contraction for streamwater pCO_2 and CO_2 evasion dynamics in an Alpine headwater stream. Catchment geomorphology is characterized by steep valley slopes confining a wide valley bottom with braided stream channels, which transit into a canyon-like channel contained within a constrained valley. This geomorphological shift caused significant groundwater upwelling thereby increasing downstream discharge. We argue that this upwelling front constitutes a control point[73] disproportionately controlling stream ecosystem processes and biogeochemistry. Our results highlight the variability of such a control point in space and time as associated with the seasonal expansion and contraction of the stream network, following the nivo-glacial hydrological regime. The influence of the control point was most pronounced during spring snowmelt when hydrological connectivity through various subsurface and surface flow paths increased stream network expansion with marked implications for streamwater biogeochemistry.

Across all seasons, the carbonate rock that dominates the catchment geology markedly contributed to streamwater DIC as indicated by its isotopic composition of -7 ‰. Elevated streamwater DIC concentration and hence elevated pH shifted the carbonate equilib-

rium towards bicarbonate and carbonate species. Thus, despite high DIC concentration, the streamwater remained only slightly supersaturated in CO_2 with respect to the atmosphere. Our findings suggest that streamwater CO_2 originates mostly from soil respiration; this is in line with findings from a boreal stream network[107], and small North American[47] and Amazonian headwater streams[108]. Our findings also agree with those from Butman & Raymond in 2011[71] reporting high contributions from soil respiration to CO_2 evasion fluxes from streams and rivers in the conterminous USA, where soil respiration contributed with 17-25 % to the evasion flux from streams and rivers, and up to 90 % from first-order streams. Our observations are also supported by previously reported respiration rates in the soils adjacent to the braided stream reaches (2800 m). In fact, Grand and colleagues in 2016[109] measured soil respiration rates in this area which were twice as high as the average (10 µmol C m^{-2} s^{-1}) in the Vallon de Nant catchment.

During stream network expansion, increasing groundwater upwelling can deliver more respiratory CO_2 from the soils to the stream. In contrary, our results suggest that direct snowmelt transported by surface runoff did not contribute to streamwater pCO_2 nor did snowmelt increase streamwater DOC concentration, as was previously reported from other studies (e.g., ref. [110]). Contrary to previous findings from boreal streams, rivers and lakes[107,111], we did not find any clear evidence that streamwater DOC could contribute to pCO_2 through ecosystem respiration.

We suggest that the remarkably low DOC concentrations together with low residence times typical for high-altitude and high-slope streams and high CO_2 evasion rates makes it difficult to detect and quantify CO_2 originating from stream ecosystem respiration. We used a mass balance approach to trace the potential contribution of stream ecosystem respiration to the streamwater δ^{13}C-DIC composition. To estimate δ^{13}C-DOC values, we subtracted 20 ‰ from the δ^{13}C-DIC (e.g., ref. [90]). Next, we inferred from mass balance equations (e.g., Equation 2:1, rewritten as the isotopic composition multiplied with concentration for DIC, DOC and DIC+DOC) that DOC could potentially enrich the δ^{13}C-DIC by 0.14 ± 0.07 ‰. To enrich δ^{13}C-DIC by 1 ‰, an additional 0.08 ± 0.02 mmol L^{-1} DOC would be required. This additional DOC would translate into an increase in the annual mean DOC concentration by 86.4 %. This approximation suggests that stream ecosystem respiration contributed only marginally to the observed streamwater pCO_2, which is in general agreement with results from a large spatial survey on the CO_2 dynamics in streams throughout the USA[38]. We argue that this apparent difference is attributable to both low biomass and low residence times typical for high-altitude and high-slope streams.

We do acknowledge that our approach based on stable isotopes can be considered as an approximation alone and is prone to large uncertainties. Furthermore, the rapid evasion of groundwater-derived CO_2 from the stream may lead to erroneous estimates of streamwater CO_2 concentration and isotopic composition as grab samples may represent streamwater that is already degassed[67]. Rapid CO_2 evasion may explain the concordance between the calculated 'pre-evasion' streamwater δ^{13}C-CO_2 and the measured values in groundwater, and between the measured streamwater δ^{13}C-CO_2 and atmospheric δ^{13}C-CO_2.

The high CO_2 evasion fluxes from the stream network were unexpected given that high-altitude streams typically have low pCO_2 and therefore low CO_2 evasion fluxes[47]. Our high-resolution sampling along the stream network identified local groundwater upwelling as a significant contributor to the areal annual CO_2 evasion fluxes. Control points mediated by the local geomorphology induced CO_2 evasion rates that were up to 60 times higher than those reported for boreal 1st-order streams[43]. This is remarkable given that the overall streamwater pCO_2 was lower than in most boreal streams[43,80]. Rather, streamwater pCO_2 in the Vallon de Nant catchment was often close to atmospheric equilibrium and bracketed by values reported from other high-altitude streams in Austria[49], USA[50] and China[48,106]. Although, the Vallon de Nant catchment stream network CO_2 evasion fluxes were orders of magnitude higher than those found in other high-altitude streams (Table 2:5), this difference was likely due to the high contribution of CO_2 from the control point along the stream network, along with the high gas-exchange. Therefore, higher gas transfer velocity rates rather than increased streamwater pCO_2 drove the observed high evasion rates within the braided reach. We acknowledge that our estimates of CO_2 evasion rates may be biased by incorrect model assumptions of the gas transfer velocity model, but since there are only very few models established for high-energy mountain streams, we consider applying the gas transfer velocity model from Ulseth and colleagues in 2019[54] to be more accurate than applying models established from large low-land rivers, such as one of the commonly used equations from Raymond and colleagues in 2012[52]. Crawford and colleagues in 2015[47] found the opposite pattern, where the equations from[52] may have led to an overestimation of the CO_2 evasion fluxes. However, the region studied in that paper was significantly different from the stream network in this study; due to the carbonate bedrock and the inputs from soil respiration, our stream network was most likely not limited by supply, as the streams studied in a study by Crawford and colleagues in 2015[47] where the streamwater pCO_2 commonly indicated undersaturation. In our study, streamwater CO_2 supersaturation within the braided reach, despite high gas transfer velocity rates, highlights the role of groundwater upwelling for the CO_2 delivery into the stream.

Our spatially highly resolved sampling allowed us to capture small-scale variations in streamwater pCO_2 and to detect control points driving CO_2 evasion fluxes at the scale of the stream network. Grab samples confined to a few individual reaches may underestimate the actual evasion fluxes at the network scale. This finding corroborates a recent study by Duvert and colleagues in 2018[37] highlighting the relevance of groundwater for the CO_2 dynamics in temperate, boreal and tropical streams.

Headwater streams comprise most of the drainage length in fluvial networks[35] and can expand and contract as a response to catchment hydrology[112]. These properties have major implications for the exchange fluxes at the terrestrial-aquatic interface[113], especially when considering the diverse surface and sub-surface flow paths connecting the stream to its terrestrial environment in small catchments[114]. Understanding the implications of this hydrological connectivity on stream biogeochemistry may therefore contribute to an enhanced understanding on spatial and temporal variability of CO_2 sources and evasion fluxes[34,37]. In the Vallon de Nant catchment, the stream network covered a four times larger surface area during the expansion in spring (35,300 m^2) compared to winter (7,100 m^2). Network expansion during spring snowmelt increased the hydrological connectivity to the groundwater and thereby the delivery of CO_2 from soil respiration and calcareous rock weathering that has likely accumulated during winter under the snowpack (similar as suggested by ref. [37]). At the same time, the magnification of the stream surface area at the interface to the atmosphere in combination with increased discharge (and turbulence) increased the CO_2 evasion flux to be 10 times larger in spring compared to winter.

Our results on the role of stream network dynamics for CO_2 sources and evasion also emphasize that we need to better apprehend the lateral carbon flux across the terrestrial-aquatic interface[18], which is at the basis of the 'boundless carbon cycle' across ecosystem boundaries[15]. This is imperative to understand future impacts of climate change on ecosystem processes and biogeochemistry of high-altitude streams. In fact, climate-induced changes of catchment hydrology are expected to impact the movement of inorganic and organic carbon from the terrestrial environment to streams[115]. Owing to the low soil buildup and the prevalence of bare rock, the terrestrial delivery of inorganic carbon species dominates over DOC deliveries to streams in high-altitude catchments – a relationship that may change in the future as vegetation cover moves uphill. This consideration would also imply an integrative view of the speciation of CO_2, HCO_3^- and CO_3^{2-} within the carbonate system to better quantify and predict the carbon balance at catchment level[115]. For instance, in the Vallon de Nant catchment, streamwater CO_2 constituted on average only 2.9 % of the DIC pool, most likely because of an average pH of 8.14. Downstream transformation of HCO_3^- to CO_2 because of pH shifts could impact CO_2 evasion rates and hence the carbon balance of the stream.

In summary, our high-resolution spatial sampling over four seasons enabled us to capture the relevance of stream network expansion and contraction and of a control point for the streamwater CO_2 dynamics in a high-altitude catchment. Despite low streamwater pCO_2, our results suggest that high-altitude streams are potential sources of CO_2 to the atmosphere. Our findings further contribute to the understanding of the biogeochemistry of glacier-fed streams now changing rapidly because of climate change[12].

2.6 Acknowledgements

The research leading to these results has received funding from the European Union's Horizon 2020 research and innovation programme under the Marie Sklodowska-Curie grant agreement No 643052 (C-CASCADES project) and from the Swiss Science Foundation grant agreement No 200021_163015 (METALP project). We want to thank M. Aguirre Morales, A. Bagnoud, M. Bensimon, G. Cotte, K. Dzubákobá, N. Escoffier, S. Flury McGinnis, A. Niayifar, R. Niederdorfer, H. Peter, P. Pramateftaki, J. Rüegg, D. Scheidweiler, P. L. Segatto and J. Thornton for field and lab assistance. We would also like to thank R. Striegl, M. Johnson and an anonymous reviewer for valuable comments on the manuscript. The authors declare that they have no conflict of interest. The data presented can be found at https://sber.epfl.ch/page-141576-en-html/published-data/.

Chapter 3 Dynamics and potential drivers of CO_2 concentration and evasion across temporal scales in high-alpine streams

Research article submitted

Contributing authors:

Åsa Horgby[1], Lluís Gómez-Gener[1], Nicolas Escoffier[2] and Tom J. Battin[1]

[1]Stream Biofilm and Ecosystem Research Laboratory, École Polytechnique Fédérale de Lausanne (EPFL), Station 2, CH-1015, Lausanne, Switzerland
[2]Institute of Earth Surface Dynamics, University of Lausanne, CH-1015, Lausanne, Switzerland

Å.H., T.J.B and L.G.G. planned and designed the research; N.E. acquired, managed and curated the data; Å.H performed the stable isotope analyses and other laboratory work and analysed the data with support from L.G.G; Å.H. wrote a first version of the manuscript; T.J.B contributed to the final version together with L.G.G. and N.E.

3.1 Abstract

Carbon dioxide (CO_2) evasion from streams greatly contributes to global carbon fluxes. Despite this, the temporal dynamics of CO_2 and its drivers remain poorly understood to date. This is particularly true for high-altitude streams. Using high-resolution time series of CO_2 concentration and runoff from sensors in twelve streams in the Swiss Alps, we studied over three years the responsiveness of both CO_2 concentration and evasion fluxes to runoff at annual scales and at the scale of the spring freshet. On an annual basis, our results show dilution responses of the streamwater CO_2 likely attributable to limited supply from sources within the catchment. Combining our sensor data with stable isotope analyses, we identify the spring freshet as a window where source limitation of the CO_2 evasion fluxes becomes relieved. CO_2 from soil respiration enters the streams during the freshet thereby facilitating CO_2 evasion fluxes that are potentially relevant for the carbon fluxes at catchment scale. Our study highlights the need for long-term measurements of CO_2 concentrations and fluxes to better understand and predict the role of streams for global carbon cycling.

3.2 Introduction

Inland waters are now recognized as important components of the global carbon cycle[13,15,28] with total carbon evasion fluxes to the atmosphere possibly as high as 3.88 Pg C yr^{-1} (ref. [28]). Among the inland waters, headwater streams — the smallest but most abundant streams in fluvial networks — are estimated to contribute approximately one third to the global carbon dioxide (CO_2) evasion flux[30]. Our understanding of the role of headwater streams for large-scale carbon fluxes is largely based on the study of headwater streams draining biomes with large carbon stocks[16,108,116] and generally attributed to the close connectivity with the terrestrial environment, which delivers large amounts of carbon, including CO_2 from soil respiration, to the headwaters[38,115]. However, not all headwater catchments are rich in organic carbon, which is particularly true for mountain catchments above the tree line.

Discharge is a master variable controlling ecological and biogeochemical processes in stream ecosystems. At catchment scale, the response of streamwater solute concentrations (*C*) to discharge, or runoff, *R,* (here we use R for the sake of cross-catchment comparability) provides information on the sources of solutes within the catchment, their size and arrangement, and mobilization and transportation to the streams (e.g., refs. [117,118]). Invariant responses of *C* to *R* are indicative of chemostasis and may reflect a uniform distribution of solutes within the catchment (e.g., in soils), where changes in hydrological connectivity and flow-paths position do not alter *C* in the streamwater. Chemodynamic responses indicates a change of *C* with *R,* where increasing *R* can either dilute or concentrate a solute in the streamwater. Responses of *C* to *R* are typically described by a simple power function, $C = aR^b$, where the exponent (*b*) indicates whether the response is chemostatic ($b = 0$) or chemodynamic (concentration: $b > 0$; dilution: $b < 0$) (e.g., refs. [117,118]).

This approach has been widely used to understand event-scale (e.g., storms) behavior of solutes and more recently also inter-annual solute dynamics in streams, and to infer drivers (e.g., source *versus* transportation limitation) that act at catchment scale (e.g., refs. [117,118]). Numerous studies have focused on the behavior of conservative solutes, including dissolved ions, but few have adopted the *C* - *R* scaling approach to gases, such as CO_2[74], to understand their temporal and spatial dynamics. Unlike nongaseous solutes that are transported downstream through advective flow, CO_2 is also outgassed vertically from the streamwater into the atmosphere (Figure 3:1).

The CO_2 evasion flux (F_{CO2}) depends on the gas exchange velocity (k_{CO2}) and the gradient between atmospheric and streamwater CO_2 concentrations. Streamwater CO_2 concentration and F_{CO2} are mutually dependent because (at oversaturation) the latter can deplete the CO_2 pool within the stream through atmospheric loss, which in turn can diminish F_{CO2}[119]. This relationship is further complicated by the dual role of *R*. As shown above, *R* drives solute dilution and concentration behavior in streams and at the same time it influences the gas exchange velocity through the water surface[52,54]. A recent survey by Liu and Raymond (2018) shows that roughly 50% of the streams and rivers throughout the USA had positive responses of CO_2 concentration to *R*, which would suggest increased CO_2 deliveries from the catchment outbalancing F_{CO2} from these systems. This is in line with observations that hydrological connectivity, as encapsulated by changes in *R* and its relationship with groundwater, can affect the transportation of CO_2 from various sources (e.g., soil respiration, geogenic origin) within the catchment to the streams[37,38,120] (Figure 3:1).

Based on the previous considerations, we present a framework based on the relationship between the responsiveness of CO_2 concentration to *R* (b_C) and the responsiveness of F_{CO2} to *R* (b_F), with the aim to gain mechanistic understanding of the dynamics of CO_2 evasion from streams and its linkage to processes operating at catchment scale (Figure 3:1). An underlying premise to this is that F_{CO2} scales with *R* similarly as *C*. That is, a $b_F > 0$ would indicate a responsiveness of F_{CO2} owing to increasing gas exchange velocity, possibly also because of no CO_2 limitation in the streamwater. A $b_F < 0$ would indicate that CO_2 depletion in the streamwater in combination with high gas exchange velocity would drive the responsiveness of F_{CO2} to *R*. We postulated that low responsiveness of both CO_2 concentration and F_{CO2} to *R* would limit F_{CO2} through low CO_2 concentration (i.e., dilution) as it happens for instance when CO_2 from terrestrial deliveries and/or in-stream respiration are reduced. Alternatively, CO_2 dilution but high F_{CO2} responsiveness to *R* indicates enhanced F_{CO2} with low CO_2 concentrations but high turnover. On the other hand, high responsiveness of both CO_2 concentration and F_{CO2} to *R* also enhances F_{CO2} but because of elevated CO_2 concentrations in the streamwater. Our conceptual framework serves as guidance to understand the balance between CO_2 supply to the stream and its outgassing from the stream, which ultimately affects the role of streams for large-scale CO_2 fluxes[74,119].

Despite the fact that mountains cover one fourth of the world's land surface[44,45], the CO_2 emission fluxes from mountain streams, including their drivers, remain poorly understood to date[47,54,120]. In this study, we use high-resolution temporal data over two consecutive years to assess the CO_2 dynamics across a range of twelve streams in the Swiss Alps across different timescales. On an annual basis, we anticipated overall limitation on the supply of CO_2 from the sources within the catchments as they are often devoid of vegetation and major soil horizons. We also expected low streamwater CO_2 concentrations resulting from the combination of low CO_2 supply and high gas exchange velocities. Furthermore, we postulate that there are windows when supply limitation becomes relieved and streams receive larger deliveries of CO_2 from sources within the catchment increasing the responsiveness of both CO_2

concentrations and F_{CO2}. We complemented sensor data with occasional measurements of the isotopic composition of CO_2 to explore its potential sources. Our findings shed new light on the CO_2 dynamics in high-altitude streams, further contributing to a better understanding of the role of these ecosystems for global carbon fluxes.

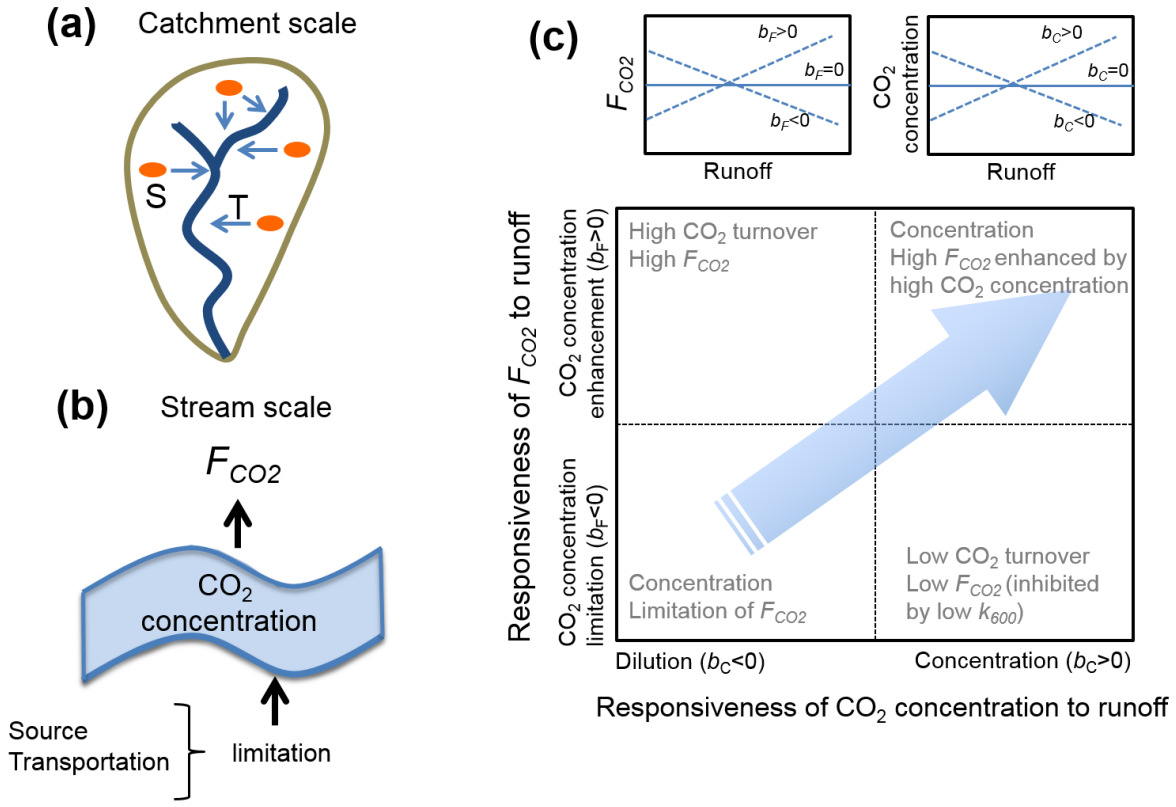

Figure 3:1 Conceptual framework proposed to study the CO_2 dynamics in streams. (a) At catchment scale, sources (S) and transportation (T) can shape the responsiveness of solutes concentration to runoff. (b) There is a mutual relationship between CO_2 evasion flux (F_{CO2}) and concentration in streams, where the latter is also influenced by source and/or transportation. The latter and F_{CO2} are both dependent on runoff. (c) The responsiveness of CO_2 concentration (b_C) and F_{CO2} (b_F) to runoff can be quantified by partial least squares regressions on log-log transformed data. The b_C to b_F space serves as a frame to explore the potential drivers on the CO_2 dynamics in streams. For instance, the domain defined by b_C<0 and b_F<0 indicates that source/transportation limits CO_2 concentration and hence F_{CO2}. Depending on the limitation the system state can move to an alternative domain (as indicated by the blue arrow) where limitation relief results in a higher responsiveness of F_{CO2} to runoff.

3.3 Methods

3.3.1 Study streams

We studied twelve streams distributed over four catchments (Valsorey, Champéry, Ferret and Vallon de Nant) in the Swiss Alps and that were selected to cover environmental gradients typical for high-altitude systems (Figure 3S:1, Table 3S:1). Five streams did not have any glacial influence (PEU, VID, VIM, VIU, and VEL), while seven streams were glacier-fed with glacier coverage ranging from 2 to 27% (VAD: 22%, VAU: 27%, FED: 2%, FEU: 4%, RIC: 6%, AND: 5%, and ANU: 7%). The drainage areas varied in size from 0.3 to 20 km^2. The average catchment altitude ranged from 1200 to 2161 m above sea level (a.s.l.); stream channel slopes ranged from 0.05 to 0.16 m m^{-1}. Catchment lithologies are dominated by carbonate sedimentary rocks (Champéry and Vallon de Nant) and metamorphic rocks (Valsorey and Ferret)[121]. Eight of the stream sites were located above the tree line, while the other four streams drained partially forested catchments (VID 0.5 %, RIC 1.2 %, AND 2.0 %, ANU 0.3 %). Vegetation cover ranged from 25 to 100%, and bare rocks from 0 to 56 %[122]. Vegetation cover decreased with increasing altitudes both for the glacierized sites (R^2=0.47, n=7, P=0.09) and the non-glacierized sites (R^2=0.84, n=5, P<0.05). Streamwater DOC concentrations were low and ranged between 111 and 448 µg C L^{-1} (ref. [122]).

3.3.2 High-frequency measurements and isotope sampling

In each stream, we measured streamwater pCO_2, temperature and depth, as well as barometric pressure every 10 minutes during two consecutive years. We prepared the pCO_2 sensors (Vaisala CARBOCAP®, GMT220, Vantaa, Finland) according to Johnson et al. (2010), where sensors were contained within a polytetrafluoroethylene (ePDFE) semi-permeable membrane sealed with liquid electrical tape. Sensors were further protected with a metal casing and powered by a solar panel. Sensors were maintained and data downloaded on average every month. Raw data were corrected according to the manufacturer's recommendations for streamwater temperatures (HOBO U24-001 Conductivity Logger, ONSET, Bourne, USA) and barometric pressure (Track-It™ Logger, Monarch Instrument, Amherst, USA). Before deployment, we tested all pCO_2 sensors in the laboratory using certified gas mixtures of CO_2 diluted in synthetic air to final concentrations of 0, 400 and 2000 ppmv. We also performed a laboratory calibration with two of our sensors, which revealed sensor accuracy of -5% and sensor response times between 2.5 and 13 minutes.

Water depth (Odyssey® Logger, Dataflow Systems Ltd., New Zealand; TruTrack Data Logger, Intech Instruments LTD, New Zealand) was converted to *Q* from sodium chloride (NaCl) slug additions[123]. Thereby, we established rating curves for each individual stream (ranging from 4 to 13 NaCl additions in FED and VID, respectively, with an average of 7). From the rating curves, we obtained discharge, which we converted to *R* by normalizing for drainage area. We determined the catchment area in ArcGIS 10.5 (Environmental Systems Research Institute, USA) from a 2-m^2 digital elevation model (Geodata © Swisstopo).

When accessible, streams were sampled on a monthly basis for the determination of the isotopic composition of streamwater CO_2 ($\delta^{13}C\text{-}CO_2$; expressed as ‰ VPDB; Vienna Pee Dee Belemnite) using glass vials sealed with rubber stoppers and metal caps. Samples were stored in the dark (4°C) pending analyses within 24h. In the laboratory, we created a headspace (in the 60 mL sample vials) with synthetic air, shook the samples (2 min) and let them equilibrate (2 h). We measured CO_2 concentrations and $\delta^{13}C\text{-}CO_2$ using a cavity ring-down spectrometer (Model G2201-*I*, Picarro Instruments, Santa Clara, CA, USA). Samples for atmospheric CO_2 were collected next to the study streams into glass vials sealed with rubber stoppers and metal caps; we injected additional 50 mL of ambient air to over-pressurize the samples, which were measured on the same Picarro G2201-*I* as above.

3.3.3 CO_2 concentration and flux calculations

At the 10-minute basis, we multiplied monitored streamwater pCO_2 with Henry's constant (K_H, mol L^{-1} atm^{-1})[124] as a function of streamwater temperature and atmospheric pressure (P_{atm}, atm) to obtain streamwater CO_2 concentration. F_{CO2} were calculated from the CO_2 gradient (ΔCO_2, mol L^{-1}) between the streamwater and the atmosphere, and the gas transfer velocity for CO_2 (k_{CO2}, m d^{-1}) (Eq. 3:1).

$$F_{CO2} = k_{CO2} \times \Delta_{CO2}$$

Equation 3:1 – CO_2 evasion flux

To estimate ΔCO_2, we first calculated median atmospheric CO_2 concentration derived from grab samples (at least 5 measurements per stream). The atmospheric CO_2 was multiplied with K_H and P_{atm} to obtain atmospheric CO_2 concentrations at saturation ($[CO_{2sat}]$, mol L^{-1}). We then subtracted CO_{2sat} from the streamwater CO_2 concentrations to obtain ΔCO_2.

Ulseth et al. (2019) recently described gas transfer velocities (k_{600}, m d^{-1}) in turbulent mountain streams as function of energy dissipation (*eD*, m^2 s^{-3}). We used this scaling relationship for streams with *eD*> 0.02 m^2 s^{-3} as

$$k_{600} = exp^{6.43+1.18 \times \ln(eD)}$$

Equation 3:2 – Gas transfer velocity for turbulent streams

where *eD* is a function of stream flow velocity (*V*, m s^{-1}), stream channel slope (*S*, m m^{-1}) and the gravity acceleration (*g,* m s^{-2}). We calculated *eD* from *V* that we derived from the hydraulic geometry scale relationship specifically established for our study streams.

$$V = 0.668 * Q^{0.365}$$

Equation 3:3 – Streamwater velocity

We converted k_{600} to k_{CO2} (m d^{-1}) (Equation 3:4) using the Schmidt scaling[51], as shown in Equation 3:5.

$$k_{CO_2} = \frac{k_{600}}{\left(\frac{600}{Sc_{CO2}}\right)^{-0.5}}$$

Equation 3:4 – Gas transfer velocity of CO_2

$$Sc_{CO2} = 1923.6 - 125.06 \times T_w + 4.3773 \times {T_w}^2 - 0.085681 \times {T_w}^3 + 0.00070284 \times {T_w}^4$$

Equation 3:5 – Schmidt scaling for CO_2

We performed all sensor corrections and flux calculations in Matlab R2017b.

3.3.4 Data analyses

We analyzed time series covering the period from August 2016 to September 2018 (three calendar years; 2016, 2017, 2018). We collapsed the 10-min interval data from the time series to daily median values of CO_2 concentration and *R*, and calculated gas transfer velocity of CO_2 (k_{CO2}) and F_{CO2}. We followed the same approach as Liu and Raymond (2018) to identify the responses of CO_2 concentration, k_{CO2}, and F_{CO2} to runoff, respectively. We used power law functions with transformed data (log(x+10)) to analyze whether the responses were chemostatic or chemodynamic, as well as the magnitude of the response[117,118]. We fitted the data using partial least squares regressions. We fitted each site and each year separately, for which we derived statistical parameters. We used $P<0.05$ as the threshold for statistical significance and the coefficient of determination, R^2, to determine the goodness of the fit. We used JMP 13 (SAS Institute Inc., Cary, USA) for all statistical analyses.

3.4 Results and discussion

3.4.1 Hydrological regimes

The hydrological regimes of our study streams are typical for high-altitude systems[125,126]. After an extended winter baseflow, where runoff was relatively stable, the freshet started between March and April depending on the altitude and exposition of the catchments. Snowmelt further shaped the hydrological regimes throughout spring and summer. As expected, summer runoff was higher in the glacier-fed streams because of the glacier ice melt. The 2016/2017 winter was milder with less precipitation than the 2017/2018 winter, which resulted in overall higher spring and summer runoff in 2018 (Figure 3S:2).

3.4.2 Streamwater CO_2 concentration dynamics

Overall, we found low streamwater CO_2 concentrations (Figure 3:S2), which is consistent with other reports on similar streams[49,50,106,120]. At a 10-minute basis, median CO_2 concentrations ranged from 22.8 to 34.6 µmol L^{-1} across all study streams during the study period, with 7.1 and 77.6 µmol L^{-1} as minimum and maximum concentrations, respectively. Daily median CO_2 concentrations covered a similar range as the 10-minute time step (ranging from 22.9 to 34.5 µmol L^{-1} across all study streams and both years). Therefore, we used the daily median for all further analyses, which would also smooth potential outliers and make estimates more robust. Despite often incomplete time series (e.g., owing to sensor malfunctioning or loss), our analysis of streamwater CO_2 concentration revealed recurrent seasonal patterns that were also similar among streams. Specifically, the CO_2 concentrations increased during the recession of the snowmelt and ice melt and further into fall baseflow. The freshet in early spring was marked by a transient increase in both runoff and CO_2 concentration in several of our streams (e.g., VAD, VAU, VIM, FED, AND, ANU).

3.4.3 Annual responsiveness of CO_2 concentration and evasion fluxes to runoff

On an annual basis, we consistently found inverse relationships between CO_2 concentration and *R* with a median annual b_C of -0.11 and ranging between -0.34 and 0.11 across streams). Only two *C-R* relationships (from VIU 2017 and VIU 2018) yielded non-significant statistic and the only positive b_C (0.11±0.03) was calculated for AND in 2016; this may be attributable to the relatively low number of daily concentrations (n=45) in AND. Five study streams (VEL, VIM, RIC, AND, ANU) showed negative but near-chemostatic behavior defined as b_C = -0.05 to 0.15 according to Godsey et al (2009) during 1 and/or 2 of the three calendar years of this study (Figure 3:2, Table 3S:2). For instance, RIC showed near-chemostatic behavior in 2016 (b_C =-0.04±0.005) and 2017 (b_C = -

0.03±0.003) but a more pronounced chemodynamic response in 2018 (b_C = -0.14±0.007). Hence, across the 34 significant *C-R* relationships, 28 indicated chemodynamic and 8 indicated near-chemostatic behavior (Table 3S:2). We attribute the inter-annual differences in b_C within sites to the gaps in the time series, particularly when different periods of the year were excluded from the analyses (Figure 3:2; Figure 3S:2).

Overall, our b_C values are lower than those reported for 1st- to 6th-order streams (b_C ranging from -0.05 to 0) and larger rivers (b_C ranging from 0.02 to 0.24) throughout the USA[74]. Low b_C values are indicative of dilution as a response to increasing runoff, which in mountain streams is certainly facilitated by an acceleration of k_{CO2} that also increases with discharge (hence also with *R*) and related hydraulics. The b_C values from our study streams are comparable to those reported from small boreal streams draining forested and peatland catchments (b_C ranging from -0.36 to -0.08)[127]. Wallin et al. (2010) found more negative responses of CO_2 concentration to discharge in streams with lower pH and hence lower carbonate buffering capacity. We did not find a similar trend, possibly also because the pH in our study streams was typically >8. Only the streams in the Valsorey catchment were transiently undersaturated in CO_2 with respect to the atmosphere. We tentatively attribute this to low dissolved inorganic carbon (DIC) concentrations in these streams (2 to 3 times lower compared to the other catchments) and thus less potential for inorganic carbon buffering.

The overall low b_C values reported here may also be linked to the sparse sources from where CO_2 may emanate. This notion is supported by the trend showing b_C values decreasing with increasing altitude (R^2=0.48, n=10, P<0.05; VID and FED were outliers and excluded from this analysis).

Near-chemostatic behavior can occur when CO_2 supply balances CO_2 export through evasion and downstream transport fluxes. We attribute the annual near-chemostatis observed in some of our streams to substantial deliveries CO_2 via groundwater. In fact, groundwater has been shown to be important for the CO_2 dynamics in the streams in the Vallon de Nant catchment (RIC, AND, ANU)[120]. In agreement with this, VEL is a mostly groundwater-fed stream within the Valsorey catchment. Beyond our mountain streams, groundwater is now being increasingly recognized to drive CO_2 concentration and fluxes in various headwater streams[37,128]. Because of the inherent link between gas exchange velocity and discharge, we found overall positive responses in k_{CO2} to runoff (100%, P<0.05) and F_{CO2} to increasing runoff, respectively (55%, P<0.05) (Table 3S:2). Of the 36 b_F, only 4 were from non-significant relationships (VAD 2018, VEL 2016, VEL 2017, AND 2016). The median b_F value for the 32 significant F_{CO2} - R relationships was 0.007, ranging from -0.14 to 0.16 across streams (Table 3S:2). In their systematic survey on US streams and rivers, Liu and Raymond (2018) found the highest b_F values (0.23 to 0.31) in small streams. We relate the different responses between their study and ours to the overall low CO_2 concentrations in our mountain streams. In fact, low streamwater CO_2 concentration reduce the CO_2 gradient between the streamwater and the atmosphere, and hence F_{CO2}. This is further supported by the inverse relationship between b_F and altitude (n=12, R^2=0.34, P<0.05) for the same reasons as discussed above.

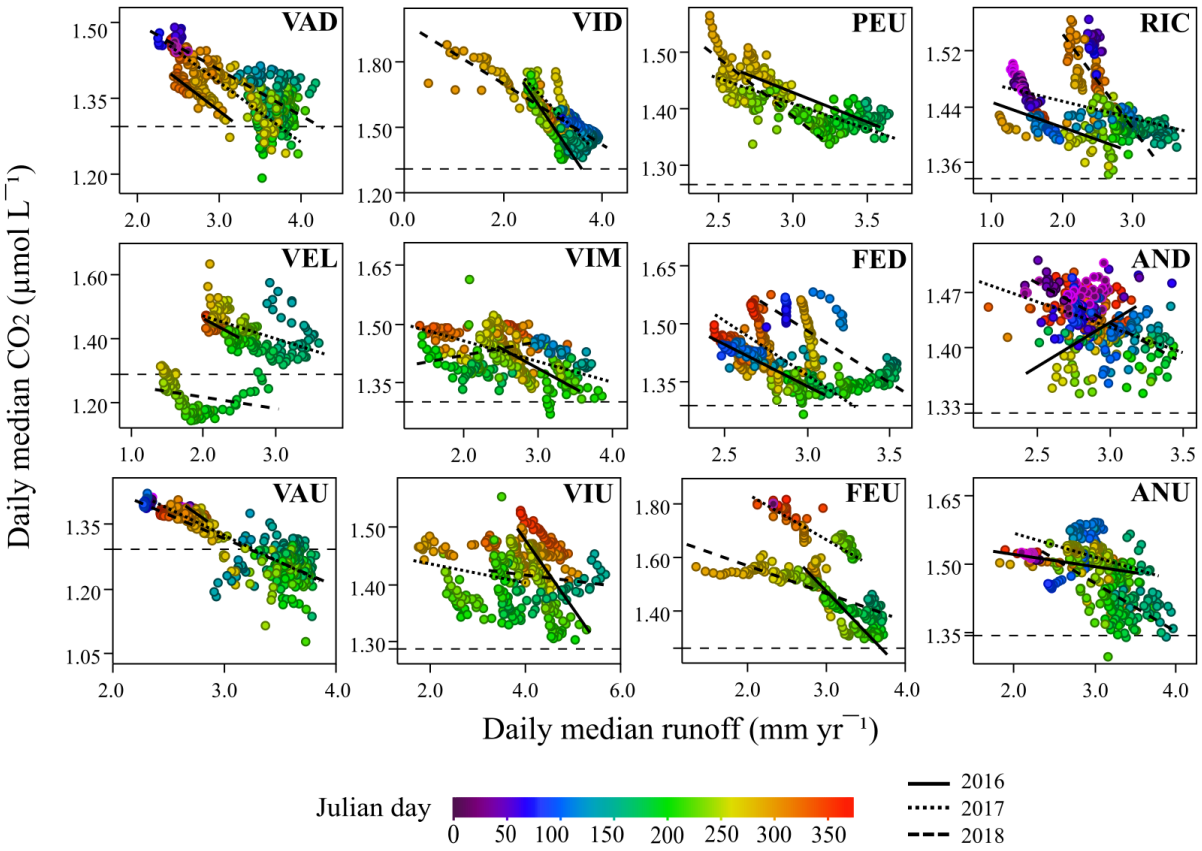

Figure 3:2 Multiannual (2016 to 2018) responses of streamwater CO_2 concentrations to runoff in twelve streams in the Swiss Alps, Shown are daily median CO_2 concentration and daily median runoff (log-log). The horizontal dotted lines represent site-specific median CO_2 saturation, determined from grab samples of atmospheric CO_2. Data are color-coded according to Julian day and the lines represent the linear regressions for each year (2016, 2017, 2018); see Table 3S:2 for regression statistics.

3.4.4 Short-time responsiveness of CO_2 to runoff and CO_2 sources

While most study streams exhibited dilution to quasi-chemostasis behavior for CO_2 concentration on an annual basis, we also detected windows with positive b_C values in five of our study streams (VAD: b_C=0.56±0.05, n=74, R^2=0.60; VAU: b_C=0.35±0.03, n=269, R^2=0.41; FED: b_C=0.23±0.01, n=865, R^2=0.32; AND: b_C=0.11±0.01, n=2592, R^2=0.63; ANU: b_C=0.14±0.01, n=2304, R^2=0.78; all with P<0.05) that were typically associated with the freshet in spring (Figure 3S:2). This short-term behavior indicates that these streams received substantial CO_2 deliveries during increasing freshet runoff.

The notion of increased CO_2 deliveries during the onset of snowmelt is further supported by our stable isotope analyses. Across all streams, stable isotope analysis consistently revealed depleted CO_2 compositions ($\delta^{13}C$-CO_2) in spring (April: median $\delta^{13}C$-CO_2: -15.81‰; March: -15.47‰; May: -14.39‰) but more enriched composition in August (-11.73‰) and later in February (-11.83‰) and January (-11.90‰) (streams were not accessible in December) (Figure 3:3). These isotopic compositions indicate CO_2 from soil respiration as a source to the streams during the spring freshet, coinciding with the hydrological activation of the headwater network. In fact, respiratory CO_2 ultimately from the heterotrophic breakdown of organic matter typically has isotopic compositions ranging from -34 to -24‰[88] and is hence more depleted than atmospheric CO_2 and CO_2 originating from carbonate precipitation at isotopic equilibrium[90]. Our observation of a respiratory CO_2 pulse during the freshet is in agreement with previous observations from high-altitude and high-latitude catchments (e.g., refs. [129,130]), and further corroborates the notion of microbial activity underneath the snow cover leading to CO_2 accumulation[131]. Increasing hydrological connectivity during snowmelt facilitates the transportation of this CO_2 via shallow groundwater flow paths to the streams[87]. The delivery of CO_2 from the terrestrial environment to streams is analogous to the DOC flushing during snowmelt[122,132], and further supports the relevance of this short window for carbon fluxes at the scale of high-altitude catchments.

Our findings reveal the window of the freshet as potentially important for carbon fluxes in high-altitude catchments. In fact, during the observed flushing events, we found on average 49 % higher F_{CO2} compared to the F_{CO2} calculated across the rest of the year. The largest difference was found in ANU, where the freshet F_{CO2} was 4.1 times higher (median: 24.8 g C m^{-2} day^{-1}) compared to the rest of the year (median: 6.1 g C m^{-2} day^{-1}). During the 16 days of the freshet, F_{CO2} from ANU increased from 14 g C m^{-2} day^{-1} (April 1, 2018) to 35 g C m^{-2} day^{-1} (April 16, 2018).

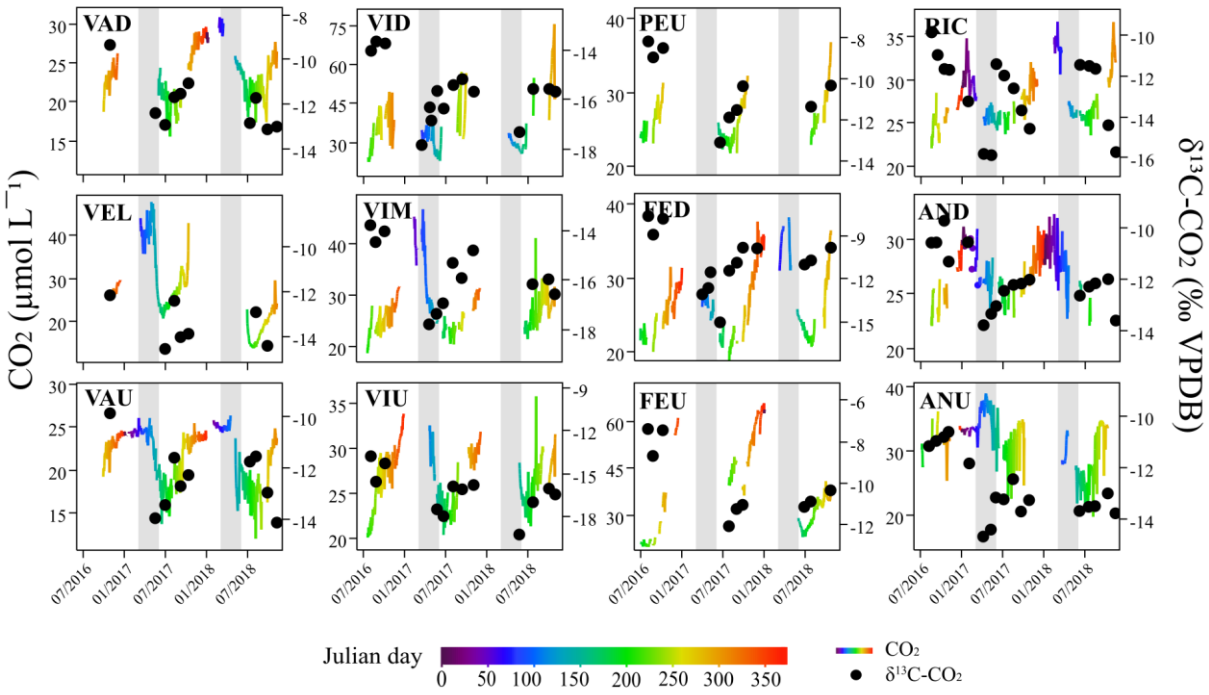

Figure 3:3 Multiannual dynamics of streamwater CO_2 concentration and isotopic composition ($\delta^{13}C$-CO_2). The isotopic composition indicates depletion during the spring freshet (March-May, as indicated by the grey bars), suggesting CO_2 from soil respiration as a possible source.

3.4.5 CO_2 dynamics across temporal scales

Our study revealed differing responsiveness of CO_2 concentration and fluxes to runoff depending on the temporal scale. In line with our conceptual framework (Figure 3:1), we found a clear transition of the CO_2 dynamics and its potential drivers from an annual to the event-driven (i.e., freshet) scale (Figure 3:4). On an annual basis, the relationship between b_F and b_C remained largely restricted to the domain where CO_2 concentration apparently limited F_{CO2}. Here, streams draining the catchments with the highest altitude tended to be at the lower end of this continuum. This is intuitive as CO_2 source limitation is more pronounced in these catchments as in those at lower altitude and with higher organic carbon stocks. The latter have higher potential to generate CO_2 from soil respiration, for instance, that can be delivered to the streams. The freshet is a window where the CO_2 source limitation becomes transiently relieved enabling an increase in F_{CO2}. This is furthermore facilitated by an accelerated gas exchange because of the increasing runoff.

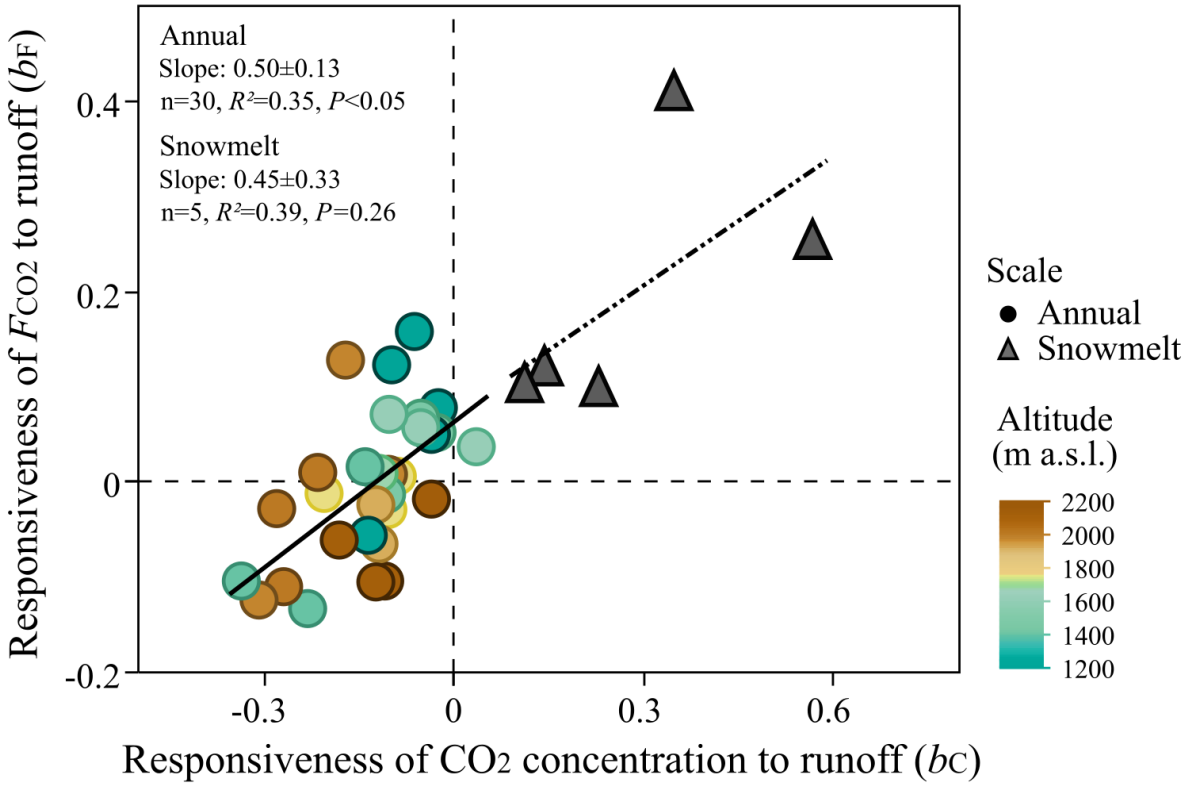

Figure 3:4 Responsiveness of F_{CO2} (b_F) and CO_2 (b_C) concentration to increasing runoff across time scales. On an annual basis, the relationship between b_F and b_C was largely constrained to the domain where CO_2 dilution governs the evasion fluxes (see also Figure 3:1). This was particularly true for high-elevation catchments. During the freshet, CO_2 source limitation became relieved, which resulted in a higher F_{CO2} responsiveness to runoff.

3.5 Conclusions

Across 12 studied mountain streams, we found the responsiveness of CO_2, and F_{CO2}, respectively, to runoff to be temporally dynamic. Our study identified varying responsiveness of CO_2 dynamics to runoff in high-altitude streams. Streamwater CO_2 dilution, likely because of source limitation, was the general response to increasing runoff on an annual basis. The spring freshet was found to be a window where source limitation was relieved and CO_2 from soil respiration flushed to the streams. This window is potentially relevant for carbon fluxes at the catchment scale and certainly susceptible to changing precipitation patterns and snowpack owing to climate change in the Alps.

3.6 Acknowledgements

We would like to thank Marta Boix Canadell, Félicie Hammer, Rémy Romanens, Mathieu Brunel and Valentin Sahli for fieldwork. The research leading to these results has received funding from the European Union's Horizon 2020 research and innovation program under the Marie Sklodowska-Curie grant agreement No 643052 (C-CASCADES) and from the Swiss National Science Foundation (No 200021_163015, METALP) to T.J.B.

3.7 Supplementary information

3.7.1 Supplementary Figures

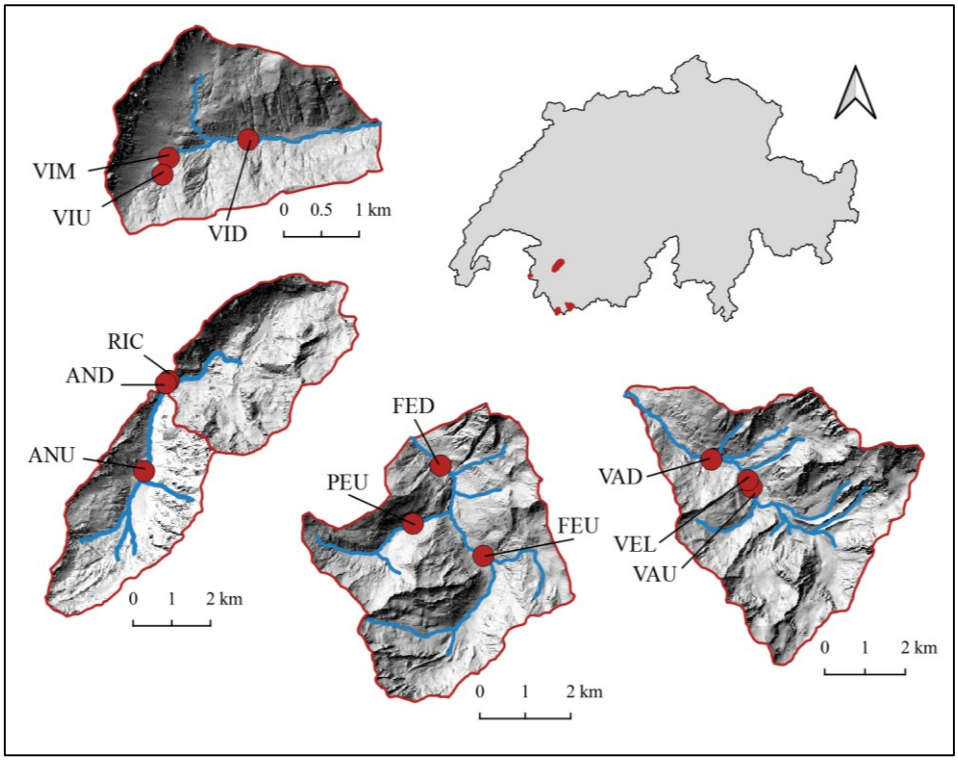

Figure 3S:1 We studied 12 stream segments in four high-altitude alpine catchments. Site ID's are abbreviations of stream names: Torrent de Valsorey Down (VAD), Torrent du Vélan (VEL), Torrent de Valsorey Up (VAU), La Vièze Down (VID), La Vièze Middle (VIM), La Vièze Up (VIU), Torrent de la Peule (PEU), Dranse de Ferret Down (FED). Dranse de Ferret Up (FEU), Richard (RIC), L'Avançon de Nant Down (AND), and L'Avançon de Nant Up (ANU) (Figure 3S:1, Table 3S:1).

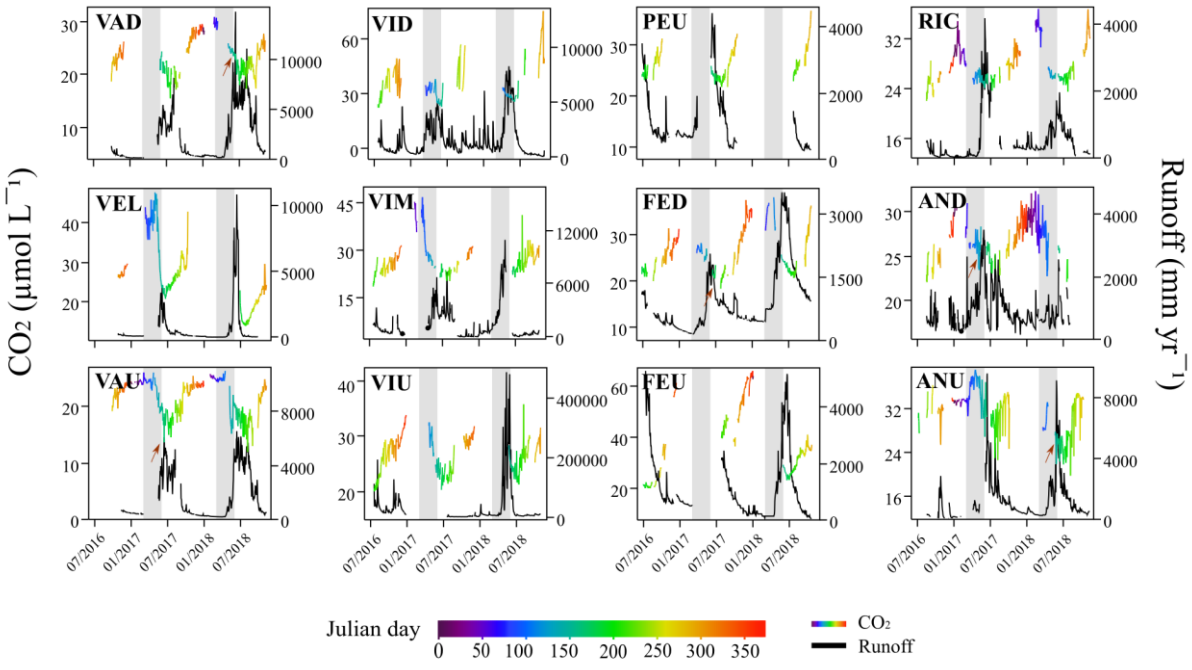

Figure 3S:2 Time series of daily median CO_2 concentration (colored according to Julian day; left y-axis) and daily median runoff (black; right y-axis). Gray bands (March-May) represent the snowmelt period and red arrows point towards the identified freshet events.

3.7.2 Supplementary Tables

Site	Latitude	Longitude	Area (km^2)	Altitude (m a.s.l.)	Slope ($m\ m^{-1}$)	Glacial coverage (%)	Median pCO_2 (µatm)	Mean pCO_2 (±std.) (µatm)	Median CO_2 ($\mu mol\ L^{-1}$)
VAD	45.93503	7.226898	23.16	1937	0.1	22.2	430	427±39	23.5
VEL	45.55677	7.147520	3.11	2161	0.08	0	465	473±132	24.5
VAU	45.92951	7.244578	18.1	2148	0.06	27.7	397	388±43	22.8
VID	46.15932	6.814734	3.64	1415	0.1	0	593	687±221	32.5
VIM	46.15701	6.801199	0.74	1630	0.16	0	501	527±84	26.1
VIU	46.15495	6.800200	0.31	1689	0.06	0	502	511±62	27.2
PEU	45.89366	7.107973	3.97	2027	0.06	0	523	525±55	25.8
FED	45.90509	7.115597	20.24	1774	0.03	1.8	454	472±57	25.3
FEU	45.88308	7.130949	9.33	1995	0.05	3.9	673	699±220	34.6
RIC	46.25352	7.110105	14.32	1200	0.14	6.2	473	486±43	26.7
AND	46.25341	7.109632	13.36	1201	0.14	4.5	454	457±26	27.3
ANU	46.23160	7.101972	8.99	1465	0.05	6.7	579	566±69	31.7

Table 3S:1 Site properties and CO_2 concentrations at the 12 study reaches.

			CO_2 vs. runoff				F_{CO2} vs. runoff			
Site	Year	n	R^2	b_C	Std. Error	*P*-value	R^2	b_F	Std. Error	*P*-value
VAD	2016	59	0.77	-0.124	0.01	<0.05	0.42	-0.024	0.00	<0.05
	2017	118	0.79	-0.119	0.01	<0.05	0.12	-0.065	0.02	<0.05
	2018	213	0.64	-0.091	0.00	<0.05	0.00	-0.010	0.01	0.426
VEL	2016	48	0.57	-0.121	0.02	<0.05	0.00	0.0004	0.00	0.912
	2017	149	0.24	-0.071	0.01	<0.05	0.01	0.004	0.00	0.387
	2018	91	0.06	-0.036	0.01	<0.05	0.35	-0.018	0.00	<0.05
VAU	2016	51	0.75	-0.182	0.01	<0.05	0.50	-0.061	0.01	<0.05
	2017	206	0.84	-0.124	0.00	<0.05	0.64	-0.105	0.01	<0.05
	2018	236	0.73	-0.110	0.00	<0.05	0.54	-0.104	0.01	<0.05
VID	2016	91	0.82	-0.337	0.02	<0.05	0.31	-0.104	0.02	<0.05
	2017	114	0.62	-0.232	0.02	<0.05	0.37	-0.133	0.02	<0.05
	2018	109	0.88	-0.141	0.01	<0.05	0.11	0.016	0.00	<0.05
VIM	2016	103	0.21	-0.103	0.02	<0.05	0.23	0.071	0.01	<0.05
	2017	104	0.59	-0.053	0.00	<0.05	0.58	0.057	0.00	<0.05
	2018	128	0.05	0.035	0.01	<0.05	0.15	0.037	0.01	<0.05
VIU	2016	151	0.31	-0.119	0.01	<0.05	0.03	0.009	0.00	<0.05
	2017	82	0.03	-0.016	0.01	0.098	0.81	0.009	0.00	<0.05
	2018	131	0.02	-0.010	0.01	0.106	0.08	0.010	0.00	<0.05
PEU	2016	72	0.72	-0.105	0.01	<0.05	0.35	-0.029	0.00	<0.05
	2017	121	0.54	-0.090	0.01	<0.05	0.06	0.006	0.00	<0.05
	2018	66	0.75	-0.206	0.01	<0.05	0.18	-0.012	0.00	<0.05
FED	2016	122	0.74	-0.216	0.01	<0.05	0.04	0.010	0.00	<0.05
	2017	158	0.46	-0.281	0.02	<0.05	0.11	-0.028	0.01	<0.05
	2018	137	0.56	-0.270	0.02	<0.05	0.64	-0.110	0.01	<0.05
FEU	2016	69	0.71	-0.309	0.02	<0.05	0.89	-0.124	0.01	<0.05
	2017	119	0.75	-0.172	0.01	<0.05	0.76	0.128	0.01	<0.05
	2018	146	0.67	-0.104	0.01	<0.05	0.04	0.008	0.00	<0.05
RIC	2016	70	0.40	-0.036	0.01	<0.05	0.51	0.050	0.01	<0.05
	2017	165	0.28	-0.025	0.00	<0.05	0.81	0.078	0.00	<0.05
	2018	173	0.68	-0.136	0.01	<0.05	0.32	-0.056	0.01	<0.05
AND	2016	45	0.21	0.110	0.03	<0.05	0.00	0.013	0.03	0.698
	2017	174	0.28	-0.063	0.01	<0.05	0.54	0.158	0.01	<0.05
	2018	117	0.30	-0.099	0.01	<0.05	0.17	0.123	0.03	<0.05
ANU	2016	45	0.27	-0.027	0.01	<0.05	0.75	0.052	0.00	<0.05
	2017	157	0.19	-0.053	0.01	<0.05	0.48	0.067	0.01	<0.05
	2018	169	0.46	-0.107	0.01	<0.05	0.03	-0.013	0.01	<0.05

Table 3S:2 Slopes of the linear regressions for daily median CO_2 concentration versus daily median runoff (b_C), and daily median F_{CO2} versus daily median runoff (b_F), respectively. All data was log 10 transformed prior to analysis. To keep potential negative CO_2 evasion fluxes, +10 was added to all F_{CO2} values prior to the logarithmic transformation.

Chapter 4 Unexpected large CO_2 evasion fluxes from turbulent streams draining the world's mountains

Research article accepted in Nature Communications

Contributing authors:

Åsa Horgby[1], Pier-Luigi Segatto[1], Enrico Bertuzzo[2], Ronny Lauerwald[3], Bernhard Lehner[4], Amber J. Ulseth[5], Torsten W. Vennemann[6] and Tom J. Battin[1]

[1]Stream Biofilm and Ecosystem Research Laboratory, École Polytechnique Fédérale de Lausanne (EPFL), Station 2, CH-1015, Lausanne, Switzerland
[2]Department of Environmental Sciences, Informatics and Statistics, University of Venice Ca' Foscari, 30123 Venezia Mestre, Italy
[3]Biogeochemistry and Earth System Modelling, Department of Geoscience, Environment and Society, Universite Libre de Bruxelles, Bruxelles, Belgium
[4]Department of Geography, McGill University, Montreal, Canada
[5]Department of Biological Sciences, Sam Houston State University, Huntsville, TX 77341, USA
[6]Institute of Earth Surface Dynamics, University of Lausanne, CH-1015, Lausanne, Switzerland

Å.H. and T.J.B. conceptualized the study; Å.H. acquired and analysed the data with the support from P.-L.S. as well as E.B., R.L., B.L., A.J.U. and T.W.V; T.J.B. wrote the manuscript with ÅH and with contributions from all other authors.

4.1 Abstract

Inland waters, including streams and rivers, are active components of the global carbon cycle. Despite the large areal extent of the world's mountains, the role of mountain streams for global carbon fluxes remains elusive. Using recent insights from gas exchange in turbulent streams, we found that areal CO_2 evasion fluxes from mountain streams equal or exceed those reported from tropical and boreal streams, typically regarded as hotspots of aquatic carbon fluxes. At the regional scale of the Swiss Alps, we present evidence that emitted CO_2 derives from lithogenic and biogenic sources within the catchment, delivered by the groundwater to the streams. At a global scale, we estimate the CO_2 evasion from mountain streams to 167 ± 1.5 Tg C yr^{-1}, which is high given their relatively low areal contribution to the global stream and river networks. Our findings shed new light on mountain streams for global carbon fluxes.

4.2 Introduction

Since 2007, when a seminal publication[133] highlighted the relevance of inland waters for the global carbon cycle, estimates of CO_2 evasion fluxes from the world's streams, rivers and lakes to the atmosphere have continuously moved upwards[28]. Current estimates of annual CO_2 evasion fluxes from inland waters are within the same range as ocean uptake fluxes of CO_2[134], although the fluxes are in the opposite direction. Streams and rivers alone are estimated to emit 650 Tg C yr^{-1} (ref. [16]) to 1800 Tg C yr^{-1} (ref. [17]) to the atmosphere, which is remarkable given that they contribute marginally to the Earth's non-glacierized land surface[36]. These fluxes are admittedly still poorly constrained, partly because of the lack of observations from various regions of the world and the poor quantification of stream networks, particularly their headwaters.

Mountains account for 25% of the Earth's land surface and the streams that drain them contribute more than a third to the global runoff[45]. Nevertheless, the role of mountain streams for global carbon fluxes has not yet been evaluated. To date, interest on CO_2 evasion fluxes has largely centered on streams and rivers draining low-altitude catchments in tropical[25,135] and boreal[107,116] regions. It is intuitive to assume that the lack of significant vegetation cover and soil carbon stocks in many mountain catchments, particularly in high-altitude catchments, have precluded research on carbon fluxes in the streams draining these systems. There are certainly exceptions to the inverse relationship between altitude and vegetation cover[136], such as the Paramo vegetation in the Andes, or more generally peatlands developing in high-altitude catchments. Furthermore, the lack of appropriate scaling relationships to predict the gas exchange velocity across the highly turbulent water surface of mountain streams has impeded the appreciation of their CO_2 evasion fluxes[54].

The few existing studies of CO_2 in mountain streams typically reveal low pCO_2 and occasionally even undersaturation relative to the atmospheric pCO_2 (e.g., refs. [47–50]). In line with this, temporally highly resolved measurements consistently indicate relatively low streamwater pCO_2 values (median: 397 to 673 µatm) throughout the year in twelve streams in the Swiss Alps (Figure 4S:1, Table 4S:1). Not unexpected, these pCO_2 values are low compared to those measured in boreal[137] and tropical[108] headwaters, for instance, and would thus support the assumption that mountain streams contribute only marginally to global carbon fluxes. However, low pCO_2 in mountain streams can also result from high evasion fluxes, owing to elevated turbulence, compared to CO_2 supply from the catchment and CO_2 production from stream ecosystem respiration. This notion is in line with a recent study by Rocher-Ros and colleagues[119] showing low CO_2 concentrations in turbulent streams with high gas exchange velocity compared to a wide range of elevated CO_2 concentrations in low-turbulence streams with reduced gas exchange velocities and little supply limitation of CO_2.

In this study, we combine recent insights[54] into the gas exchange through the turbulent water surface of mountain streams with novel streamwater CO_2 concentration data to estimate CO_2 evasion fluxes from Swiss mountain streams, as well as from the mountain streams worldwide. We found unexpectedly high areal CO_2 evasion fluxes from these streams driven by high gas exchange velocities and a constant CO_2 supply from both biogenic and lithogenic sources. To our knowledge, this is the first large- scale attempt to estimate CO_2 evasion fluxes from mountain streams.

4.3 Results and discussion

4.3.1 Scaling relationships and parameter simulation

To quantify CO_2 evasion fluxes, streamwater CO_2 concentration and exchange velocities must be estimated. Many current upscaling approaches involve aggregation of streamwater pCO_2, estimated from pH, DIC and alkalinity, into a single median value over very large regions (e.g., European Alps or Andes). This is then combined with gas exchange velocities at the stream or catchment scale[17,71]. While this approach has been often used for estimating regional and global CO_2, it might provide erroneous estimates[119]. We therefore opted for an alternative upscaling strategy involving similar spatial scales for streamwater CO_2 concentration and gas exchange velocity for each mountain stream individually.

We estimated streamwater CO_2 concentration from a linear regression model (R^2 = 0.39, P<0.001) based on observations from 323 streams from the world's major mountain ranges (Methods; Figure 4S:2). The streams included in the model drain catchments covering a broad range of lithologies, dominated by carbonate rocks (37%), siliciclastic sedimentary rocks (20%) and metamorphic rocks (20%). Furthermore, they cover similar mountain regions as those included in the Global River Chemistry database (GLORICH)[46] database and often used for upscaling[16,17] (Methods). Due to the low pCO_2 in mountain streams, we exclusively used measured CO_2 concentrations since CO_2 concentrations calculated from alkalinity, DIC and pH are prone to substantial errors[17,30,57], which is the reason why they are often aggregated over larger regions. The model retained altitude (partial correlation: -0.65, P<0.001), soil organic carbon content (partial correlation: 0.10, P<0.001) and discharge (partial correlation: -0.09, P<0.001) as predictors. Altitude affects streamwater CO_2 concentration along several lines. Streamwater temperature, terrestrial net ecosystem production (NEP)[136]

and soil organic carbon content decrease with increasing altitude; NEP and soil organic carbon content are positively related to carbon fluxes in inland waters in general[23,138]. Besides elevation, discharge also scales broadly with channel slope and bed roughness in mountain streams[54], all of them conducive to accelerated gas exchange and hence lower streamwater CO_2 concentration moving upstream.

We calculated the normalized gas exchange velocity k_{600} (for CO_2 at 20°C) using a recently published scaling relationship based on energy dissipation (*eD*), which is the product of flow velocity, channel slope and the gravity acceleration[54]. This relationship accounts for the high turbulence owing to steep-channel slopes and elevated streambed roughness of mountain streams. Channel width and flow velocity were calculated from hydraulic geometry scaling laws derived for mountain streams with an annual discharge smaller than 2.26 $m^3\ s^{-1}$ (Methods, Figure S4:3). Channel slope was determined using streamlines combined with digital elevation models (DEM) (Methods). We acknowledge that this approach does not account for the step-pool structure in mountain streams that can locally increase channel slope[139]. Our slope estimates are therefore conservative (Methods). Moreover, we retained only streams with a predicted *eD* smaller than 1.052 $m^2\ s^{-3}$ to be within the boundary of the input data used for the gas exchange model (ref. [54]). In addition, we restricted the upper elevation boundary to 4938 m (a.s.l), corresponding to the highest sampling location included in our CO_2 model.

Rather than directly predicting streamwater temperature, channel width, flow velocity, CO_2 concentration, and temperature dependent CO_2 exchange velocity (k_{CO2}), we computed each of these parameters using Monte Carlo simulations with 10,000 iterations for each individual stream (Methods). Thereby we were able to propagate the error associated with each of these parameters into an uncertainty related to cumulative (e.g., regional or global) CO_2 evasion fluxes. We used the typology proposed by Meybeck and colleagues[45] for the identification of mountain catchments as those with an average altitude higher than 500 m above sea level (a.s.l.) and an average relief roughness exceeding 20 to 40‰ depending on elevation as computed from digital elevation models (DEM) (Methods). A similar classification of mountains was also used to assess the relevance of mountains for water resources[140]. We then defined streams draining these regions as mountain streams.

4.3.2 CO_2 evasion fluxes from Swiss mountain streams

In a first step, we applied our upscaling approach to Switzerland where the availability of a high-resolution DEM (2 m) and accurate discharge data allowed us to reliably predict streamwater CO_2 concentrations and gas exchange velocity. Applying our selection criteria (i.e., restricting according to the mountain stream classifications, discharge and *eD*), we retained 23,343 streams (86% of them belonging to 1st to 4th Strahler order) for which we computed a median k_{600} of 116 m d^{-1} (7.5 and 650 m d^{-1}, 5th and 95th confidence interval quantiles, CI, respectively). The median of the corresponding temperature-corrected gas exchange velocities for CO_2 (k_{CO2}) was 86.4 m d^{-1} (CI: 6.0 and 462 m d^{-1}) (Figure 4:1a). These numbers are higher than those used to calculate regional and global estimates of CO_2 evasion from streams and rivers[16,17]. We attribute this difference to the novel scaling relationships for k_{600} (ref. [54]) that we used and that take into account the role of turbulence in accelerating gas exchange in mountain streams.

We estimate median streamwater pCO_2 of 705 µatm (CI: 380 and 1224 µatm) for the Swiss streams (Figure 4:1b). By combining predicted streamwater CO_2 concentrations with k_{CO2} we compute a median areal CO_2 evasion flux of 3.5 kg C m^{-2} yr^{-1} (CI: -0.5 and 23.5 kg C m^{-2} yr^{-1}) (Figure 4:1c). These areal fluxes are unexpectedly high, equivalent or even higher than those reported for the Amazon[135,141] and boreal[42,116] streams, which, among the inland waters, are typically considered as major emitters of CO_2 to the atmosphere. Over the 23,343 streams, these areal fluxes result in a total CO_2 evasion flux of 0.248±0.012 Tg C yr^{-1} from small Swiss mountain streams.

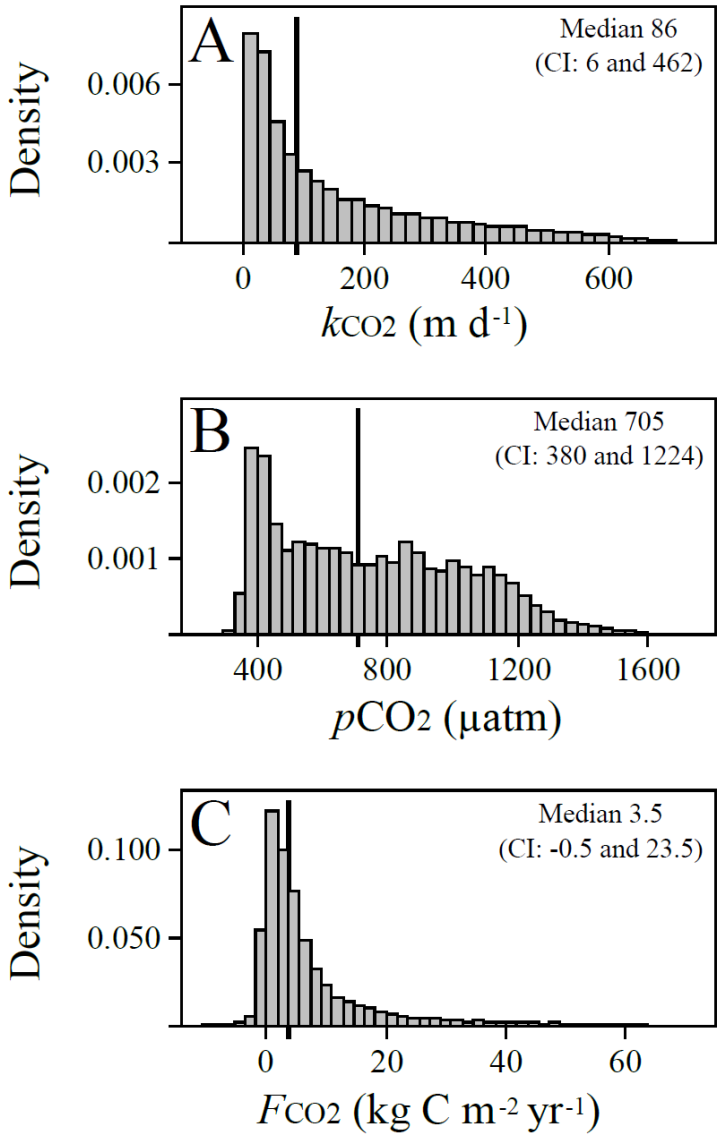

Figure 4:1 Patterns of CO_2 in streams in the Swiss Alps. The distributions of k_{CO2} (A), pCO_2 (B) and areal CO_2 fluxes (F_{CO2}) (C) for 23,343 mountain streams in Switzerland.

4.3.3 Potential sources of CO_2 in Swiss mountain streams

It is intuitive to assume that high evasion fluxes rapidly deplete CO_2 stocks in turbulent mountain streams and therefore cause the consistently low pCO_2 in these streams[119]. However, pCO_2 above saturation as often observed in mountain streams would imply a continuous supply of CO_2 able to sustain the high evasion fluxes. Groundwater is recognized as a potentially important delivery route of CO_2 into headwater streams[37,38,120,128]. To explore the potential of such CO_2 deliveries from groundwater into mountain streams in Switzerland, we applied a simple mass balance for CO_2 fluxes assuming that all CO_2 within a stream segment originates from groundwater discharge (Methods). Solving the mass balance for the groundwater CO_2 concentration in 3858 streams, we found that a median CO_2 concentration of 105 µmol L^{-1} in the groundwater, equivalent to a median pCO_2 of 2195 µatm (CI: 42 and 38,867 µatm) would be required to sustain in principle the CO_2 evasion flux from these streams (Figure 4:2a). This median value is indeed closely bracketed by measured pCO_2 (1343 to 4267 µatm) in the groundwater within two of our Swiss study catchments (Table 4S:2). Available data on groundwater CO_2 concentrations in mountain catchments are rare, and we therefore compare the expected groundwater CO_2 concentrations derived from our mass balance calculations also with data that are not necessarily from such catchments. For instance, maximum pCO_2 measured in groundwater in headwater catchments in Belgium, Czech Republic and Laos (Methods) were close to our expected 95th CI quantile of 51,647 µatm. Not unexpected, the variation of our estimates is large given the wide range of hydrological (e.g., fed by groundwater, snowmelt and glacier ice melt), geomorphological and geological characteristics of these streams and their catchments. Moreover, due to the lack of appropriate data, we were not able to include alkalinity as a

potential sink for CO_2 in the mass balance[72]. Nevertheless, the agreement between estimated and reported CO_2 concentrations suggests that groundwater CO_2 contributions are potentially relevant to sustain the CO_2 evasion fluxes from mountain streams.

Our notion of external CO_2 sources to the mountain streams was further supported by various lines of geochemical evidence (Methods; Supplementary Note 1, Figure 4S:4; Figure 4S:5). The streamwater ion balance suggests that the streams are representative for headwaters draining catchments with carbonate rock[30,46] (Figure 4S:4), and more important, that they are carbonate buffered to saturation (median calcite saturation index ranging from 2.48 to 4.11). This would imply a continuous supply of dissolved inorganic carbon (DIC) to the streams with new CO_2 re-equilibrating due to CO_2 evasion. As a further result, streamwater alkalinity was elevated (median: 2.05 meq L^{-1}; range: 0.94 to 2.85 meq L^{-1}), even beyond the threshold where DIC from carbonate weathering can drive CO_2 supersaturation in numerous lakes worldwide[142]. Therefore, in conjunction with respiratory CO_2 from soils, the dissolution of carbonate minerals can be a potential source to the CO_2 evasion flux from the mountain streams.

The notion of a lithogenic CO_2 source is further supported by stable isotope analyses of streamwater DIC (Methods). Across our study streams (n=134), we found $\delta^{13}C$ values ranging from -11.6 to -1.76‰ VPDB (median: -5.8, CI: -9.9 and -2.5) (Figure 4:2b, Figure 4S:5). Overall, these values are closely bracketed by reported isotopic compositions for soil organic matter (ranging from -30 to -24[90]) and carbonate rocks (close to zero[90]) as two end-members of the $\delta^{13}C$ variability continuum[90,143]. This implies contributions from both the respiration of organic carbon and lithogenic sources to the streamwater DIC pool. Given the overall very low concentrations of dissolved organic carbon (DOC; 254 ± 124 µg C $liter^{-1}$; Methods) in our study streams, we suggest that most of the depleted DIC is from respiratory CO_2 from soils and delivered by groundwater to the streams. The delivery of DIC from lithogenic sources (mostly carbonate weathering) into streams and its subsequent outgassing as CO_2 into the atmosphere is increasingly being recognized[72,82,120]. However, the underlying processes seem less evident and certainly require more attention in the future. We suggest that depending on the carbonate buffering capacity, both dissolution of atmospheric CO_2 (but also from soil respiration) could lower the pH in the soil water, groundwater and ultimately in the streamwater. If the streamwater is already saturated in CO_2 with respect to the atmosphere, DIC would be converted into CO_2 that may ultimately outgas from the stream[72]. Furthermore, cold water can dissolve more CO_2, which facilitates the dissolution of carbonates in the soil water and groundwater; if these waters warm in the stream, carbonates can re-precipitate with the concurrent release of CO_2 (ref. [144]). We suggest that this retrograde solubility further adds to the CO_2 outgassing from streams when colder groundwater transports dissolved carbonates to warmer streamwater in summer. Whereas the relative effect of pH changes on streamwater pCO_2 may outweigh the effects of temperature, we suggest that their combination can be important for the conversion of bicarbonates to carbonic acid (and CO_2) in mountain streams.

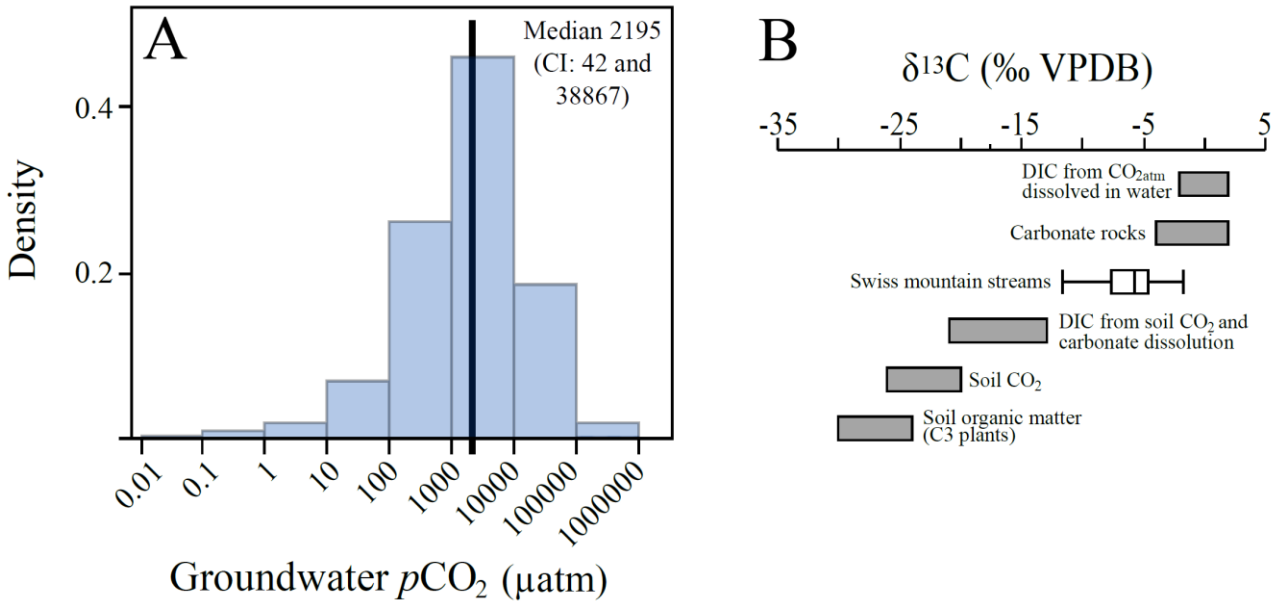

Figure 4:2 Sources of CO_2 in streams in the Swiss Alps. (A) Estimated groundwater pCO_2 in Swiss mountain catchments. (B) Isotopic compositions of dissolved inorganic carbon ($\delta^{13}C$-DIC) indicates biogenic (e.g., soil respiration) as well as geogenic sources (more enriched) (‰ Vienna Pee Dee Belemnite, VPDB). End-members are adopted from refs. [90,143]. The box plot shows median and quartile $\delta^{13}C$-DIC compositions repedetly sampled across the 12 Swiss sites (n=134; 7 to 15 samples per stream) (calculated in JMP 13, SAS Institute Inc., USA).

4.3.4 CO_2 evasion fluxes from the world's mountain streams

In a second step, we extrapolated our findings from the Swiss Alps to assess the CO_2 evasion fluxes from the world's mountain streams. The accuracy of geomorphological and hydrological parameters extracted from DEMs and other maps depends on their spatial resolution. Therefore, before transferring our approach from the Swiss streams, we compared the statistical distributions of elevation, stream slope, discharge obtained from our high-resolution dataset with those obtained from low-resolution data available for approaches at the global scale (Supplementary Note 2). We found surprisingly good agreement between both approaches (Figure 4S:6), and were therefore confident to proceed with the upscaling of CO_2 fluxes from mountain streams at the global scale. Here we used the Global River Classification (GloRiC) database[145], an extended version of HydroSHEDS, that describes drainage networks of Earth's surface in 15 arc-second (~500 m) spatial resolution including the networks above the 60°N latitude. These northern regions were poorly represented in previous estimates of global CO_2 evasion fluxes from streams and rivers[16,17]. Discharge data included in the GloRiC database were used to infer stream flow velocity and channel width (Methods). Rather than presenting streamwater pCO_2, we present the CO_2 gradient (ΔCO_2) as the difference between streamwater and atmospheric CO_2 concentration. In combination with k_{CO2}, ΔCO_2 is useful to understand the drivers of the CO_2 fluxes and to evaluate the spatial distribution of potential sources and sinks of CO_2.

Using the same selection criteria as for the Swiss mountain streams, we retained a total of 1,872,874 stream segments for which we calculated a global median k_{600} of 31.4 m d^{-1} (CI: 4.6 and 460 m d^{-1}) and a corresponding median k_{CO2} of 25.6 m d^{-1} (CI: 3.5 and 411 m d^{-1}) (Figure 4S:7a). These are 3.7 and 3.4 times lower, respectively, than the average gas exchange velocity calculated for the Swiss streams. The skewed distribution of global k_{CO2} towards smaller values may result from the abundant streams draining large plateaus (e.g., interior Tibetan Plateau, Altiplano) (Figure 4S:7a). We predicted a median streamwater pCO_2 of 737 µatm (CI: 317 and 1644 µatm) (Figure 4S:7b), which are lower than the global predictions of 2400 to 3100 µatm from studies that were likely biased towards larger streams and rivers[16,17]. However, our values are comparable with pCO_2 values reported from streams that drain mountain regions[16,47] and that were not included in our predictive model for streamwater CO_2 concentration. Overall, this agreement corroborates our CO_2 model and Monte Carlo simulation approach. We calculated a median global areal CO_2 evasion flux of 1.1 kg C m^{-2} yr^{-1} (CI: -0.54 and 32 kg C m^{-2} yr^{-1}) (Figure 4S:7c). Overall, we found negative CO_2 fluxes in 10.8 % of the streams (that is, these streams are potential sinks of atmospheric CO_2).

Overall, the spatial distribution of k_{CO2}, ΔCO_2 and areal CO_2 fluxes followed the variation of mountain topology (Figure 4:3). For instance, streams (median elevation: 4236 m a.s.l.; CI: 2676 and 4886 m a.s.l.) draining the inner Tibetan Plateau have low pCO_2 (median: 288 µatm; CI: 194 and 449 µatm) translating into a negative median ΔCO_2 of -56 mg C m^{-3} (CI: -105 and 23 mg C m^{-3}). Similar CO_2 concentrations close to equilibrium were also reported by others for streams[146] and lakes[147] on the Tibetan Plateau**.** These gradients result in an overall negative areal CO_2 flux of -0.36 kg C m^{-2} yr^{-1} (CI: -4.29 and 0.87 kg C m^{-2} yr^{-1}) (Figure 4S:8). Our estimates would therefore suggest that the Tibetan Plateau streams potentially act as a net sink (total flux: -1.46 Tg C yr^{-1}; CI: -1.52 and -1.39 Tg C yr^{-1}) of atmospheric CO_2. On the other hand, tropical mountain streams generally exhibited higher ΔCO_2 values, likely due to terrestrial inputs of CO_2 from soil respiration[108] and the in-stream degradation of terrestrial plant material[91]. At higher elevations, outside the tropical biome, lower ΔCO_2 values were compensated by high k_{CO2} because of steep stream channels, which resulted in high areal CO_2 fluxes.

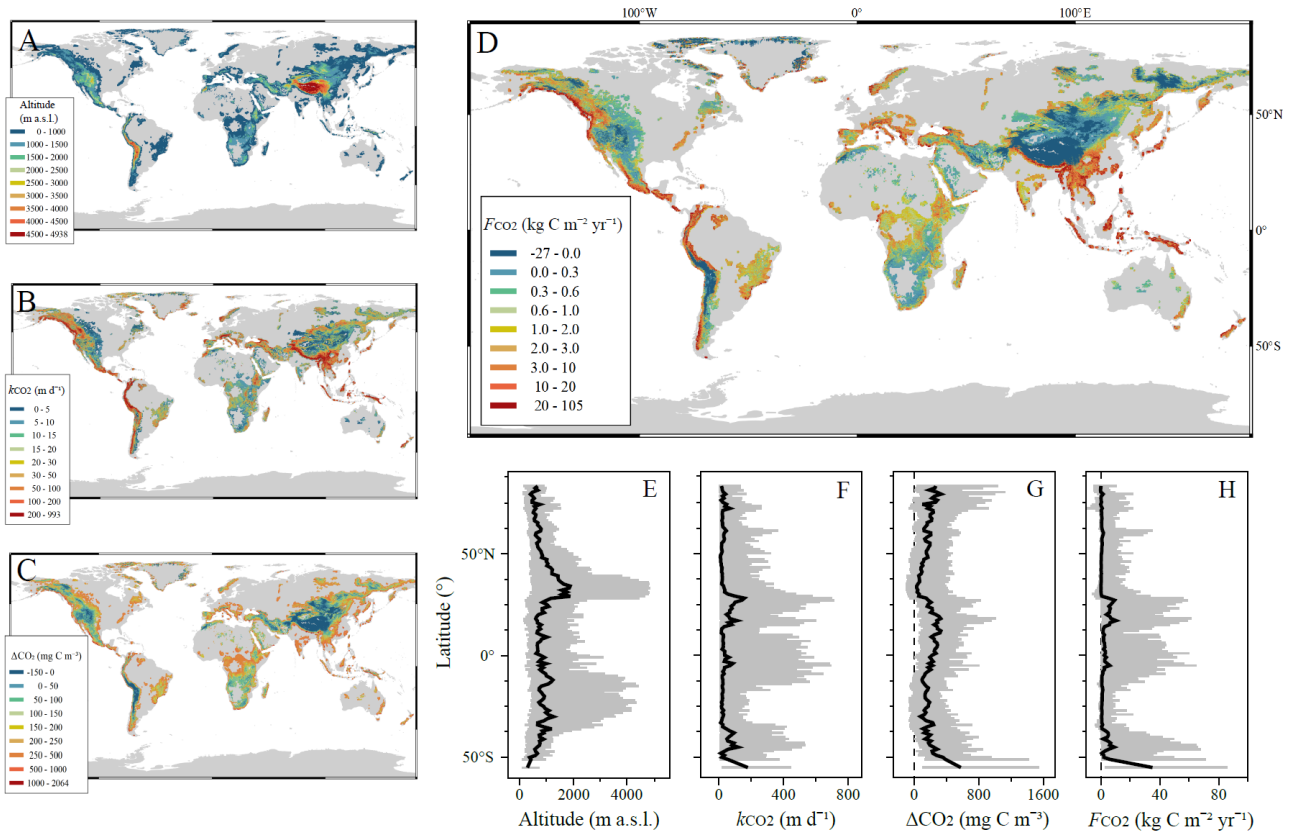

Figure 4:3 Global distributions of CO_2 in mountain streams. (A) Altitude of mountain streams, where mountains as defined according to ref. [45]. Panels B, C and D show the global distribution of predicted CO_2 exchange velocities (k_{CO2}), CO_2 gradients between the streamwater and the atmosphere (ΔCO_2) and the areal CO_2 fluxes (F_{CO2}), respectively. Panels E, F, G, and H show the latitudinal transects of these same parameters at 1-degree resolution (shown are median values in black and 5% and 95% confidence intervals in grey).

We estimated the net global CO_2 evasion flux from mountain streams by cumulating the average positive and negative CO_2 fluxes calculated from Monte Carlo simulations (10,000 iterations) for 1,872,874 streams (Methods). We obtained a net global CO_2 evasion flux of 166.6 Tg C yr^{-1} (CI: 165.9 and 167.4 Tg C yr^{-1}) from mountain streams. The magnitude of this evasion flux is high given that the mountain streams included in this study cover a surface area of 34,979 km^2, which corresponds to 4.5% or 6.0% of the global extent of streams and rivers as recently published by ref. [36] (773,000 km^2) and as calculated from GloRiC (587,630 km^2), respectively (Methods). Our estimate of the global net CO_2 evasion flux from mountain streams is within the same range as the total CO_2 evasion fluxes from tropical streams (excluding the large rivers and their floodplains) (160 to 470 Tg C yr^{-1}) [16,17,135] and substantially higher than those reported from the boreal-arctic streams and rivers (14 to 40 Tg C yr^{-1})[16,148].

As for the Swiss Alps, we suggest that, in the absence of major soil development within the catchment, DIC derived from carbonates may contribute in conjunction with soil respiratory CO_2 to the outgassing from these streams. This assumption would be supported by the fact that many of the world's streams drain catchments containing carbonate rocks[30,121,149] and that many of them have an alkalinity (median: 1.51 meq L^{-1}; CI: 0.09, 5.13 meq L^{-1}; from GLORICH[46]) that is relevant for DIC from carbonate dissolution to drive CO_2 supersaturation[142]. Our findings thus contribute to increasing understanding that CO_2 from carbonate dissolution plays a hitherto poorly recognized role for the CO_2 evasion fluxes from inland waters[37,120,142]. Alternatively, the oxidation of rock-bound carbon (i.e., petrogenic carbon) can be a source of CO_2[150], especially in glacierized catchments regularly exposed to frost shattering[151]. This is often the case with mountain streams.

Therefore, we propose that groundwater deliveries of geogenic and hence ancient CO_2, besides the CO_2 from soil respiration, is a significant contributor to the CO_2 efflux from mountain streams. This would be facilitated by topographic roughness of mountain regions generating longer groundwater flow pathways and by bedrock fractures enhancing permeability and deep infiltration, and ultimately resulting in longer residence times of water within mountain catchments[152]. Deeper infiltration and extended residence times of groundwater would also increase the concentration of weathering products[153] in the groundwater that enters mountain streams.

4.3.5 Temporal variations

The extrapolation of CO_2 fluxes from streams and rivers to a regional or global scale rarely takes into account the temporal variability of the fluxes[16,17]. This runs against the recognition that CO_2 fluxes from streams and rivers can change on a seasonal and diurnal basis[49,66]. Furthermore, depending on the zero degree isotherm[154], mountain streams can fall dry, or they are snow-covered during winter. Factoring this variability into an upscaling effort of gas fluxes is difficult though exposition, terrain slope and groundwater upwelling all are factors that affect the snow cover locally. For instance, even during winter mountain streams can have reaches without snow cover, which serve as hotspots for outgassing of CO_2 that has accumulated upstream from groundwater deliveries into the snow-covered channel.

To assess the potential inaccuracy emanating from the temporal variation of CO_2 fluxes for our upscaling, we compared the median CO_2 flux (on an annual basis) calculated from the continuous measurements (every 10 minutes) with the predicted annual CO_2 flux in several of our Swiss study streams with rather complete time series (Supplementary Note 3). We found good congruence between the measured and predicted fluxes (R^2 = 0.68, P=0.02, slope = 0.93±0.28), which we consider as a further proof of the robustness of our scaling approach (Figure 4S:9).

4.3.6 Uncertainties and limitations

Upscaling of CO_2 evasion fluxes from streams and rivers is not an easy task and requires an element of simplification and speculation. This is particularly true for small mountain streams. A first level of uncertainty emanates from the definition of a mountain and the spatial resolution and aggregation used to identify mountain regions. We used the parsimonious aggregation approach at a 0.5° spatial resolution as previously done to quantify runoff in mountain regions[45,140]. We recognize that applying the filters (e.g., spatial resolution, relief, altitude) differently may lead to different global maps of mountain streams[45,140].

Channel width is inherently difficult to estimate for small streams. Rather estimating channel width from hydromorphological scaling relationships that also require information on hydraulic resistance[34,36], we derived channel width from hydraulic scaling relationships specifically established for mountain streams in combination with discharge from the GloRiC database[145]. Discharge is available at the level of spatial resolution required for upscaling CO_2 fluxes, whereas parameters for hydraulic resistance are not. Furthermore, by using discharge to infer width and velocity, but also to predict streamwater CO_2 concentration, we constrain errors to the same source. Our approach yielded a minimum stream channel width of 0.32 m, which is identical with the stream width reported by Allen and colleagues[34] as the characteristic most abundant stream width in headwater catchment.

The overall uncertainty associated with our regional and global CO_2 fluxes appears small compared to previous upscaling studies[16,17]. This is inherent to the structure of our uncertainty computation that assumes that errors in the estimation of fluxes at the stream segment level are independent. Therefore, summing up largely uncertain stream segment fluxes results in a global estimate with a small uncertainty compared to the median value, because errors average out if they are independent[155]. This is analogous to the reduction of the coefficient of variation of the sum of identically distributed, independent random variables, as predicted by the central limit theorem. Assuming that errors are fully independent is an approximation, of course, as is the assumption of fully correlated error as the opposite extreme. Therefore, we also computed the uncertainty with the latter assumption (Methods) and found a larger uncertainty associated with the total flux for the mountain streams in Switzerland (CI: -0.107 and 0.939 Tg C yr^{-1}) and worldwide (CI: -27.7 to 561.9 Tg C yr^{-1}). The large discrepancy between the two uncertainty approaches is not unexpected and the real uncertainty is probably somewhere between both approaches.

In summary, our study reveals small streams of the world's mountains as an important yet hitherto poorly appreciated component of the global carbon cycle. High turbulence, induced by elevated channel slopes and streambed roughness, accelerates the evasion of CO_2 delivered from geogenic and biogenic sources by the groundwater into the mountain streams. The proper integration of the CO_2 evasion from mountain streams will further reduce the uncertainties around global carbon fluxes in inland waters.

4.4 Acknowledgements

We are grateful to Alba Algerich, James Thornton, Paul del Giorgio, Andrea Popp, Anne Marx, Clément Duvert, Catherine Kuhn, Lishan Ran, Steven Bouillon, Bin Qu, Vincent De Staercke, Michail Stylllas, Matteo Tolsano and Peter Raymond. We acknowledge the help of Nicolas Escoffier, Valentin Sahli, Rémy Romanens, Félicie Hammer, Amin Niayifar and Marta Boix Canadell with fieldwork. Peter Raymond provided useful comments on an earlier version of the manuscript. Financial support came from the European Union's Horizon 2020 research and innovation programme under the Marie Skłodowska-Curie grant agreement No 643052 (C-CASCADES project) and the Swiss Science Foundation (SNF, 200021_163015) to T.J.B.

4.5 Material and methods

4.5.1 On-line measurement of pCO_2 in Swiss streams

We operated 12 sensor stations in high-altitude Alpine catchments; 4 catchments with 3 stations in each (Figure 4S:1). Site elevation ranges from 1200 to 2161 m a.s.l., stream slope from 0.033 to 0.160 m m-1 and annual mean discharge from 0.02 – 2.26 m3 s-1. At the stations, we measured streamwater pCO_2 continuously (10 minute intervals) during two years (2016-2018) (Table 4S:1). Prior to deployment, we prepared the pCO_2 sensors (Vaisala CARBOCAP® Carbon Dioxide Transmitter Series, GMT220, Finland) with a porous polytetrafluoroethylene (ePDFE) semi-permeable membrane that we sealed with liquid electrical tape[63]. We protected our water-proof pCO_2 sensors with fine grained mash, PVC tube, and metal casing. We connected the sensors to two 12-volt batteries in series coupled with solar panels located at the streambed side.

4.5.2 Geochemical analyses and potential CO_2 sources

Filtered streamwater samples (Mixed Cellulose Ester filter, 0.22 µm) were repeatedly collected for the analyses of cation and anion concentrations between 2016 and 2018 in twelve study streams in the Swiss Alps and analyzed using ion chromatography (ICS-3000 Dionex, Sunnyvale, CA, USA). We also sampled streamwater for dissolved organic carbon (DOC) concentration. For DOC, we filtered (GF/F filters, Whatman) streamwater into 40 mL acid-washed and pre-combusted glass vials and analyzed within 1 to 3 days (Sievers M5310c TOC Analyzer, GE Analytical Instruments, USA). The accuracy of the instrument is ± 2%, precision <1% and detection limit 1.83 µmol C L^{-1}.

Furthermore, we measured concentrations and the isotopic composition of dissolved inorganic carbon (DIC; δ^{13}C-DIC). Samples for DIC concentration and δ^{13}C-DIC were collected in 12 mL glass vials and filtered (Mixed Cellulose Ester filter, 0.22-µm) to retain the dissolved fraction. In the laboratory, we injected 2 mL streamwater into pre-flushed (synthetic air, pCO_2<5 ppm) exetainers containing 300 µL of 85% orthophosphoric acid. Samples were then shaken (2 min) and equilibrated over night at room temperature. DIC samples were analyzed on a G2201-*I* Picarro Instrument (Santa Clara, CA, USA) as CO_2 released from the reaction with orthophosphoric acid. There are three possible sources of DIC: atmospheric CO_2, weathered carbonates, and soil-derived respired CO_2. Weathering and atmospheric exchange enriches the DIC stable isotope signature[86,92] where atmospheric CO_2 and rock carbonate will largely overlap in their δ^{13}C-DIC value if the rock is originally of marine origin. In contrary, contributions from respiration deplete the isotopic signature, depending on the plant type and diagenetic state of the decomposed organic matter[90,143].

4.5.3 Stream hydraulic geometry

We established hydraulic geometry scaling relationships from mountain streams in the Swiss Alps (Figure 4S:1), where we derived annual mean stream channel width (*w*), depth (*z*) and flow velocity (*v*) from annual mean discharge (Q) as follows (see also Figure 4S:3).

$$w = 7.104 \times Q^{0.447}$$

Equation 4:1 – Hydraulic scaling: stream channel width

$$z = 0.298 \times Q^{0.222}$$

Equation 4:2 – Hydraulic scaling: stream channel depth

$$v = 0.668 \times Q^{0.365}$$

Equation 4:3 – Hydraulic scaling: streamwater velocity

We performed a total of 141 slug releases where we added sodium chloride (NaCl) at the top of each reach (in average 12 slugs per site) and measured the change in specific conductivity at the bottom of the reaches. By measuring the change in specific conductivity, which we converted to mass by applying a pre-established relationship between specific conductivity and the conductivity potential of the added NaCl, we estimated discharge. We also estimated the travel time as the time for the NaCl to reach the bottom of the reach (i.e. the peak in the specific conductivity). To obtain average flow velocity we divided reach length by the travel time. We also measured stream width and stream depth.

In comparison to previous scaling relationships[52], our relationships are more representative for mountain streams, where steeper slopes induce higher flow velocities and narrower channels. Annual mean discharges ranged from 0.02 to 2.26 m^3 s^{-1} in our study

streams (n = 12) in the Swiss Alps. The maximum annual mean discharge was used as an upper boundary within which we consider our hydraulic geometry scaling valid, and we therefore restricted our data for all further analyses to streams with maximal annual mean discharge of 2.26 $m^3\ s^{-1}$. Hence we restrained our definition of mountain streams further and consider our estimates of CO_2 fluxes from mountain streams as conservative as we discarded streams with $Q > 2.26\ m^3\ s^{-1}$.

4.5.4 CO_2 flux calculations

We estimated the gas transfer velocity (k_{600}, m d^{-1}) using the following piece-wise power-law relationships as recently published by Ulseth and colleagues

$$\ln(k_{600})\ for\ eD > 0.02 = 1.18 \times \ln(eD)\ + 6.43$$

Equation 4:4 – Gas transfer velocity: high-energy streams

$$\ln(k_{600})\ for\ eD < 0.02 = 0.35 \times \ln(eD)\ + 3.10$$

Equation 4:5 – Gas transfer velocity: low-energy streams

where *eD* is the stream energy dissipation rate, which is the product of slope, flow velocity and the gravity acceleration. In order to use this gas transfer velocity equation, we restricted the streams used for our analyses to those where *eD* did not exceed 1.052 $m^2\ s^{-3}$, which was the maximum *eD* used in scaling relationship by Ulseth and colleagues[4].

To convert k_{600} into k_{CO2}, we calculated CO_2 saturation ($[CO_{2sat}]$ as

$$[CO_{2sat}] = 400.40 \times \frac{P_{atm}}{P_{std}} \times KH$$

Equation 4:6 – CO_2 saturation

using annual mean atmospheric CO_2 in 2017 (400.40 µatm) measured at Jungfraujoch, Switzerland (World Data Centre for Greenhouse Gases (WDCGG), Japan, 2018). Then, by multiplying with the Henry constant (K_H, mol L^{-1} atm^{-1}) and the ratio between atmospheric pressure (P_{atm}, atm) and standard pressure of 1 atmosphere (P_{std}, atm) we calculated the CO_2 saturation ($[CO_{2sat}]$, mol L^{-1}).

In Equation 4:7, P_{atm} changes with elevation (E),

$$P_{atm} = P_0 \times \frac{T_b}{T_b + \lambda \times E}^{\frac{g \times m}{R \times \lambda}}$$

Equation 4:7 – Atmospheric pressure

where P_0 is the International standard atmosphere (ISA) values of sea level pressure (101,325 Pa) and T_b is an assumed sea level temperature of 19°C (292.15 K). λ is the temperature lapse rate (-0.0065 K m^{-1}), g is the gravity acceleration (9.80616 m s^{-2}), m is the molecular weight of dry air (0.02897 kg mol^{-1}), and R is the gas constant (8.3143 J mol^{-1} K^{-1}). We multiplied the values derived from Equation 4:7 with 9.86923×10^{-6} to obtain P_{atm} in atmospheres[156].

K_H is a function of water temperature (T_K, Kelvin), where A (108.3865), B (0.01985076), C (-6919.53), D (-40.4515) and E (669365) are constants[124].

$$K_H = 10^{A+B\times(T_K)+\frac{C}{T_K}+D\times log10(T_K)+\frac{E}{{T_K}^2}}$$

Equation 4:8 – Henry's constant

To estimate streamwater temperature, we extracted gridded air temperatures[157], which we translated into streamwater temperatures according to a relationship between streamwater temperature (T_w) and air temperature (T_{air})[16].

$$T_w = 3.941 \pm 0.007 + 0.818 \pm 0.0004 \times T_{air}$$

Equation 4:9 – Streamwater temperature

We used the temperature-dependent Schmidt scaling (Equation 4:10)[51] to convert k_{600} (Equation 4:4 and 4:5 respectively) to k_{CO2} (Eq. 4:11).

$$Sc_{CO2} = 1923.6 - 125.06 \times T_w + 4.3773 \times {T_w}^2 - 0.085681 \times {T_w}^3 + 0.00070284 \times {T_w}^4$$

Equation 4:10 - Schmidt scaling for CO_2

$$k_{CO_2} = \frac{k_{600}}{\left(\frac{600}{Sc_{CO2}}\right)^{-0.5}}$$

Equation 4:11 – Gas transfer velocity of CO_2

To estimate streamwater CO_2, we collected data from Swiss Alpine streams, which we combined with stream data from Austria[49], Kenya[158], U.S.A (A. Agerich, *personal communication*; ref. [50]; C. Kuhn, *personal communication*; P. del Giorgio, *personal communication*; P. Raymond, *personal communication*), Brazil[159], Tibet and China (refs. [48,106], L. Ran *personal communication*), and New Zealand (V. De Staercke, M. Styllas, and M. Tolsano, *personal communication*). We restricted our data set to only encompass mountain streams[45] with annual mean discharges[145] below 2.26 $m^3\ s^{-1}$. We predicted streamwater CO_2 concentration from a linear regression model using mean channel elevation (E)[160,161], mean annual discharge (Q)[145] and soil organic carbon content (SOC, g kg^{-1})[162] (Figure 4S:2), that we extracted with QGIS using the Point sampling tool. The model is based on a collection of 323 direct measurements of streamwater CO_2 concentration from mountain streams that were selected according to our selection criteria (i.e., elevation, relief, discharge). The regression model

$$\ln(\mathrm{CO_2}) = -0.647 \pm 0.052 \times \ln(E) - 0.094 \pm 0.014 \times \ln(\mathrm{Q}) + 0.099 \pm 0.029 \times \ln(\mathrm{SOC}) + 7.287 \pm 0.427$$

Equation 4:12 – CO_2 prediction model

explained 39% of the variation (R^2 = 0.39, n = 323, p<0.0001) in streamwater CO_2 concentration.

Finally, areal CO_2 fluxes (g C $m^{-2}\ d^{-1}$) were calculated as

$$F_{CO2} = k_{CO2} \times \Delta_{CO2}$$

Equation 4:13 – Areal CO_2 evasion fluxes

where the CO_2 gradient ΔCO_2 (converted to g C m^{-3}) is the CO_2 gradient between the streamwater and the atmosphere. To estimate total fluxes, we first estimated stream area (A) from stream width as derived from the hydraulic scaling relationships (Equation 4:1) and stream length (L) defined in the stream network dataset for Swiss (Federal Office for the Environment (FOEN) Switzerland, 2013) and global[145] streams. The total CO_2 flux per stream was then calculated as areal CO_2 fluxes multiplied with stream area.

4.5.5 Monte Carlo simulations and uncertainties

We used Monte Carlo (Matlab 2017b) approaches to simulate the parameters (i.e., streamwater CO_2 concentration, channel width, streamwater temperature, flow velocity and k_{CO2}) required for the calculation of CO_2 evasion fluxes and to estimate related uncertainties for each individual stream. We used two different approaches to quantify the uncertainty. A first approach was based on the assumption that errors in the calculation of F_{CO2} for each stream were independent. For each stream and for each of the 10,000 iterations, we perturbed the various scaling relationships by randomly extracting error approximations from their corresponding residual probability distribution. We thereby created for each Monte Carlo simulation a random extraction of the streamwater CO_2 concentration, stream width, streamwater temperature, flow velocity and k_{CO2} values for all streams, and finally 10,000 estimates of areal CO_2 evasion fluxes (according to Equation 4:13). We classified the upper 99.5 percentiles of all slope, streamwater CO_2 and areal CO_2 flux estimates as outliers and removed them from further analysis, to avoid unrealistically inflated values. Then, for each iteration, we derived a total flux by summing up the fluxes from all streams accounting for their contributing area. We thereby obtained 10,000 total flux estimates, from which we extracted the mean CO_2 evasion flux as well as the 5th and 95th percentiles as confidence intervals. For this approach, the largest uncertainty was related to the k_{600} model, while the hydraulic scaling relationships (for flow velocity and width), the streamwater temperature and streamwater CO_2 model contributed less to the overall uncertainty. The streamwater CO_2 concentrations, k_{CO2} and areal CO_2 fluxes reported in our study refer to the means obtained from the 10,000 iterations. The propagated CO_2 fluxes were summed to obtain a total estimate of the annual CO_2 evasion flux. As a consequence, the errors introduced at the different iterations average out. This resulted in a narrow CO_2 flux distribution due to the assumption of independent errors.

A second approach was based on the assumption that all errors in the calculation of F_{CO2} for each stream were perfectly dependent on each other. Thus, instead of summing the F_{CO2} across all streams and then draw the distribution from the different iterations, we used the distributions derived for each stream from the Monte Carlo simulations, from which we calculated the mean and confidence intervals. Then, we summed all means and confidence intervals separately to obtain the total F_{CO2} estimate and the uncertainties. With this approach, we obtained much larger uncertainties compared to the first approach. Because, under the assumption of error dependency, the percentiles of the total F_{CO2} distribution equal the sum of the percentiles of the single stream distributions. Reality is probably somewhere in between the two approaches and we therefore decided to report uncertainties estimated with both approaches.

4.5.6 Definition of mountain streams

We defined mountain streams as those draining terrain with an elevation above 500 m a.s.l. and more than 20 to 40‰ in relief roughness depending on elevation[45]. This approach was previously used to estimate water resources and runoff from the world's mountains[45,140]. We used the Global Multi-resolution Terrain Elevation Data (GMTED2010)[160], which we aggregated to 0.5˚ using mean elevations (ArcGIS 10.5, Aggregate tool). We derived relief roughness from the DEM (QGIS 3.2.1. with GRASS 7.4.1, Roughness tool) where relief roughness was calculated as the difference in a pixel's maximum and minimum elevation divided by half the pixel length.

4.5.7 Groundwater CO_2 mass balance

We calculated the groundwater CO_2 concentration that would be required in principle to sustain the CO_2 evasion fluxes from 3858 mountain streams in the Swiss Alps. To do so, we first estimated the flow between stream segments (From/To Node tool, Arc Hydro, Esri 2011). Then, we established a mass balance similar to refs. [37,71], where the difference in discharge (Q, $m^3\ s^{-1}$) between two stream segments, x and x+1, is assumed to be due to groundwater inflow (Q_{GW}). Therefore, the groundwater CO_2 concentration (C_{GW}, $\mu mol\ m^{-3}$) can be calculated as;

$$C_{GW} = \frac{f_x + (CQ)_{x+1} - (CQ)_x}{Q_{GW}}$$

Equation 4:14 – Groundwater CO_2 mass balance

where f_x is the CO_2 evasion flux ($\mu mol\ s^{-1}$), and C ($\mu mol\ m^{-3}$) is the CO_2 concentration in the streamwater.

Groundwater mass balance indicated that a median groundwater pCO_2 of 2195 µatm (CI: 42 and 38,867 µatm) would be required to sustain the CO_2 evasion flux from Swiss streams (computed for n = 3858). We compared the results obtained from the groundwater mass balance with groundwater pCO_2 data sampled in two of our study catchments; catchment B (Figure 4S:1) had a median groundwater pCO_2 of 1343 µatm (CI: 245 and 1936 µatm, n = 9; Table 4S:2) and catchment C had a median groundwater pCO_2 of 4267 µatm (CI: 2230 and 6303 µatm, n = 2; Table 4S:2). Yet, those few measurements of groundwater pCO_2 may underestimate groundwater CO_2 concentrations; measurements of groundwater pCO_2 in Belgium[163], Laos and Czech Republic (C. Duvert, *personal communication*) are 10-fold higher with measured values up to almost 50,000 µatm (highest measured value: 47,374).

4.5.8 Extrapolating CO_2 evasion

For Switzerland, we used the stream network from the Swiss Federal Office for the Environment (FOEN, 2013), which we combined with mean simulated natural annual discharge data (1981-2000) (FOEN, 2016). We created a node layer (Node tool) in QGIS and we extracted elevation data (Point sampling tool) from a highly resolved (2 m) digital elevation model (DEM) (Geodata © swisstopo). Prior to sampling, we resampled (nearest neighbor, median, 3-pixel radius in SAGA GIS 2.3.2) the DEM to remove outliers. We calculated stream slopes (Matlab 2017b) as the elevation difference per stream divided by the predefined stream length (FOEN, 2013). We extracted SOC content[162] for every node, which we averaged to mean values per stream. Similarly, we extracted monthly air temperatures[157], which we averaged over the year and converted to streamwater temperature[16] (Equation 4:9).

We estimated global CO_2 fluxes from mountain streams using a similar approach as for the Swiss streams. We used the GloRiC stream network at 15 arc-seconds (~500 m) spatial resolution, including streams north of 60˚ latitude[145]. To estimate stream channel slopes, we first resampled the DEMs to remove outliers (nearest neighbor, median value in a 3-pixel radius) in SAGA GIS 2.3.2. We used the SRTM 90 m[161], which we combined with the 30 s GMTED elevation layer[160] for streams above 60˚N. We created a node layer from the GloRiC stream network from which we extracted elevation (Node tool, QGIS) and calculated stream gradients (Matlab 2017b) as the elevation difference per stream divided by the predefined stream length[145]. We used the discharge from Dallaire and colleagues.

For every node, we also extracted the geopredictors required in the CO_2 model; soil organic carbon content[162] and air temperature[157] which we converted to streamwater temperature[16].

To approximate the total global stream area, we used all the streams and discharge data included in the GloRiC data set[145] and inferred width from the hydraulic scaling relationship equations for larger rivers[52]. In other words, since we wanted an approximate estimate for all streams and rivers, we used a well-established hydraulic scaling relationship (ref. [52]) to estimate stream width, which we combined with stream lengths from the GloRiC dataset. We summed all stream areas to estimate a total stream surface area (to estimate the stream area of mountain streams we used our own scaling hydraulic relationship to obtain stream width).

4.6 Supplementary Information

4.6.1 Supplementary Note 1

Marx and colleagues showed in 2017[30] that small streams (catchment sizes <30 km^2) have high geochemical variability but are skewed towards the carbonate end-member. This it related to short residence times in small headwater catchments, which favors fast weathered bedrock, such as carbonate bedrock weathering, rather than silicate weathering[30]. We repeated this analysis from Marx and colleagues using the same database, the Global River Chemistry database (GLORICH)[46], together with data from our Swiss monitoring stations. The geochemical characterization shows that the Swiss sites are indeed influenced by carbonate bedrock weathering (Figure 4S:4).

4.6.2 Supplementary Note 2

We evaluated differences between geopredictors for Swiss streams derived from data sets with different resolutions (highly resolved Swiss dataset and lower resolved globally available dataset; Figure 4S:6) to be confident that the stream channel slopes (Figure 4S:6a) stream altitude (Figure 4S:6b) and stream discharge (Figure 4S:6c) did not deviate considerably depending on data resolution. The distributions of the data were similar for the two datasets, although slope was somewhat lower in the high-resolution data set (median 0.039 m m^{-1}, CI: 0.004 and 0.176 m m^{-1}) compared to the low-resolution data set (median 0.055 m m^{-1}, CI: 0.004 and 0.222 m m^{-1}). Altitude was slightly higher in the high-resolution data set (median 902 m, CI: 415 and 2185 m) compared to the low-resolution data set (median 834 m, CI: 406 and 2141 m). Discharge was similar between the high-resolution data set (median 0.38 m^3 s^{-1}, CI: 0.09 and 1.77 m^3 s^{-1}) and the low-resolution data set (median 0.38 m^3 s^{-1}, CI: 0.12 and 1.82 m^3 s^{-1}).

Moreover, for all our monitoring stations in the Swiss Aps (Figure 4S:1) we measured stream channel slope every 10 meters' distance in the field using a dGPS system. We then compared the difference in stream channel slopes calculated for whole stream reaches with channel slopes calculated from segments of 10 m in length each. We found that in average the slope is underestimated by 0.022 m m^{-1} when using mean reach slope and not considering the variations in slopes along a stream reach. The maximum slope measured along the reach (10 m sub-reaches) deviated significantly from the mean reach slopes, and was up to 0.60 m m^{-1} higher. Across all 12 catchments, the maximum slope was 0.42 m m^{-1} higher compared to the reach slope. This suggests that the k_{CO2} values may be even higher than estimated in this study for Switzerland (median 86.4 m d^{-1}, CI: 6.0 and 461.9 m d^{-1}) and for mountain streams worldwide (median 25.6 m d^{-1}, CI: 3.5 and 410.6 m d^{-1}). Predicted streamwater pCO_2 was similar in Swiss streams (median 705 µatm, CI: 380 and 1224 µatm) and at the global extent (median 737 µatm, CI: 317 and 1644 µatm). 10.8% of the Swiss mountain streams, and the same proportion of the mountain streams worldwide has negative ΔCO_2 meaning that they fall below atmospheric saturation. The median areal CO_2 fluxes are higher from Swiss mountain streams (median 3.6 kg C m^{-2} yr^{-1}, CI: -0.5 and 23.5 kg C m^{-2} yr^{-1}) compared to mountain streams worldwide (median 1.1 kg C m^{-2} yr^{-1}, CI: -0.5 and 32.1 kg C m^{-2} yr^{-1}) (Figure 4S:7).

4.6.3 Supplementary Note 3

Estimating CO_2 fluxes based on mean or median values of CO_2 and discharge, instead of highly resolved data, may induce errors due to the temporal variability. We compared CO_2 fluxes derived from measured data at 10-minute time steps with CO_2 fluxes predicted using our CO_2 prediction model combined with Q from GloRiC. Due to data availability, this analysis was possible at 7 of our 12 high-altitude Alpine monitoring stations. Despite high temporal variability in CO_2 fluxes, we found median areal fluxes at the monitoring stations corresponding relatively well to the areal fluxes that we predicted in our study where the slope between F_{CO2} predicted by the model and F_{CO2} calculated from 10-minute time series was -0.921 ± 0.284 (R^2 = 0.68, n = 7, P = 0.0022) (Figure 4S:9).

4.6.4 Supplementary Figures

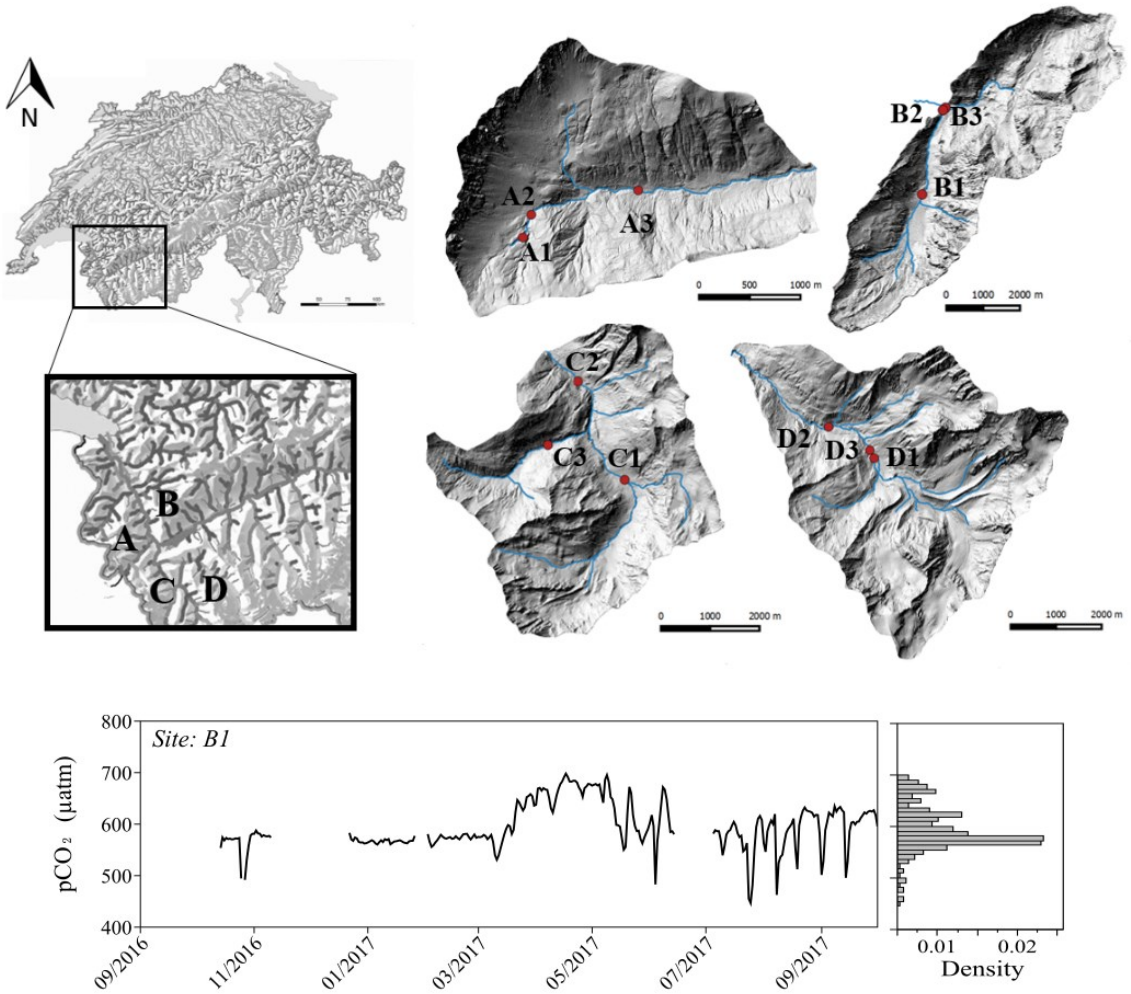

Figure 4S:1 We continuously monitored pCO2 in 12 streams located in 4 Alpine catchments in Switzerland. Our 12 mountain stream monitoring stations measured streamwater pCO_2 levels close to saturation throughout the year (median pCO_2 397 to 673 µatm, Table 4S:1).

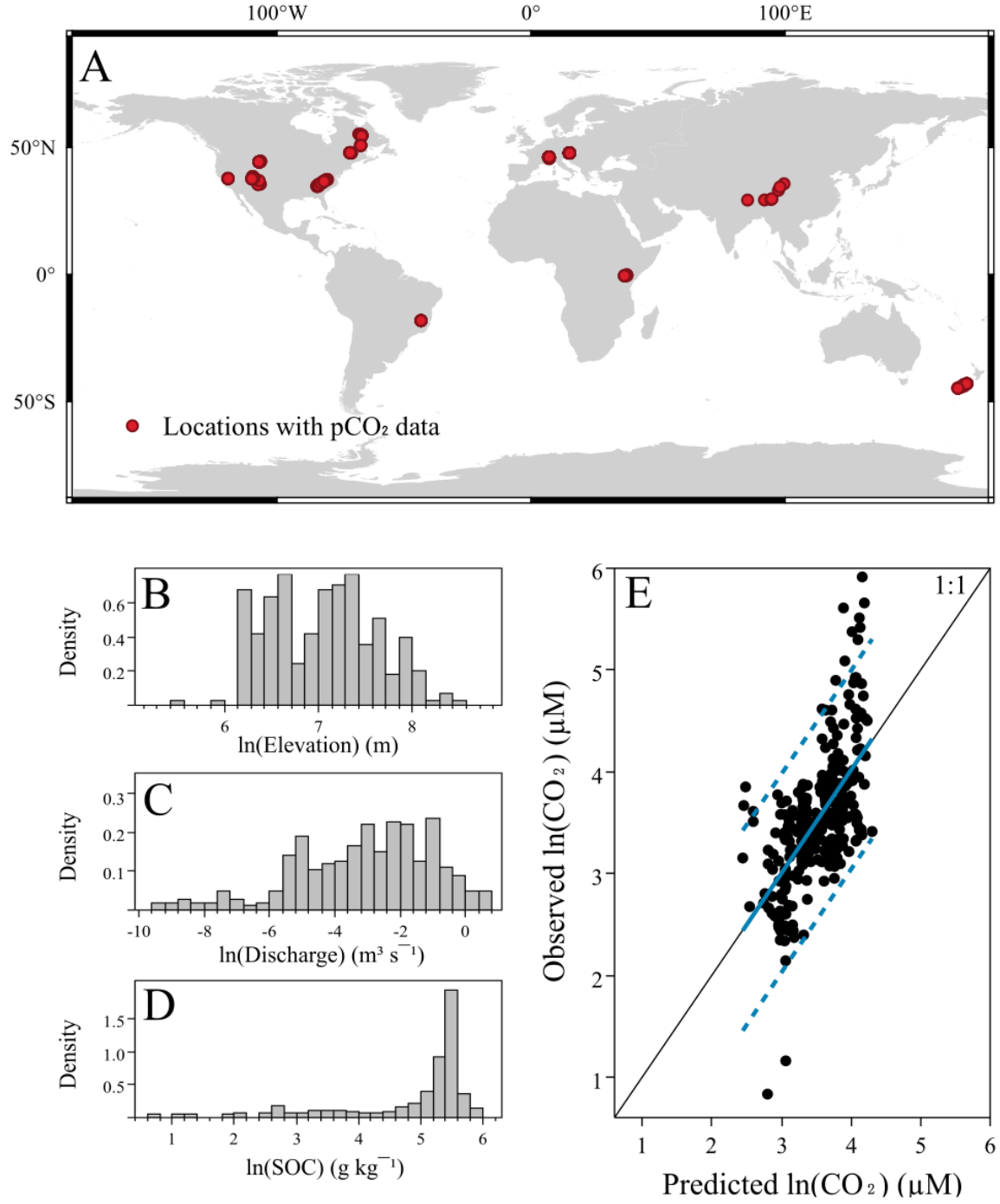

Figure 4S:2 Data input of the CO_2 model. Sampling locations for the mountain stream CO_2 data used for the prediction model (A). Shown are also density distributions of elevation (B), discharge (C) and soil organic carbon (SOC) (D), used as input parameters for the prediction of streamwater CO_2 concentrations (E). Observed versus predicted CO_2 followed the 1:1 line (blue) and fell within the 95% prediction confidence intervals (dashed blue lines) except for at very high CO_2 concentrations were CO_2 was underpredicted.

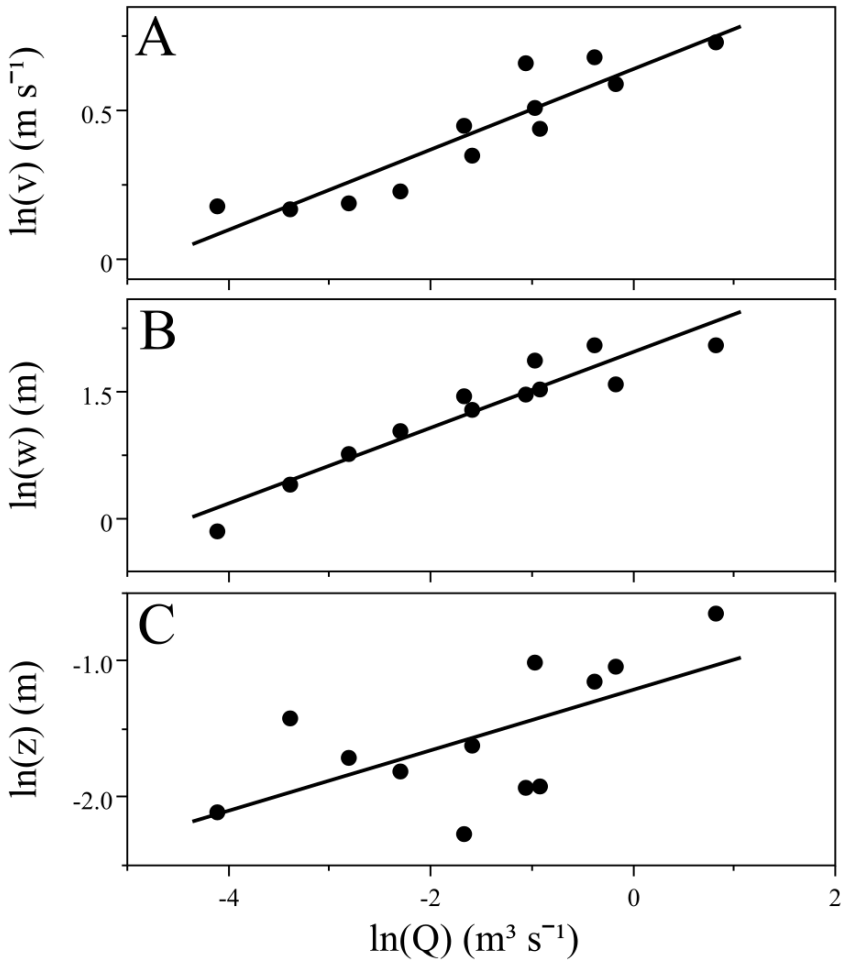

Figure 4S:3 Hydraulic scaling relationship (natural log) between annual average stream discharge (Q) and flow velocity (v), stream width (w) and stream depth (z). The relationships are derived from 141 measurements (7-17 measurements per sites) at 12 mountain stream monitoring stations in the Swiss Alps (velocity: $\ln(v) = 0.365 \times \ln(Q) - 0.403$, R^2 = 0.87; width: $\ln(w) = 0.447 \times \ln(Q) + 1.961$, R^2 = 0.90; depth: $\ln(z) = 0.222 \times \ln(Q) - 1.212$, R^2 = 0.39).

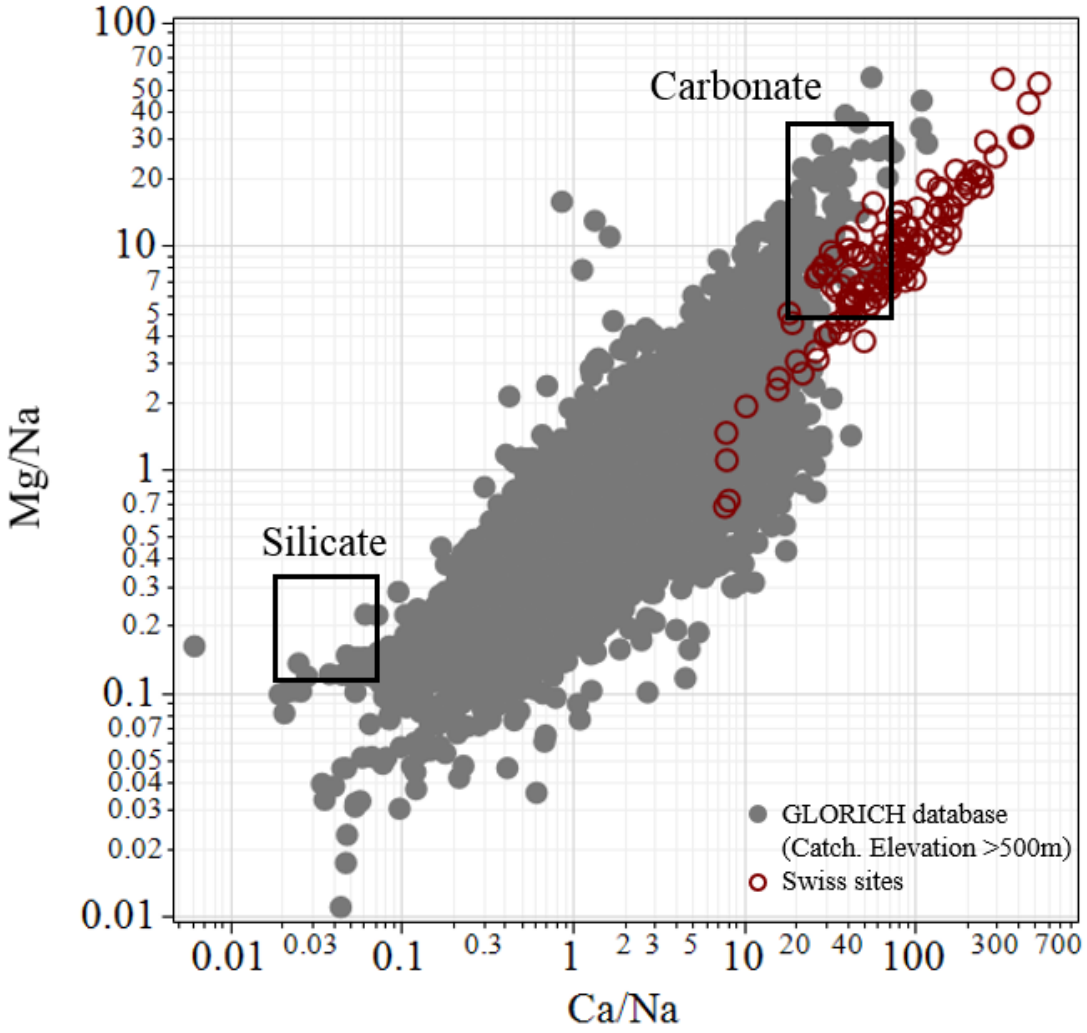

Figure 4S:4 Water samples from the Swiss sites (red) are all close to the carbonate end-member in this Na^+-normalized mixing diagram. The Swiss sites have similar Mg^{2+}/Na^+ and Ca^{2+}/Na^+ molar ratios as the carbonated sites in the GLORICH database (gray)[30,46,149].

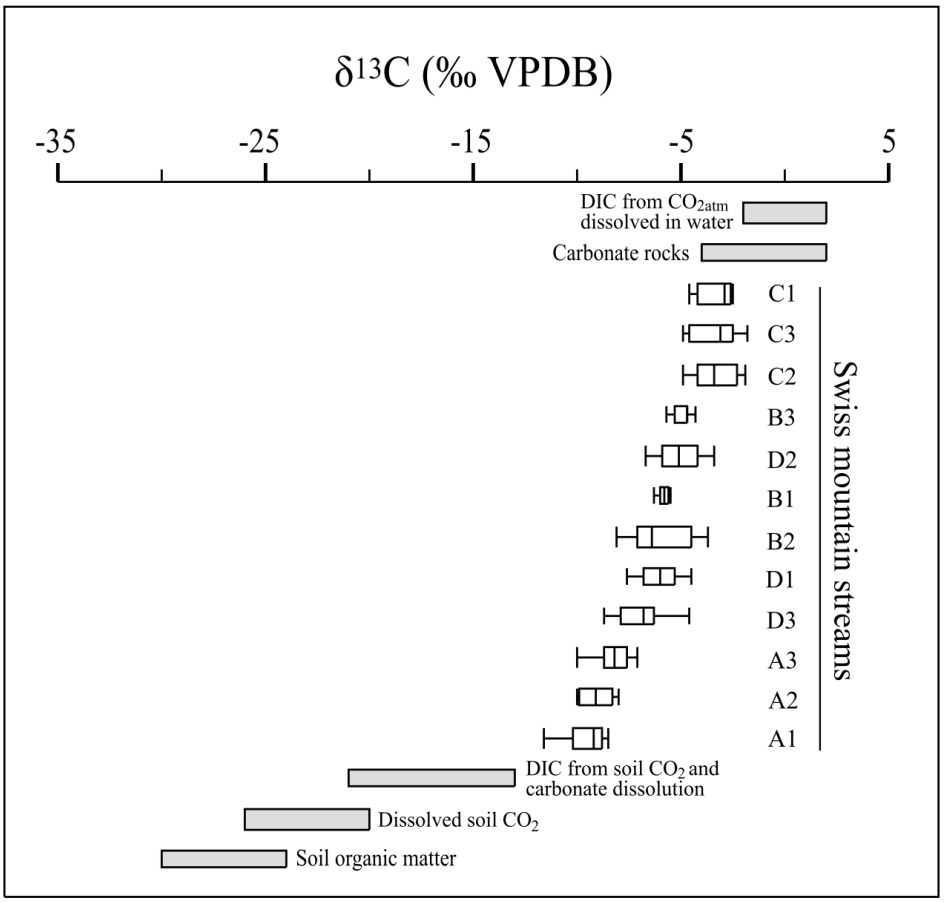

Figure 4S:5. Isotopic composition of the streamwater DIC (δ13C-DIC) for the 12 study streams (7 to 15 samples per stream). End-members are adopted from refs. [90,143]. The box plots show median and quartile δ13C-DIC compositions (calculated in JMP 13, SAS Institute Inc., USA).

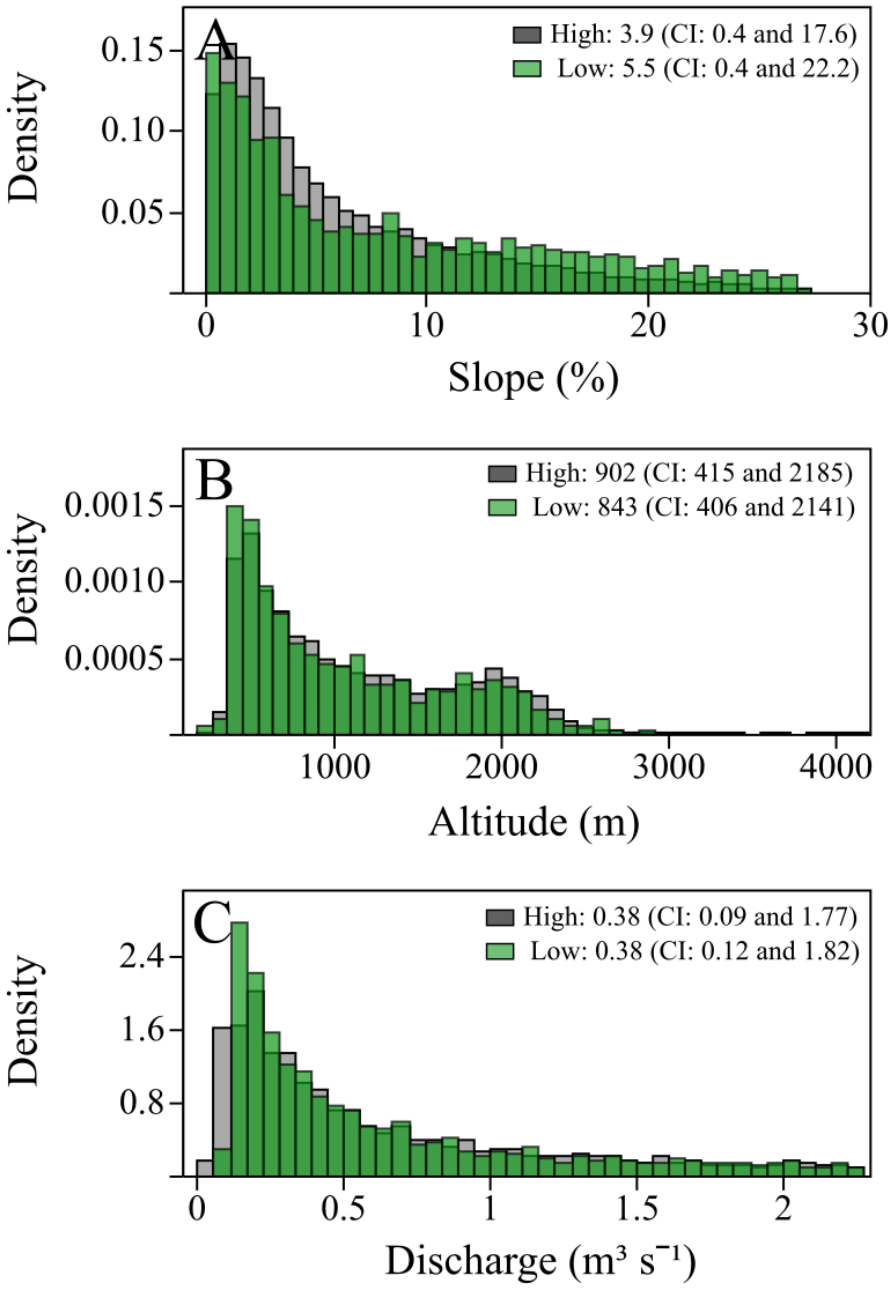

Figure 4S:6 Distributions of the main input parameters used for estimation of CO_2 fluxes. Slope (A), altitude (B) and discharge (C) of Swiss mountain streams derived from the high-resolution (grey) and low-resolution (green) data sets.

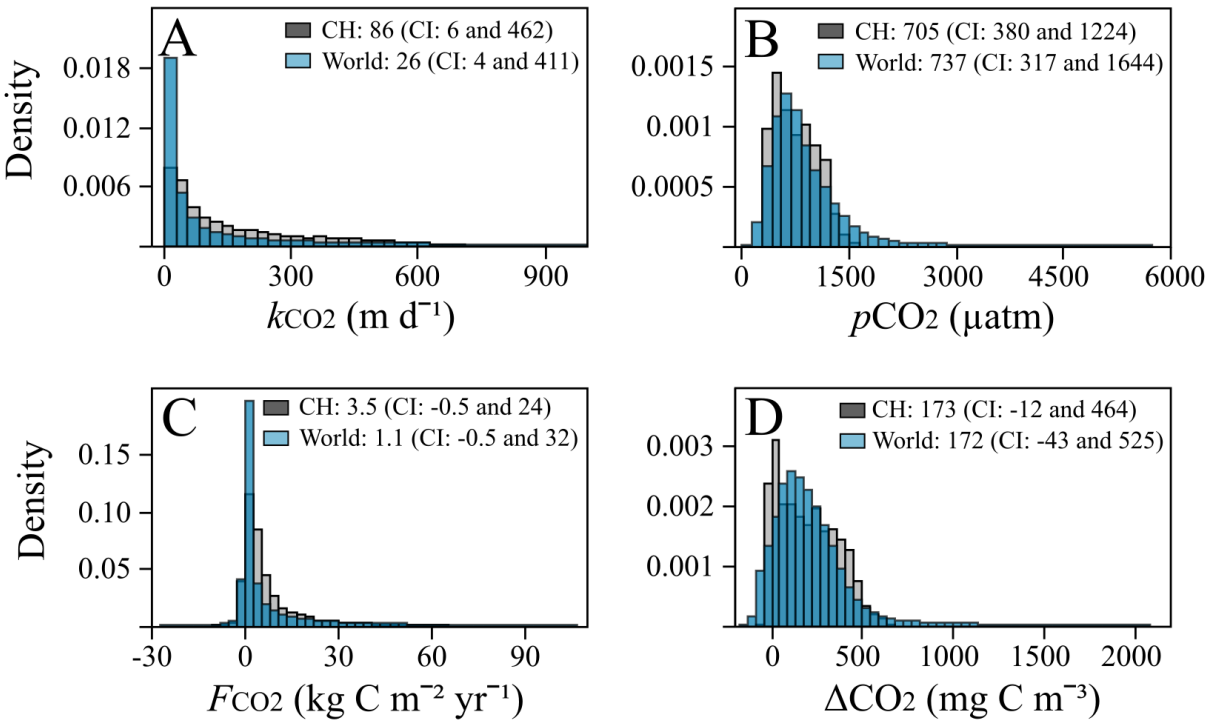

Figure 4S:7 Density distributions of k_{CO2} (A), pCO_2 (B), F_{CO2} (C) and ΔCO_2 (D) calculated for 23,343 Swiss mountain streams (CH; grey) and 1,872,874 mountain streams worldwide (World; blue).

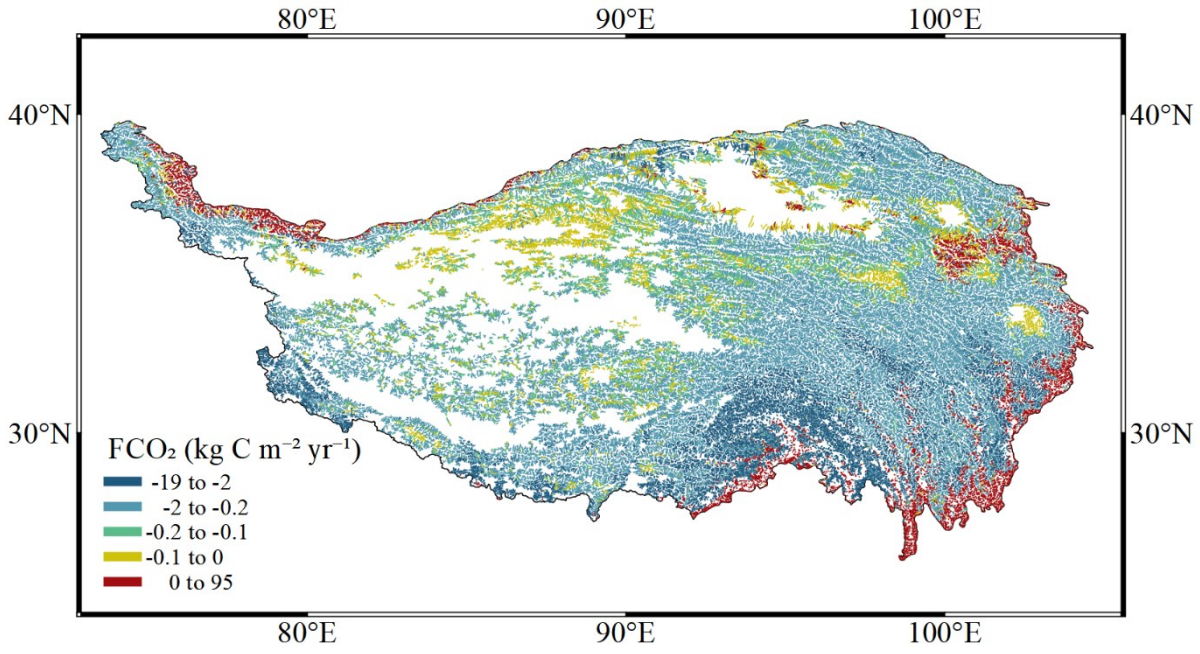

Figure 4S:8 Most streams at the Tibetan plateau are predicted to be undersaturated in CO_2 with the respect to the atmosphere likely acts as a CO_2 sink. Streamwater pCO_2 was mainly undersaturated with respect to the atmosphere (median 288 µatm, CI: 194 and 449 µatm) and 88% of the streams had negative CO_2 fluxes.

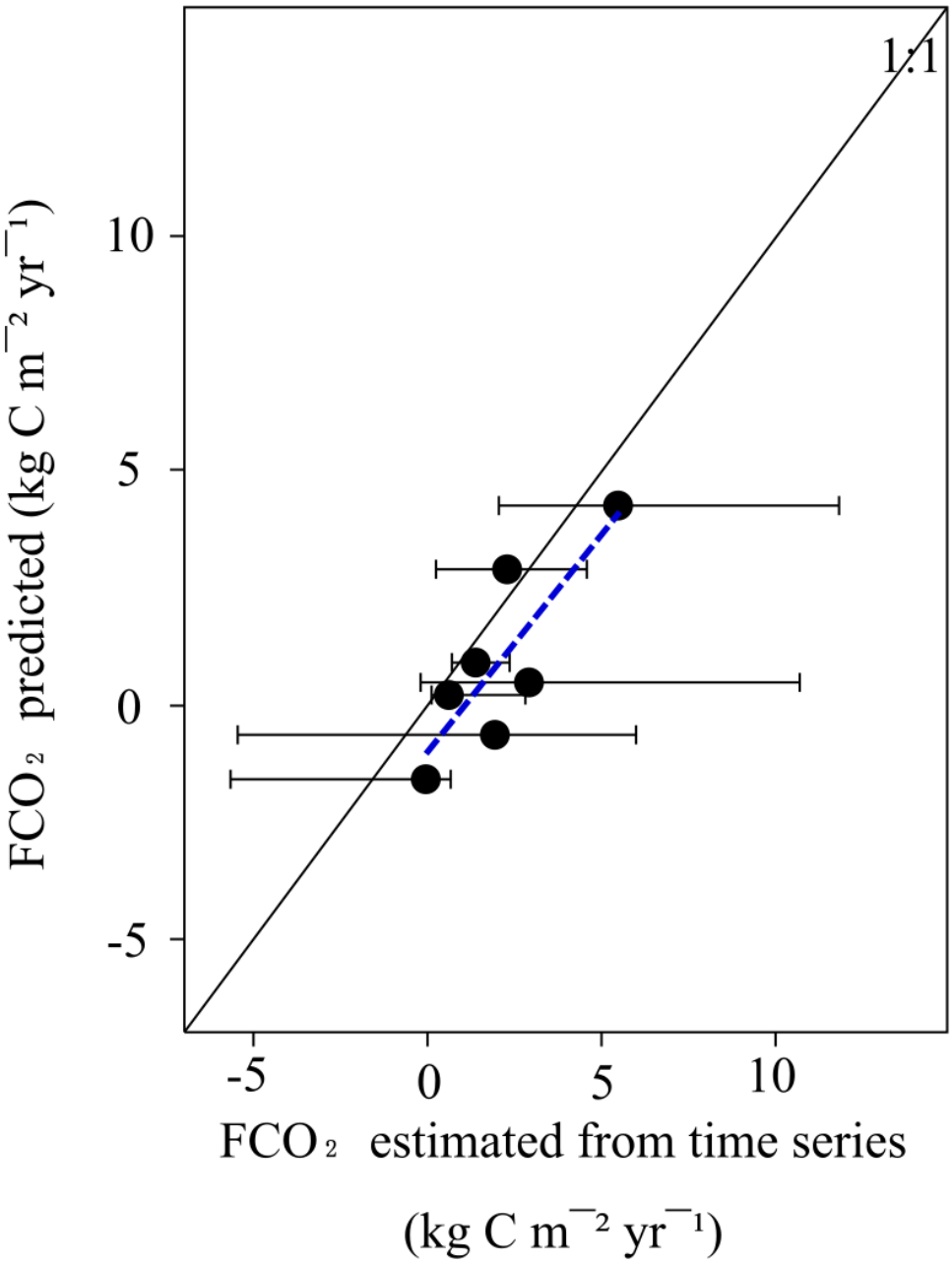

Figure 4S:9 The predicted CO_2 flux corresponded well to the median CO_2 flux estimated from time series (10-minute time steps). Median values (black dots) and 95% confidence intervals (error bars) of F_{CO2} predicted from the CO_2 model versus median values based on time series (Predicted $F_{CO2} = 0.926 \pm 0.284 \times$ Measured $F_{CO2} - 0.981 \pm 0.752$, R^2 = 0.68, n = 7, P=0.022). Units are expressed in kg C m^{-2} yr^{-1} for consistency with other flux estimates reported in this study.

4.6.5 Supplementary Tables

Site	Latitude	Longitude	Altitude (m)	Slope (m m^{-1})	Mean (±std.) pCO_2 (µatm)	Median pCO_2 (µatm)
A1	46.1549	6.80020	1689	0.056	511±62	502
A2	46.1570	6.80120	1630	0.16	527±84	501
A3	46.1593	6.81473	1415	0.097	687±221	593
B1	46.2316	7.10197	1465	0.048	566±69	579
B2	46.2534	7.10963	1201	0.137	457±26	454
B3	46.2535	7.11011	1200	0.138	486±43	473
C1	45.8831	7.13095	1995	0.054	699±220	673
C2	45.9051	7.11560	1774	0.033	472±57	454
C3	45.8937	7.10797	2027	0.059	525±55	523
D1	45.9295	7.24458	2148	0.059	388±43	397
D2	45.9350	7.22690	1937	0.103	427±39	430
D3	45.5568	7.14752	2161	0.078	473±132	465

Table 4:S1 Stream characteristics at the 12 Alpine monitoring stations.

Catchment	Latitude	Longitude	Groundwater pCO_2 (µatm)	Reference
A	46.2305	7.10042	748	Åsa Horgby, *unpublished data*
A	46.2296	7.10156	1789	Åsa Horgby, *unpublished data*
A	46.2296	7.10156	976	Andrea Popp, James Thornton, *personal communication*
A	46.2296	7.10152	245	Andrea Popp, James Thornton, *personal communication*
A	46.2295	7.1012	1936	Andrea Popp, James Thornton, *personal communication*
A	46.2305	7.10042	1729	Andrea Popp, James Thornton, *personal communication*
A	46.2305	7.10042	1362	Andrea Popp, James Thornton, *personal communication*
A	46.2301	7.10035	1343	Andrea Popp, James Thornton, *personal communication*
A	46.2301	7.10035	1072	Andrea Popp, James Thornton, *personal communication*
B	45.8831	7.13095	6303	Lluís Gómez Gener, *personal communication*
B	45.8831	7.13095	2230	Lluís Gómez Gener, *personal communication*

Table 4:S2 Groundwater pCO_2 data, sampled adjacent to mountain streams in Switzerland.

Chapter 5 Conclusions

5.1 Achieved results

We are facing a climate emergency. To be able to assess this threat properly, we need to understand the underlying mechanisms and drivers – both for the anthropogenic carbon cycle as well as the natural carbon cycle. Therefore, in order to better understand the transfer of carbon from land to ocean, and the processes occurring along this journey, the Carbon Cascades from Land to Ocean in the Anthropocene project (C-CASCADES) was founded. As one of 15 PhD students in this project, I focused on CO_2 dynamics and CO_2 fluxes in the start of the land to ocean aquatic continuum: Alpine headwater streams.

In my thesis, I studied the importance of spatiotemporal CO_2 dynamics for CO_2 evasion fluxes from high-altitude streams. My research revealed unexpectedly high CO_2 evasion fluxes from mountain streams and highlights the need to better include mountain streams in the assessment of regional and global carbon budgets.

CO_2 sources and transport pathways can vary considerably at different spatial (reach, catchment and regional) and temporal (annual, seasonal, event) scales. In chapter 2, my co-authors and I found large spatial variability in streamwater CO_2 concentration due to heterogeneous deliveries of respiratory CO_2 from soils adjacent to the streams. This is critical since regions of CO_2 supersaturation might function as "control points" that significantly alter downstream biogeochemistry as well as driving CO_2 evasion fluxes. Moreover, CO_2 concentration dynamics and evasion fluxes might not only vary spatially but also temporally, as shown in chapter 3. There, we showed how CO_2 concentration and evasion fluxes could differ substantially at shorter timescales (i.e., during snowmelt) compared to the annual dynamics. This advocates for high resolution sampling both at spatial and temporal scales, since sporadic sampling of a few locations within a stream network might risk neglecting this heterogeneity.

Spatiotemporal heterogeneity also creates issues for upscaling attempts. In chapter 4, my co-authors and I present a first effort to upscale CO_2 evasion fluxes from small mountain streams worldwide. In this chapter, we developed a simple CO_2 prediction model using literature data and general geopredictors. We then compared modeled CO_2 evasion fluxes (annual scale) with fluxes calculated from CO_2 time series (presented in Chapter 3). We found good agreement between the two estimates (linear regression slope: 0.93±0.28) although with an offset (intercept: -0.98±0.75). Hence, the incapability of including spatiotemporal heterogeneity and CO_2 hotspots in our global estimates may have led to an underestimation of the amount of CO_2 that is evaded from the world's mountain streams. Nevertheless, despite the uncertainty related to the spatiotemporal heterogeneity of CO_2 fluxes from mountain streams, our estimates of 167 ± 1.5 Tg C yr^{-1} corresponds to a substantial amount of the total estimate of CO_2 emissions from all inland waters.

From the chapters in this thesis, the following conclusions can be derived:

(1) Mountain streams may play an important and yet unrecognized role in the global carbon cycle. In chapter 2, my co-authors and I estimated CO_2 evasion fluxes at the catchment scale, and in chapter 4 we estimated CO_2 evasion fluxes from mountain streams at a global scale. In both studies, we argue for significantly higher CO_2 evasion fluxes from mountain streams compared to previous global estimates and emphasize that mountain streams must be better included in the global carbon cycle.

(2) The transport of soil-derived CO_2 to mountain streams is fundamental for streamwater CO_2 dynamics due to several reasons: first, directly by increasing streamwater CO_2 and inducing CO_2 evasion fluxes. Secondly, by lowering streamwater pH. pH controls the speciation of dissolved inorganic carbon (DIC), where lower pH induces conversion of bicarbonate to CO_2. This positive feedback from CO_2 additions to streams with high DIC concentrations, such as many mountain streams, cannot be overlooked.

(3) CO_2 dynamics in mountain streams depend highly on the CO_2 supply from the catchments. I show in chapter 2 how the hydrological connectivity between the stream and its catchment controls CO_2 deliveries to the stream, and thereby the CO_2 supply. The hydrological connectivity is largely driven by snowmelt. In chapter 3, I show how streamwater CO_2 concentrations are diluted with increasing flow on an annual basis, but that snowmelt events flush catchment-derived CO_2 to the

streams. Thus, spatial and temporal variability in CO_2 supply determine whether and when mountain streams, typically with low CO_2 concentrations, act as CO_2 sources or sinks to the atmosphere.

(4) Mountain streams are highly susceptible to climate change. This thesis highlights the role of runoff as a master variable for streamwater CO_2 concentrations and CO_2 evasion fluxes. Therefore, due to ongoing and future climate change, and subsequent shifts in hydrological regimes and groundwater flow paths (as well as vegetation cover) it is crucial to better understand the drivers and mechanisms of CO_2 sources, CO_2 supply and transport pathways for quantification of CO_2 evasion fluxes from mountain streams.

5.2 Future development

In my thesis, I have investigated the role of spatiotemporal variations in CO_2 sources and transportation pathways for CO_2 evasion fluxes from mountain streams. This research has included both intense field and laboratory work, especially during the first years. As with all practical work, it takes time, leaving opportunities for related studies. There are two major subjects that I think require more attention in future research: firstly, better incorporation of the inorganic carbon fluxes and the interactions between lithology and CO_2 evasion, and secondly, increased spatial coverage of mountain streamwater CO_2 monitoring.

The first major subject for future development is to better constrain interactions between the organic and the inorganic carbon fluxes and what those interactions may have on streamwater CO_2 dynamics and ultimately on CO_2 evasion fluxes. In all chapters of my thesis, we discuss the relationship between CO_2 and carbonates and how the carbonate speciation impacts streamwater CO_2 in streams located in catchments with carbonate bedrock. As discussed most extensively in the fourth chapter of my thesis, the interplay between carbonate buffering, pH and streamwater temperature might be of great importance for streamwater CO_2 concentrations and CO_2 evasion fluxes from mountain streams. We found that with increasing altitude, DIC derived from carbonates gains more importance relative to soil-derived DIC. We relate this switch to the increasing influences of carbonate buffering capacity, lowering of pH due to dissolution of atmospheric CO_2 and inputs of soil-derived CO_2 at higher altitudes. We also discuss that CO_2 evasion (and loss in CO_2) may force re-equilibration within the DIC pool, and that increasing temperatures may induce re-precipitation of carbonates due to the retrograde solubility of carbonates. This is in agreement to what, for instance, Marcé and colleagues found in lakes[142], however, very little is known about those processes in streams. Studying streams with low CO_2 concentrations, such as mountain streams may reveal controlling drivers that are not shown, or not significant, for CO_2 evasion fluxes in more carbon-rich aquatic environments. Thus, I would recommend future work along those lines. One way to approach this work could be to use radioactive carbon isotopes ($\delta^{14}C$) to determine the age of the CO_2 in the streamwater, and preferably also the age of the CO_2 that is evading form the streams, since this would inform about the origin of the CO_2.

The second major subject for future development concerns the spatial coverage of mountain streamwater CO_2 monitoring. Very few direct CO_2 measurements from mountain streams exist. In the fourth chapter of my thesis, I present a map of all CO_2 measurements that my co-authors and I found from small mountain streams around the world. In total, there are 323 measurements. These measurements are not only scarce but also heavily biased towards the temperate mountain regions of the world, located in Europe and North America. From South America, Africa and Asia, there are almost no direct measurements of streamwater CO_2 from small mountain streams. Adding to this, many mountain regions in those parts of the world differ substantially in terms of soil cover and vegetation, compared to the Alps, for instance. As an example, mountain streams located in tropical regions are likely to have higher deliveries of catchment-derived organic carbon as well as higher rates of in-stream productivity. At a global scale, this may lead to very different spatiotemporal patterns CO_2 concentrations and evasion fluxes from mountain streams. Furthermore, those differences may have large consequences for upscaling attempts of CO_2 emissions, and there is thus a need of higher spatiotemporal coverage of CO_2 data from mountain streams worldwide.

In summary, I would recommend further studies focusing on capturing different types of mountain streams, across altitudinal gradients as well as a variety of lithologies and biomes. Geographical areas that require more attention are South America, Africa and Asia. By accounting for differences in lithology and vegetation coverage, interactions within the carbonate system could be further constrained. Drivers of streamwater CO_2 concentrations and gas exchange might vary spatially, and temporally, which has the potential to lead to erroneous estimates of CO_2 evasion rates. While it is difficult to recommend an optimal strategy for developing a global monitoring network of pCO_2 and gas exchange rates in mountain streams, what is clear is that more measurements are needed, and that spatiotemporal drivers of CO_2 dynamics and evasion fluxes should be considered in further studies.

References

[1] Tans, P. & Keeling, R. *Trends in Atmospheric Carbon Dioxide.* National Oceanic and Atmospheric Administration, Earth System Research Laboratory, Global Monitoring Division (NOAA/ESRL) (2019).

[2] IPCC*. Climate Change 2014: Synthesis Report*. Intergovernmental Panel of Climate Change (IPCC) (2014).

[3] Climate Emergency Declaration. Available at: https://climateemergencydeclaration.org/climate-emergency-declarations-cover-15-million-citizens/ (Accessed: 14th June 2019).

[4] Lowell, T. V. As climate changes, so do glaciers. *PNAS USA* 97, 1351–1354 (2000).

[5] Paul, F., Kääb, A., Maisch, M., Kellenberger, T. & Haeberli, W. Rapid disintegration of Alpine glaciers observed with satellite data. *Geophys. Res. Lett.* 31, L21402 (2004).

[6] Shakun, J. D. et al. Regional and global forcing of glacier retreat during the last deglaciation. *Nature Commun.* 6, 8059 (2015).

[7] Dyurgerov, M. B. & Meier, M. F. Twentieth century climate change: Evidence from small glaciers. *PNAS* 97, 1406–1411 (2000).

[8] Huss, M., Hock, R., Bauder, A. & Funk, M. 100-year mass changes in the Swiss Alps linked to the Atlantic Multidecadal Oscillation. *Geophys. Res. Lett.* 37, L10501 (2010).

[9] Zemp, M., Haeberli, W., Hoelzle, M. & Paul, F. Alpine glaciers to disappear within decades? *Geophys. Res. Lett.* 33, L13504 (2006).

[10] Milano, M., Reynard, E., Bosshard, N. & Weingartner, R. Simulating future trends in hydrological regimes in Western Switzerland. *J. Hydrol.: Regional Studies* 4, 748–761 (2015).

[11] CH2018. *CH2018 - Climate Scenarios for Switzerland, Technical Report*. National Centre for Climate Services (2018).

[12] Milner, A. M. et al. Glacier shrinkage driving global changes in downstream systems. *PNAS* 114, 9770–9778 (2017).

[13] Cole, J. J. et al. Plumbing the Global Carbon Cycle: Integrating Inland Waters into the Terrestrial Carbon Budget. *Ecosystems* 10, 172–185 (2007).

[14] IPCC. *Climate Change 2013: The Physical Science Basis. Contribution of Working Group I to the Fifth Assessment Report of the Intergovernmental Panel on Climate Change* (Cambridge University Press, 2013).

[15] Battin, T. J. et al. The boundless carbon cycle. *Nature Geosci.* 2, 598–600 (2009).

[16] Lauerwald, R., Laruelle, G. G., Hartmann, J., Ciais, P. & Regnier, P. A. G. Spatial patterns in CO_2 evasion from the global river network. *Global Biogeochem. Cycles* 29, 534–554 (2015).

[17] Raymond, P. A. et al. Global carbon dioxide emissions from inland waters. *Nature* 503, 355–359 (2013).

[18] Regnier, P. et al. Anthropogenic perturbation of the carbon fluxes from land to ocean. *Nature Geosci.* 6, 597–607 (2013).

[19] Bastviken, D., Tranvik, L. J., Downing, J. A., Crill, P. M. & Enrich-Prast, A. Freshwater Methane Emissions Offset the Continental Carbon Sink. *Science* 331, 50–50 (2011).

[20] Beaulieu, J. J. et al. Nitrous oxide emission from denitrification in stream and river networks. *PNAS* 108, 214–219 (2011).

[21] Borges, A. V., Abril, G. & Bouillon, S. Carbon dynamics and CO_2 and CH_4 outgassing in the Mekong delta. *Biogeosciences* 15, 1093–1114 (2018).

[22] Deemer, B. R. et al. Greenhouse Gas Emissions from Reservoir Water Surfaces: A New Global Synthesis. *BioScience* 66, 949–964 (2016).

[23] Hastie, A. et al. CO_2 evasion from boreal lakes: Revised estimate, drivers of spatial variability, and future projections. *Glob. Change Biol.* 24, 711–728 (2018).

[24] Kokic, J., Wallin, M. B., Chmiel, H. E., Denfeld, B. A. & Sobek, S. Carbon dioxide evasion from headwater systems strongly contributes to the total export of carbon from a small boreal lake catchment. *J. Geophys. Res. Biogeosci.* 120, 2014JG002706 (2015).

[25] Borges, A. V. et al. Globally significant greenhouse-gas emissions from African inland waters. *Nature Geosci.* 8, 637–642 (2015).

[26] Ran, L., Lu, X. X. & Liu, S. Dynamics of riverine CO_2 in the Yangtze River fluvial network and their implications for carbon evasion. *Biogeosciences* 14, 2183–2198 (2017).

[27] Sarma, V. V. S. S. et al. High CO_2 emissions from the tropical Godavari estuary (India) associated with monsoon river discharges. *Geophys. Res. Lett.* 38, (2011).

[28] Drake, T. W., Raymond, P. A. & Spencer, R. G. M. Terrestrial carbon inputs to inland waters: a current synthesis of estimates and uncertainty. *Limnol. Oceanogr. Lett.* 3, 132–142 (2018).

[29] Argerich, A. et al. Comprehensive multiyear carbon budget of a temperate headwater stream. *J. Geophys. Res. Biogeosci.* 1306–1315 (2016).

[30] Marx, A. et al. A review of CO_2 and associated carbon dynamics in headwater streams: a global perspective. *Rev. Geophys.* 55, 560–585 (2017).

[31] Tranvik, L. J. et al. Lakes and reservoirs as regulators of carbon cycling and climate. *Limnol. Oceanogr.* 54, 2298–2314 (2009).

[32] Holgerson, M. A. & Raymond, P. A. Large contribution to inland water CO_2 and CH_4 emissions from very small ponds. *Nature Geosci.* 9, 222–226 (2016).

[33] Sawakuchi, H. O. et al. Carbon Dioxide Emissions along the Lower Amazon River. *Front. Mar. Sci.* 4, (2017).

[34] Allen, G. H. et al. Similarity of stream width distributions across headwater systems. *Nature Commun.* 9, 610 (2018).

[35] Downing, J. A. et al. Global abundance and size distribution of streams and rivers. *Inland Waters* 2, 229–236 (2012).

[36] Allen, G. H. & Pavelsky, T. M. Global extent of rivers and streams. *Science* 361, 585–588 (2018).

[37] Duvert, C., Butman, D. E., Marx, A., Ribolzi, O. & Hutley, L. B. CO_2 evasion along streams driven by groundwater inputs and geomorphic controls. *Nature Geosci.* 11, 813 (2018).

[38] Hotchkiss, E. R. et al. Sources of and processes controlling CO_2 emissions change with the size of streams and rivers. *Nature Geosci.* 8, 696–699 (2015).

[39] Campeau, A., Lapierre, J.-F., Vachon, D. & del Giorgio, P. A. Regional contribution of CO_2 and CH_4 fluxes from the fluvial network in a lowland boreal landscape of Québec. *Global Biogeochem. Cycles* 28, 57–69 (2014).

[40] Öquist, M. G., Wallin, M., Seibert, J., Bishop, K. & Laudon, H. Dissolved inorganic carbon export across the soil/stream interface and its fate in a boreal headwater stream. *Environ. Sci. Technol.* 43, 7364–7369 (2009).

[41] Wallin, M. B. et al. Spatiotemporal variability of the gas transfer coefficient (K_{CO2}) in boreal streams: Implications for large scale estimates of CO_2 evasion. *Global Biogeochem. Cycles* 25, GB3025 (2011).

[42] Teodoru, C. R., del Giorgio, P. A., Prairie, Y. T. & Camire, M. Patterns in pCO_2 in boreal streams and rivers of northern Quebec, Canada. *Global Biogeochem. Cycles* 23, GB2012 (2009).

[43] Humborg, C. et al. CO_2 supersaturation along the aquatic conduit in Swedish watersheds as constrained by terrestrial respiration, aquatic respiration and weathering. *Global Change Biol.* 16, 1966–1978 (2010).

[44] Kapos, V., Rhind, J., Edwards, M., Price, M. F. & Ravilious, C. Developing a map of the world's mountain forests (CABI Publishing, Wallingford, UK, 2000).

[45] Meybeck, M., Green, P. & Vörösmarty, C. A New Typology for Mountains and Other Relief Classes. *MT Res. Dev.* 21, 34–45 (2001).

[46] Hartmann, J., Lauerwald, R. & Moosdorf, N. A Brief Overview of the GLObal RIver Chemistry Database, GLORICH. *Procedia Earth Planet.* 10, 23–27 (2014).

[47] Crawford, J. T., Dornblaser, M. M., Stanley, E. H., Clow, D. W. & Striegl, R. G. Source limitation of carbon gas emissions in high-elevation mountain streams and lakes. *J. Geophys. Res. Biogeosci.* 120, 2014JG002861 (2015).

[48] Ran, L. et al. Riverine CO_2 emissions in the Wuding River catchment on the Loess Plateau: Environmental controls and dam impoundment impact. *J. Geophys. Res. Biogeosci.* 122, 1439–1455 (2017).

[49] Schelker, J., Singer, G. A., Ulseth, A. J., Hengsberger, S. & Battin, T. J. CO_2 evasion from a steep, high gradient stream network: importance of seasonal and diurnal variation in aquatic pCO_2 and gas transfer. *Limnol. Oceanogr.* 61, 1826–1838 (2016).

[50] Kuhn, C. et al. Patterns in stream greenhouse gas dynamics from mountains to plains in northcentral Wyoming. *J. Geophys. Res. Biogeosci.* 122, 2173–2190 (2017).

[51] Wanninkhof, R. Relationship between wind speed and gas exchange over the ocean revisited. *Limnol. Oceanogr.: Methods* 12, 351–362 (2014).

[52] Raymond, P. A. et al. Scaling the gas transfer velocity and hydraulic geometry in streams and small rivers. *Limnol. Oceanogr.* 2, 41–53 (2012).

[53] Hall, R. O., Kennedy, T. A. & Rosi-Marshall, E. J. Air–water oxygen exchange in a large whitewater river. *Limnol. Oceanogr.* 2, 1–11 (2012).

[54] Ulseth, A. J. *et al.* Distinct air–water gas exchange regimes in low- and high-energy streams. *Nature Geosci.* 12, 259–263 (2019).

[55] Dickson, A. G., Sabine, C. L. & Christian, J. R. *Guide to best practices for ocean CO_2 measurements* (North Pacific Marine Science Organization, Sidney, Canada 2007).

[56] Mook, W. G., Bommerson, J. C. & Staverman, W. H. Carbon isotope fractionation between dissolved bicarbonate and gaseous carbon dioxide. *Earth Planet. Sc. Lett.* 22, 169–176 (1974).

[57] Abril, G. et al. Technical Note: Large overestimation of pCO_2 calculated from pH and alkalinity in acidic, organic-rich freshwaters. *Biogeosciences* 12, 67–78 (2015).

[58] Lapierre, J.-F. & del Giorgio, P. A. Geographical and environmental drivers of regional differences in the lake pCO_2 versus DOC relationship across northern landscapes. *J. Geophys. Res.* 117, G03015 (2012).

[59] Fasching, C., Behounek, B., Singer, G. A. & Battin, T. J. Microbial degradation of terrigenous dissolved organic matter and potential consequences for carbon cycling in brown-water streams. *Sci. Rep.* 4, 4981 (2014).

[60] Gatland, J. R., Santos, I. R., Maher, D. T., Duncan, T. M. & Erler, D. V. Carbon dioxide and methane emissions from an artificially drained coastal wetland during a flood: Implications for wetland global warming potential. *Earth's Future* 1698–1716 (2016).

[61] Crawford, J. T. et al. Basin scale controls on CO_2 and CH_4 emissions from the Upper Mississippi River. *Geophys. Res. Lett.* 43, 1973–1979 (2016).

[62] Crawford, J. T. et al. CO_2 and CH_4 emissions from streams in a lake-rich landscape: patterns, controls, and regional significance. *Global Biogeochem. Cycles* 28, 2013GB004661 (2014).

[63] Johnson, M. S. et al. Direct and continuous measurement of dissolved carbon dioxide in freshwater aquatic systems—method and applications. *Ecohydrol.* 3, 68–78 (2010).

[64] de Fátima F. L. Rasera, M., Krusche, A. V., Richey, J. E., Ballester, M. V. R. & Victória, R. L. Spatial and temporal variability of pCO_2 and CO_2 efflux in seven Amazonian Rivers. *Biogeochemistry* 116, 241–259 (2013).

[65] Giesler, R. et al. Spatiotemporal variations of pCO_2 and δ^{13}C-DIC in subarctic streams in northern Sweden. *Global Biogeochem. Cycles* 27, 176–186 (2013).

[66] Peter, H. et al. Scales and drivers of temporal pCO_2 dynamics in an Alpine stream. *J. Geophys. Res. Biogeosci.* 119, 1078–1091 (2014).

[67] Deirmendjian, L. & Abril, G. Carbon dioxide degassing at the groundwater-stream-atmosphere interface: isotopic equilibration and hydrological mass balance in a sandy watershed. *J. Hydrol.* 558, 129–143 (2018).

[68] Laudon, H. et al. The role of biogeochemical hotspots, landscape heterogeneity, and hydrological connectivity for minimizing forestry effects on water quality. *Ambio* 45, 152–162 (2016).

[69] McClain, M. E. et al. Biogeochemical hot spots and hot moments at the interface of terrestrial and aquatic ecosystems. *Ecosystems* 6, 301–312 (2003).

[70] Brown, L. E., Hannah, D. M. & Milner, A. M. Alpine stream habitat classification: an alternative approach incorporating the role of dynamic water source contributions. *Arctic, Antarctic, and Alpine Research* 35, 313–322 (2003).

[71] Butman, D. & Raymond, P. A. Significant efflux of carbon dioxide from streams and rivers in the United States. *Nature Geosci.* 4, 839–842 (2011).

[72] Duvert, C. et al. Groundwater-derived DIC and carbonate buffering enhance fluvial CO_2 evasion in two Australian tropical rivers. *J. Geophys. Res. Biogeosci.* 124, 312–327 (2019).

[73] Bernhardt, E. S. et al. Control points in ecosystems: moving beyond the hot spot hot moment concept. *Ecosystems* 20, 665–682 (2017).

[74] Liu, S. & Raymond, P. A. Hydrologic controls on pCO_2 and CO_2 efflux in US streams and rivers. *Limnol. Oceanogr. Lett.* 3, 428–435 (2018).

[75] Barnett, T. P., Adam, J. C. & Lettenmaier, D. P. Potential impacts of a warming climate on water availability in snow-dominated regions. *Nature* 438, 303–309 (2005).

[76] Grace, J., Berninger, F. & Nagy, L. Impacts of Climate Change on the Tree Line. *Ann. Bot.* 90, 537–544 (2002).

[77] Lane, S. N., Bakker, M., Gabbud, C., Micheletti, N. & Saugy, J.-N. Sediment export, transient landscape response and catchment-scale connectivity following rapid climate warming and Alpine glacier recession. *Geomorphology* 277, 210–227 (2017).

[78] IPCC. Global warming of 1.5℃: *Summary for Policymakers*. Intergovernmental Panel of Climate Change (IPCC) (2018).

[79] Stanley, E. H. et al. The ecology of methane in streams and rivers: patterns, controls, and global significance. *Ecol. Monogr.* 86, 146171 (2016).

[80] Crawford, J. T., Striegl, R. G., Wickland, K. P., Dornblaser, M. M. & Stanley, E. H. Emissions of carbon dioxide and methane from a headwater stream network of interior Alaska. *J. Geophys. Res. Biogeosci.* 118, 482–494 (2013).

[81] Ulseth, A. J., Bertuzzo, E., Singer, G. A., Schelker, J. & Battin, T. J. Climate-induced changes in spring snowmelt impact ecosystem metabolism and carbon fluxes in an Alpine stream network. *Ecosystems* 21, 373–390 (2018).

[82] Campeau, A. et al. Stable carbon isotopes reveal soil-stream DIC linkages in contrasting headwater catchments. *J. Geophys. Res. Biogeosci.* 123, 2017JG004083 (2018).

[83] Amiotte Suchet, P., Probst, J. & Wolfgang, L. Worldwide distribution of continental rock lithology: implications for the atmospheric/soil CO_2 uptake by continental weathering and alkalinity river transport to the oceans. *Global Biogeochem. Cycles* 17, (2003).

[84] Kendall, C. & Caldwell, E. A. Fundamentals of isotope geochemistry, in *Isotope Tracers in Catchment Hydrology* (eds. Kendall, C. & McDonnell, J. J.) 51–86 (Elsevier Science, Amsterdam, The Netherlands, 1998).

[85] Venkiteswaran, J. J., Schiff, S. L. & Wallin, M. B. Large carbon dioxide fluxes from headwater boreal and sub-boreal streams. *PLOS ONE* 9, e101756 (2014).

[86] Finlay, J. C. Stable-carbon-isotope ratios of river biota: implications for energy flow in lotic food webs. *Ecology* 82, 1052–1064 (2001).

[87] Doctor, D. H. et al. Carbon isotope fractionation of dissolved inorganic carbon (DIC) due to outgassing of carbon dioxide from a headwater stream. *Hydrol. Process.* 22, 2410–2423 (2008).

[88] Wang, Y. et al. Carbon Cycling in Terrestrial Environments in *Isotope Tracers in Catchment Hydrology* (eds. Kendall, C. & McDonnell, J. J.) 577–610 (Elsevier Science, Amsterdam, The Netherlands, 199, 1998).

[89] Still, C. J., Berry, J. A., Collatz, G. J. & DeFries, R. S. Global distribution of C3 and C4 vegetation: carbon cycle implications. *Global Biogeochem. Cycles* 17, 6-1-6–14 (2003).

[90] Clark, I. D. & Fritz, P. *Environmental Isotopes in Hydrogeology* (Lewis Publishers, New York, USA, 1997).

[91] Mayorga, E. et al. Young organic matter as a source of carbon dioxide outgassing from Amazonian rivers. *Nature* 436, 538–541 (2005).

[92] Polsenaere, P. & Abril, G. Modelling CO_2 degassing from small acidic rivers using water pCO_2, DIC and δ^{13}C-DIC data. *Geochim. et Cosmochim. Acta* 91, 220–239 (2012).

[93] Spötl, C. & Vennemann, T. W. Continuous-flow isotope ratio mass spectrometric analysis of carbonate minerals. *Rapid Commun. Mass Sp.* 17, 1004–1006 (2003).

[94] Parnell, A. simmr: A Stable Isotope Mixing Model (2016). R package version 0.3, http://CRAN.R-project.org/package=simmr

[95] Barthold, F. K. *et al.* How many tracers do we need for end member mixing analysis (EMMA)? A sensitivity analysis. *Water Resour. Res.* 47, W08519 (2011).

[96] Killick, R., Haynes, K. & Eckley, I. A. changepoint: an R package for changepoint analysis (2016). R package version 2.2.2, http://CRAN.R-project.org/package=changepoint

[97] Killick, R. & Eckley, I. A. changepoint: an R package for changepoint analysis. *J. Stat. Softw.* 58, 1–19 (2014).

[98] Keeling, C. D. The concentration and isotopic abundances of atmospheric carbon dioxide in rural areas. *Geochim. Cosmochim. Acta* 13, 322–334 (1958).

[99] Miller, J. B. & Tans, P. P. Calculating isotopic fractionation from atmospheric measurements at various scales. *Tellus B* 55, 207–214 (2003).

[100] Campeau, A. et al. Multiple sources and sinks of dissolved inorganic carbon across Swedish streams, refocusing the lens of stable C isotopes. *Sci. Rep.* 7, 9158 (2017).

[101] Pataki, D. E. et al. The application and interpretation of Keeling plots in terrestrial carbon cycle research. *Global Biogeochem. Cycles* 17, 1022 (2003).

[102] Weyhenmeyer, G. A., Kortelainen, P., Sobek, S., Müller, R. & Rantakari, M. Carbon dioxide in boreal surface waters: a comparison of lakes and streams. *Ecosystems* 15, 1295–1307 (2012).

[103] Zhang, J., Quay, P. D. & Wilbur, D. O. Carbon isotope fractionation during gas-water exchange and dissolution of CO_2. *Geochim. et Cosmochim. Acta* 59, 107–114 (1995).

[104] Wanninkhof, R. Relationship between wind speed and gas exchange over the ocean. *J. Geophys. Res. Oceans* 97, 7373–7382 (1992).

[105] Jähne, B. et al. On the parameters influencing air-water gas exchange. *J. Geophys. Res. Oceans* 92, 1937–1949 (1987).

[106] Qu, B. et al. Greenhouse gases emissions in rivers of the Tibetan Plateau. *Sci. Rep.* 7, 16573 (2017).

[107] Campeau, A. & del Giorgio, P. A. Patterns in CH_4 and CO_2 concentrations across boreal rivers: major drivers and implications for fluvial greenhouse emissions under climate change scenarios. *Glob. Change Biol.* 20, 1075–1088 (2014).

[108] Johnson, M. S. et al. CO_2 efflux from Amazonian headwater streams represents a significant fate for deep soil respiration. *Geophys. Res. Lett.* 35, (2008).

[109] Grand, S., Rubin, A., Verrecchia, E. P. & Vittoz, P. Variation in soil respiration across soil and vegetation types in an Alpine valley. *PLOS ONE* 11, e0163968 (2016).

[110] Sommerfeld, R. A., Musselman, R. C., Reuss, J. O. & Mosier, A. R. Preliminary measurements of CO_2 in melting snow. *Geophys. Res. Lett.* 18, 1225–1228 (1991).

[111] Lapierre, J.-F., Guillemette, F., Berggren, M. & del Giorgio, P. A. Increases in terrestrially derived carbon stimulate organic carbon processing and CO_2 emissions in boreal aquatic ecosystems. *Nature Commun.* 4, 2972 (2013).

[112] Godsey, S. E. & Kirchner, J. W. Dynamic, discontinuous stream networks: hydrologically driven variations in active drainage density, flowing channels and stream order. *Hydrol. Process.* 28, 5791–5803 (2014).

[113] Williamson, C. E., Dodds, W., Kratz, T. K. & Palmer, M. A. Lakes and streams as sentinels of environmental change in terrestrial and atmospheric processes. *Front. Ecol. Environ.* 6, 247–254 (2008).

[114] Fisher, S. G., Sponseller, R. A. & Heffernan, J. B. Horizons in stream biogeochemistry: flowpaths to progress. *Ecology* 85, 2369–2379 (2014).

[115] Tank, S. E., Fellman, J. B., Hood, E. & Kritzberg, E. S. Beyond respiration: controls on lateral carbon fluxes across the terrestrial-aquatic interface. *Limnol. Oceanogr. Lett.* 3, 76–88 (2018).

[116] Wallin, M. B. et al. Evasion of CO_2 from streams – the dominant component of the carbon export through the aquatic conduit in a boreal landscape. *Glob. Change Biol.* 19, 785-797 (2013).

[117] Godsey, S. E., Kirchner, J. W. & Clow, D. W. Concentration–discharge relationships reflect chemostatic characteristics of US catchments. *Hydrol. Process.* 23, 1844–1864 (2009).

[118] Meybeck, M. & Moatar, F. Daily variability of river concentrations and fluxes: indicators based on the segmentation of the rating curve. *Hydrol. Process.* 26, 1188–1207 (2012).

[119] Rocher-Ros, G., Sponseller, R. A., Lidberg, W., Mörth, C.-M. & Giesler, R. Landscape process domains drive patterns of CO_2 evasion from river networks. *Limnol. Oceanogr. Lett.* 4, 87–95 (2019).

[120] Horgby, Å., Boix Canadell, M., Ulseth, A. J., Vennemann, T. W. & Battin, T. J. High-resolution spatial sampling identifies groundwater as driver of CO_2 dynamics in an Alpine stream network *J. Geophys. Res. Biogeosciences* 124, 1961-1976 (2019).

[121] Hartmann, J. & Moosdorf, N. The new global lithological map database GLiM: A representation of rock properties at the Earth surface. *Geochem. Geophys. Geosyst.* 13, Q12004 (2012).

[122] Boix Canadell, M., Escoffier, N., Ulseth, A. J., Lane, S. N. & Battin, T. J. Alpine glacier shrinkage drives shift in dissolved organic carbon export from quasi-chemostasis to transport-limitation. *Geophys. Res. Lett.* (2019).

[123] Gordon, N. D., McMahon, T. A., Finlayson, B. L., Gippel, C. J. & Nathan, R. J. *Stream Hydrology: an introduction for ecologists* (John Wiley, Chichester, UK, 2004).

[124] Plummer, L. N. & Busenberg, E. The solubilities of calcite, aragonite and vaterite in CO_2-H_2O solutions between 0 and 90°C, and an evaluation of the aqueous model for the system $CaCO_3$-CO_2-H_2O. *Geochim. Cosmochim. Acta* 46, 1011–1040 (1982).

[125] Hannah, D. M., Kansakar, S. R., Gerrard, A. J. & Rees, G. Flow regimes of Himalayan rivers of Nepal: nature and spatial patterns. *J. Hydrol.* 308, 18–32 (2005).

[126] Milner, A. M., Brown, L. E. & Hannah, D. M. Hydroecological response of river systems to shrinking glaciers. *Hydrol. Process.* 23, 62–77 (2009).

[127] Wallin, M., Buffam, I., Öquist, M., Laudon, H. & Bishop, K. Temporal and spatial variability of dissolved inorganic carbon in a boreal stream network: concentrations and downstream fluxes. *J. Geophys. Res. Biogeosciences* 115, G02014 (2010).

[128] Lupon, A. et al. Groundwater inflows control patterns and sources of greenhouse gas emissions from streams. *Limnol. Oceanogr.* 64, 1545–1557 (2019).

[129] Dinsmore, K. J. et al. Contrasting CO_2 concentration discharge dynamics in headwater streams: a multi-catchment comparison. *J. Geophys. Res. Biogeosciences* 118, 445–461 (2013).

[130] Dinsmore, K. J. & Billett, M. F. Continuous measurement and modeling of CO_2 losses from a peatland stream during stormflow events. *Water Resour. Res.* 44, (2008).

[131] Mast, M. A., Wickland, K. P., Striegl, R. T. & Clow, D. W. Winter fluxes of CO_2 and CH_4 from subalpine soils in Rocky Mountain National Park, Colorado. *Global Biogeochem. Cycles* 12, 607–620 (1998).

[132] Boyer, E. W., Hornberger, G. M., Bencala, K. E. & McKnight, D. M. Effects of asynchronous snowmelt on flushing of dissolved organic carbon: a mixing model approach. *Hydrol. Process.* 14, 3291–3308 (2000).

[133] Cole, J. J. & Caraco, N. F. Carbon in catchments: connecting terrestrial carbon losses with aquatic metabolism. *Mar. Freshwater Res.* 52, 101–110 (2001).

[134] Gruber, N. et al. The oceanic sink for anthropogenic CO_2 from 1994 to 2007. *Science* 363, 1193–1199 (2019).

[135] Richey, J. E., Melack, J. M., Aufdenkampe, A. K., Ballester, V. M. & Hess, L. L. Outgassing from Amazonian rivers and wetlands as a large tropical source of atmospheric CO_2. *Nature* 416, 617–620 (2002).

[136] Wang, Q., Ni, J. & Tenhunen, J. Application of a geographically-weighted regression analysis to estimate net primary production of Chinese forest ecosystems. *Global Ecol. Biogeogr.* 14, 379–393 (2005).

[137] Wallin, M. B. et al. Carbon dioxide and methane emissions of Swedish low-order streams—a national estimate and lessons learnt from more than a decade of observations. *Limnol. Oceanogr. Lett.* 3, 156–167 (2018).

[138] Butman, D. et al. Aquatic carbon cycling in the conterminous United States and implications for terrestrial carbon accounting. *PNAS* 113, 58–63 (2016).

[139] Montgomery, D. R., Buffington, J. M., Smith, R. D., Schmidt, K. M. & Pess, G. Pool Spacing in Forest Channels. *Water Resour. Res.* 31, 1097–1105 (1995).

[140] Viviroli, D., Dürr, H. H., Messerli, B., Meybeck, M. & Weingartner, R. Mountains of the world, water towers for humanity: Typology, mapping, and global significance. *Water Resour. Res.* 43, (2007).

[141] Almeida, R. M., Pacheco, F. S., Barros, N., Rosi, E. & Roland, F. Extreme floods increase CO_2 outgassing from a large Amazonian river. *Limnol. Oceanogr.* 62, 989–999 (2017).

[142] Marcé, R. et al. Carbonate weathering as a driver of CO_2 supersaturation in lakes. *Nature Geosci.* 8, 107–111 (2015).

[143] Pawellek, F. & Veizer, J. Carbon cycle in the upper Danube and its tributaries: $\delta^{13}C_{DIC}$ constraints. *Isr. J. Earth Sci.* 43, 187–194 (1994).

[144] Drysdale, R., Lucas, S. & Carthew, K. The influence of diurnal temperatures on the hydrochemistry of a tufa-depositing stream. *Hydrol. Process.* 17, 3421–3441 (2003).

[145] Dallaire, C. O., Lehner, B., Sayre, R. & Thieme, M. A multidisciplinary framework to derive global river reach classifications at high spatial resolution. *Environ. Res. Lett.* 14, 024003 (2019).

[146] Ran, L. et al. CO_2 outgassing from the Yellow River network and its implications for riverine carbon cycle. *J. Geophys. Res. Biogeosci.* 120, 1334–1347 (2015).

[147] Yan, F. et al. Lakes on the Tibetan Plateau as Conduits of Greenhouse Gases to the Atmosphere. *J. Geophys. Res. Biogeosci.* 123, 2091–2103 (2018).

[148] Aufdenkampe, A. K. et al. Riverine coupling of biogeochemical cycles between land, oceans, and atmosphere. *Front. Ecol. Environ.* 9, 53–60 (2011).

[149] Gaillardet, J., Dupré, B., Louvat, P. & Allègre, C. J. Global silicate weathering and CO_2 consumption rates deduced from the chemistry of large rivers. *Chem. Geol.* 159, 3–30 (1999).

[150] Hemingway, J. D. et al. Microbial oxidation of lithospheric organic carbon in rapidly eroding tropical mountain soils. *Science* 360, 209–212 (2018).

[151] Horan, K. et al. Mountain glaciation drives rapid oxidation of rock-bound organic carbon. *Sci. Adv.* 3, e1701107 (2017).

[152] Jasechko, S., Kirchner, J. W., Welker, J. M. & McDonnell, J. J. Substantial proportion of global streamflow less than three months old. *Nature Geosci.* 9, 126–129 (2016).

[153] Maher, K. The dependence of chemical weathering rates on fluid residence time. *Earth Planet. Sc. Lett.* 294, 101–110 (2010).

[154] Harris, G. N., Bowman, K. P. & Shin, D.-B. Comparison of freezing-level altitudes from the NCEP reanalysis with TRMM precipitation radar brightband data. *J. Climate* 13, 4137–4148 (2000).

[155] Rouaud, M. *Probability, Statistics and estimation: propagation of uncertainties in experimental measurement* (Lulu Press, Morrisville, USA, 2013).

[156] Dodson, R. & Marks, D. Daily air temperature interpolated at high spatial resolution over a large mountainous region. *Clim. Res.* 8, 20 (1997).

[157] Fick, S. E. & Hijmans, R. J. Worldclim 2: New 1-km spatial resolution climate surfaces for global land areas. *Int. J. Climatol.* 37, 4302-4315 (2017).

[158] Bouillon, S. et al. Distribution, origin and cycling of carbon in the Tana River (Kenya): a dry season basin-scale survey from headwaters to the delta. *Biogeosciences* 6, 2475–2493 (2009).

[159] Leibowitz, Z. W., Brito, L. A. F., De Lima, P. V., Eskinazi-Sant'Anna, E. M. & Barros, N. O. Significant changes in water pCO_2 caused by turbulence from waterfalls. *Limnologica* 62, 1–4 (2017).

[160] Danielson, J. J. & Gesch, D. B. Global multi-resolution terrain elevation data 2010 (GMTED2010). *U.S. Geological Survey Open-File Report* 2011-1073 (2011).

[161] Jarvis, A., Reuter, H. I., Nelson, A. & Guevara, E. Hole-filled SRTM for the globe Version 4. *CGIAR-CSI SRTM 90m Database*, http://srtm.csi.cgiar.org (2008).

[162] Hengl, T. et al. SoilGrids1km — Global soil information based on automated mapping. *PLOS ONE* 9, e105992 (2014).

[163] Jurado, A. et al. Occurrence of greenhouse gases in the aquifers of the Walloon Region (Belgium). *Sci. Tot. Environ.* 619–620, 1579–1588 (2018).

Åsa HORGBY

Rue du Maupas 36B, 1004 Lausanne, Switzerland
+41 78 867 67 74, asa.horgby@gmail.com

PROFILE: PhD in biogeochemistry with good analytical, organizational and social skills.

HOBBIES: Hiking, outdoor sports, travelling, gardening

EXPERIENCE: I am finishing a **PhD in Environmental Engineering, specialized in biogeochemistry and stream ecology**. In my research, I focused on CO_2 dynamics in mountain streams, where the CO_2 is coming from and how much that is evaded to the atmosphere. I work in a team of international scientists, where I **organize** and conduct **field** campaigns, analyze biogeochemical samples in the **laboratory** and performing **statistical** analyses. I am **innovative**, **focused** and **social** and like to work in dynamic projects.

EDUCATION

2015 – present École polytechnique fédérale de Lausanne (EPFL), Switzerland
PhD student in Civil and Environmental Engineering
Thesis: "Spatiotemporal drivers of CO_2 dynamics and evasion fluxes from mountain streams"
Supervised by Prof. T. Battin

2013-2015 Uppsala University, Sweden
Master degree in Earth Science Hydrology/Hydrogeology
Thesis: "The usability of remote sensing data for flood inundation modelling: a case study of the Mississippi River"
Supervised by Prof. G. di Baldassarre

2010-2013 Uppsala University, Sweden
Bachelor degree in Earth Science
Thesis: "Effects on drinking water quality due to irrigation in the Koga area of Merawi, Ethiopia"
Supervised by Prof. K. Bishop and Dr. J.M. Mayotte

WORK AND INTERNSHIPS

2015 Internship at Kongsberg Maritime Contros, Germany: working with the calibration of CO_2 and CH_4 sensors

2014 Erasmus ambassador, International Office of Uppsala University, Sweden: event planning, budgeting and informing

2013 Internship at the Administrative County Board of Östergötland, Environmental Protection department, Sweden
Status classification of water resources, risk classification of contaminated soils

SKILLS

Communication skills: Swedish (mother tongue), English (fluent), German (A2/B1), French (A2/B1)
Teaching assistantships: organizing and teaching laboratory experiments for students, teaching laboratory analysis techniques and sensor construction, chairing scientific discussions with students
Field work: extensive fieldwork experience and organization of practical work
Laboratory work: laboratory expertise concerning carbon concentrations and carbon isotopic compositions
Computer skills: good knowledge in the geographical information systems software GIS, QGIS and SAGA, moderate knowledge in various statistical and hydrological software such as JMP, R, Matlab and LISFLOOD-FP
Science communication: a talk international conferences (Vienna April 2018; Lausanne May 2019; Zagreb July 2019)

PUBLICATIONS

Horgby, Å., Boix Canadell, M., Ulseth, A.J., Vennemann, T.W., Battin, T.J., 2019. High-resolution spatial sampling identifies groundwater as driver of CO_2 dynamics in an Alpine stream network. Journal of Geophysical Research: Biogeosciences. Doi: 10.1029/2019JG005047

Horgby, Å., Segatto, P.L., Bertuzzo, B., Lauerwald, R., Lehner, B., Ulseth, A.J., Vennemann, T.W., Battin, T.J., Unexpected large evasion fluxes of carbon dioxide from turbulent streams draining the world's mountains. *Accepted in Nature Communications*

**Ce document a été imprimé au Centre d'impression EPFL,
imprimerie climatiquement neutre, certifiée myClimate.**